

**NOVEL APPROACHES TO TOXICITY TESTING
IN *DAPHNIA MAGNA***

by

NADINE SUZANNE TAYLOR

A thesis submitted to
The University of Birmingham
for the degree of
DOCTOR OF PHILOSOPHY

School of Biosciences
The University of Birmingham
March 2010

UNIVERSITY OF
BIRMINGHAM

University of Birmingham Research Archive

e-theses repository

This unpublished thesis/dissertation is copyright of the author and/or third parties. The intellectual property rights of the author or third parties in respect of this work are as defined by The Copyright Designs and Patents Act 1988 or as modified by any successor legislation.

Any use made of information contained in this thesis/dissertation must be in accordance with that legislation and must be properly acknowledged. Further distribution or reproduction in any format is prohibited without the permission of the copyright holder.

Abstract

Current regulatory risk assessment strategies have several limitations, such as linking subcellular changes to higher-level biological effects, and an improved knowledge-based approach is needed. Ecotoxicogenomic techniques have been proposed as having the potential to overcome the current limitations, providing greater mechanistic information for ecotoxicological testing. In this thesis, metabolomics is explored as a novel method for toxicity testing using *Daphnia magna*. Initially I evaluated the potential application of Fourier transform ion cyclotron resonance mass spectrometry (FT-ICR MS) based metabolomics for use in regulatory toxicity testing. Subsequently, I aimed to use this approach to discriminate between toxicant modes of action (MOA) and to link toxicant induced metabolic effects to reduced reproductive output in *D. magna*. FT-ICR MS metabolomics was determined to be a feasible approach for toxicity testing of both whole-organism homogenates and haemolymph of *D. magna*. It is capable of discriminating between life-stages of *D. magna* as well as determining toxicant-induced metabolic effects. Highly predictive multivariate classification models were capable of significantly discriminating between four different toxicant MOAs; achievable in both haemolymph and whole-organism extracts, with the latter being the more information-rich sample type. Multivariate regression models were predictive of reduced reproductive output in *D. magna* following toxicant exposure, and determined that a metabolic biomarker signature was significantly able to predict the reproductive output of *D. magna*. Ultimately this research has concluded that an FT-ICR MS metabolomics approach for use in regulatory toxicity testing using *Daphnia magna* is both viable and can provide valuable information.

Acknowledgements

I would like to thank my supervisor, Dr Mark Viant, for all his help and unwavering enthusiasm throughout my PhD. I also extend my thanks to all members of the Viant research group for their varied input, advice and guidance with my research. I offer my thanks to the Natural Environment Research Council for funding this PhD and the Stress Biology and Ecotoxicology Research Group at Reading University for their advice on *Daphnia* and providing the animals to initiate our culture at Birmingham.

In addition I'd like to thank specific members of the 4th floor, Huw, Rhiannon, Rachael, Leda and Chib for the many tea breaks and social events that continually made me smile. Particular thanks go to Rhiannon for all her help in starting the *Daphnia* culture, helping to keep the little critters alive and for keeping me calm!

Finally, to my Mum, Dad and Leon for your continual support, tireless encouragement and your absolute belief in me; thank you.

CHAPTER ONE: General Introduction	1
1.1 Introduction	2
1.2 Ecotoxicology and selection of test species	3
1.2.1 Current approaches in regulatory ecotoxicological testing.....	4
1.2.2 Limitations of current strategies	9
1.3 The potential of omics in regulatory ecotoxicological testing	11
1.4 Metabolomics	13
1.4.1 Metabolomics in ecotoxicology	14
1.5 <i>Daphnia magna</i>	21
1.5.1 <i>Daphnia magna</i> and regulatory toxicity testing	25
1.5.2 <i>Daphnia magna</i> and ecotoxicogenomics	25
1.6 Metabolomics analysis platforms	27
1.6.1 NMR spectroscopy	30
1.6.2 Mass spectrometry	31
1.6.3 FT-ICR MS	33
1.7 Metabolomics data analysis	35
1.8 Research aims	39
CHAPTER TWO: Materials and Methods	40
2.1 Culturing of <i>Daphnia magna</i>	41
2.1.1 Preparation of nutritional supplement Marinure	41
2.1.2 Culture of <i>Chlorella vulgaris</i> algal stock	42
2.1.3 Preparation of <i>Chlorella vulgaris</i> algal feed	42
2.1.4 Preparation of Baker’s Yeast	43
2.2 Toxicity exposures and animal capture	45
2.3 Metabolite extraction	45
2.3.1 Whole organism homogenates	45
2.3.2 Haemolymph	46
2.4 FT-ICR mass spectrometry	47
2.5 Data pre-processing	48
2.6 Putative identification of empirical formulae and metabolites	54
2.7 Statistical analysis	55
2.7.1 Multivariate statistics	55
2.7.2 Univariate Statistics	57
CHAPTER THREE: Optimisation and validation of FT-ICR MS based metabolomics using whole organism homogenates of <i>Daphnia magna</i>	58
3.1 Introduction	59
3.2 Materials and Methods	60
3.2.1 Biomass optimisation study	60
3.2.2 Copper toxicity testing	61

3.2.3	Metabolite extraction and FT-ICR mass spectrometry	61
3.2.4	Data processing and peak identification	62
3.2.5	Statistical analysis	62
3.3	Results and Discussion	63
3.3.1	Biomass optimisation study	63
3.3.2	Acute copper range-finding study	69
3.3.3	Acute copper toxicity metabolomics study	71
3.3.4	Identification of empirical formulae and metabolites	82
3.3.5	Biochemical interpretation	88
3.3.6	Applicability of SIM-stitching DI FT-ICR for metabolomics	90
3.4	Conclusion	92
 CHAPTER FOUR: Optimisation and validation of FT-ICR MS based metabolomics using <i>Daphnia magna</i> haemolymph		94
4.1	Introduction	95
4.2	Materials and Methods	96
4.2.1	<i>Daphnia magna</i> exposures and haemolymph extraction	96
4.2.2	FT-ICR MS metabolomics	97
4.2.2.1	Initial haemolymph study	97
4.2.2.2	Cadmium toxicity study	97
4.2.3	Transcriptomics	98
4.3	Results and Discussion	99
4.3.1	Initial metabolomics study	99
4.3.2	Metabolomics cadmium toxicity study	102
4.3.3	Key findings from transcriptomic cadmium toxicity study	109
4.3.4	Relevance of findings to cadmium toxicity	109
4.4	Conclusion	113
 CHAPTER FIVE: Discriminating toxicant modes of action via changes in the daphnid metabolome		114
5.1	Introduction	115
5.2	Materials and Methods	116
5.2.1	Optimisation of FT-ICR MS analysis of individual daphnid haemolymph ..	116
5.2.2	Determination of sub-lethal concentrations	117
5.2.3	Adult <i>Daphnia magna</i> acute toxicity studies	117
5.2.4	Animal capture and metabolite extraction	118
5.2.5	FT-ICR MS, data processing and metabolite identification	119
5.2.6	Statistical analysis	120
5.3	Results and Discussion	121
5.3.1	Optimisation of FT-ICR MS analysis of individual daphnid haemolymph ..	121
5.3.2	Determination of sublethal concentrations	122

5.3.3	Effects of individual toxicants on whole organism and haemolymph metabolomes	124
5.3.4	Multivariate models for discriminating toxicant modes of action	132
5.3.5	Whole organism metabolome provides more discriminatory predictive models	137
5.4	Conclusion	139
CHAPTER SIX: Discovering metabolic markers that are predictive of reduced reproductive output in <i>Daphnia magna</i>		140
6.1	Introduction	141
6.2	Materials and Methods	143
6.2.1	Determination of sub-lethal concentrations	143
6.2.2	<i>Daphnia magna</i> chronic exposures	143
6.2.3	Metabolite extraction, FT-ICR MS, data processing and putative peak identification	144
6.2.4	Statistical analysis	145
6.3	Results and Discussion	147
6.3.1	Chronic toxicant exposures of <i>Daphnia magna</i>	147
6.3.2	Metabolic effects of toxicant exposure	148
6.3.3	Effects of chronic toxicant exposure on the reproductive output of <i>D. magna</i>	151
6.3.4	Development of predictive multivariate models	154
6.3.4.1	Development of optimal predictive models using each toxicant	156
6.3.5	Discovery of biomarkers predictive of reduced reproductive output in <i>D. magna</i>	161
6.3.5.1	Potential biomarker of reduced reproductive output in <i>D. magna</i>	166
6.4	Conclusion	168
CHAPTER SEVEN: Final Conclusions and Future Work		169
7.1	The feasibility of FT-ICR MS-based metabolomics for toxicity testing using <i>Daphnia magna</i>	170
7.2	The FT-ICR MS-based metabolomics approach using <i>Daphnia magna</i> haemolymph	172
7.3	The discrimination of toxicant MOA via changes in the daphnid metabolome	174
7.4	The discovery of metabolic markers which are predictive of reduced reproductive output in <i>Daphnia magna</i>	177
7.5	Future work	180
7.6	Final conclusions	182
CHAPTER EIGHT: References		184
CHAPTER NINE: Appendix		207

List of Figures

	Page
Figure 1.1 Images of (a) an adult female daphnid and (b) neonates	23
Figure 1.2 Graphical representation of parthenogenetic reproductive lifecycle of <i>Daphnia magna</i>	24
Figure 1.3 The trade-off between analytical platforms and the objectives of metabolomics	28
Figure 3.1 Representative FT-ICR mass spectra of whole-organism extracts of 30 <i>D. magna</i> neonates in (a) positive ion and (b) negative ion mode	64
Figure 3.2 Summary of peaks detected in biomass optimisation study; (a) graphical depiction of unique and overlapping peaks and (b) total number of peaks detected with associated technical variability	66
Figure 3.3 PCA scores plot of <i>D. magna</i> biomass optimisation study	68
Figure 3.4 Dose-mortality relationship from an acute waterborne copper exposure of <i>D. magna</i> neonates	70
Figure 3.5 PCA scores plots of (a) negative ion and (b) positive ion data of <i>D. magna</i> neonate copper toxicity study	73
Figure 3.6 PLS-DA scores plots of (a) negative ion and (b) positive ion data of <i>D. magna</i> neonate copper toxicity study	75
Figure 4.1 Representative FT-ICR mass spectra of pooled haemolymph extracts of 3 <i>D. magna</i> adults in negative ion mode	100
Figure 4.2 Graphical depiction of the peaks detected in an FT-ICR mass spectrum of pooled <i>D. magna</i> haemolymph extracts	101
Figure 4.3 PCA scores plot from cadmium toxicity study of <i>D. magna</i> haemolymph	103
Figure 4.4 Section (m/z 265-295) of a representative negative ion FT-ICR spectrum of <i>D. magna</i> pooled haemolymph; highlighting putatively identified signals from inosine, uridine and palmitic acid	108
Figure 4.5 Summary model of sub-lethal cadmium toxicity in <i>D. magna</i>	110

Figure 5.1	PCA scores plots from analysis of FT-ICR mass spectra of <i>D. magna</i> (a) haemolymph and (b) whole organism homogenates following Cd exposure, (c) haemolymph and (d) whole organism homogenates following DNP exposure, (e) haemolymph and (f) whole organism homogenates following fenvalerate exposure, and (g) haemolymph and (h) whole organism homogenates following propranolol exposure.	127
Figure 5.2	PLS-DA scores plots depicting LV1 against LV2 for (a) haemolymph and (b) whole organism homogenates, and LV2 against LV3 for (c) haemolymph and (d) whole organism homogenates of <i>D. magna</i> exposed to each of four toxicants.	134
Figure 6.1	PCA scores plot from analysis of the negative ion FT-ICR mass spectra from the <i>D. magna</i> chronic studies following exposure to (a) Cd, (b) DNP and (c) Propranolol	150
Figure 6.2	Bar charts of the reproductive output of individual <i>D. magna</i> following 21 d exposure to (a) Cd, (b) DNP and (c) Propranolol	153
Figure 6.3	Correlation between measured and predicted reproductive output for individual daphnids, the latter derived from a PLS-R model and the metabolic signatures of individual daphnids following exposure to (a) Cd, (b) DNP and (c) propranolol	155
Figure 6.4	Plots of the ranked absolute regression vectors generated from the building of PLS-R models using metabolic and reproductive output data from individual <i>D. magna</i> following 21 d exposure to (a) Cd, (b) DNP and (c) Propranolol	158
Figure 6.5	Plots of the R^2 values of increasing numbers of peaks (ranked by absolute regression vector) incorporated into the building of PLS-R models using metabolic and reproductive output data from individual <i>D. magna</i> following a 21 d exposure to (a) Cd, (b) DNP and (c) Propranolol	159
Figure 6.6	Correlation between measured and predicted reproductive output for individual daphnids, the latter derived from an optimal PLS-R model and the metabolic signatures of individual daphnids following exposure to (a) Cd, (b) DNP and (c) propranolol	160
Figure 6.7	Venn diagrams depicting the common peaks from (a) the optimal PLS-R models of individual daphnids following exposure to Cd, DNP and propranolol and (b) the mean of 3 random permutations of the same data	163

List of Tables

		Page
Table 1.1	Summary of the OECD guidelines for toxicity testing in aquatic environments	7
Table 1.2	Summary of previously reported studies utilising metabolomics approaches in aquatic organisms	17
Table 2.1	Composition of media for culturing <i>D. magna</i>	43
Table 2.2	Composition of Bolds Basal Medium for culturing <i>C. vulgaris</i>	44
Table 2.3	Table of peaks used to calibrate negative ion spectra of <i>D. magna</i> haemolymph samples	51
Table 2.4	Table of peaks used to calibrate the positive and negative ion spectra of <i>D. magna</i> whole-organism homogenate samples	52
Table 3.1	Summary of the total number of peaks in the positive and negative ion datasets of <i>D. magna</i> neonates exposed to copper	71
Table 3.2	Summary of the top weighted peaks following PLS-DA of both positive and negative ion analyses of <i>D. magna</i> neonates exposed to copper	77
Table 3.3	Comparison of the PLS weightings and PCA loadings from the multivariate analyses of the <i>D. magna</i> neonate copper toxicity study; (a) negative ion and (b) positive ion data	80
Table 3.4	Summary of significantly changing amino acids and indicators of oxidative stress in <i>D. magna</i> neonates exposed to copper	85
Table 4.1	Summary of the total number of peaks in the dataset from pooled <i>D. magna</i> haemolymph extracts exposed to cadmium	102
Table 4.2	Summary of peaks detected in pooled <i>D. magna</i> haemolymph samples that change significantly upon cadmium exposure	105
Table 5.1	Results from 24 hr <i>D. magna</i> neonate acute toxicity study summarising the mean mortality rate for each nominal concentration	123
Table 5.2	Calculated LC ₅₀ values from 24 hr neonate exposures using PROBIT analysis	124

Table 5.3	Peaks identified in the FT-ICR mass spectra that directly related to parent toxicants. These were subsequently removed from the metabolic datasets prior to statistical analysis	125
Table 5.4	Summary of <i>p</i> -values from Student's t-tests of PC scores between control (n=10) and exposed (n=10) samples, for Cd, DNP, fenvalerate and propranolol	128
Table 5.5	Number of peaks that significantly changed concentration (FDR<0.05, relative to controls) and their proportion relative to the total number of peaks detected, following exposure to cadmium, DNP, fenvalerate and propranolol	129
Table 5.6	"Optimal model" and "permuted" classification error rates for each of the six exposure classes, and their mean value, for both haemolymph and whole organism homogenates of <i>D. magna</i>	136
Table 6.1	The total number of peaks detected and the proportion of peaks that significantly changed concentration (FDR<0.05) between the control and high dose groups, following chronic exposure of <i>D. magna</i> to cadmium, DNP and propranolol	151
Table 6.2	Summary of the common peaks the optimal PLS-R models of individual <i>D. magna</i> following exposure to cadmium, DNP and propranolol	164
Table 6.3	Summary of the common peaks the optimal PLS-R models of individual <i>D. magna</i> following exposure to cadmium, DNP and propranolol	165

Abbreviations

ANOVA	Analysis of Variance
BBM	Bolds Basal Medium
(c)DNA	(complementary) deoxyribonucleic acid
Cd	Cadmium
COMET	Consortium on Metabonomic Toxicology
DI FT-ICR MS	Direct Infusion Fourier Transform Ion Cyclotron Resonance Mass Spectrometry
DI(MS)	Direct Infusion (Mass Spectrometry)
DMSO	Dimethyl sulfoxide
DNP	2,4-dinitrophenol
FDR	False Discovery Rate
FT-ICR MS	Fourier Transform Ion Cyclotron Resonance Mass Spectrometry
GC-MS	Gas Chromatography - Mass Spectrometry
g-log	Generalised – log
GSH	Reduced glutathione
GST	Glutathione-S-transferase
HPLC	High Performance Liquid Chromatography
LC ₅₀	50% of the Lethal Concentration
LC-MS	Liquid Chromatography - Mass Spectrometry
MOA	Mode of Action
(m)RNA	(messenger) ribonucleic acid
MS	Mass Spectrometry

MT	Metallothionein
(n)ESI	(nano) Electrospray Ionisation
NMR	Nuclear Magnetic Resonance
OECD	Organisation for Economic Cooperation and Development
PCA	Principal Components Analysis
PLS-DA	Partial Least Squares Discriminant Analysis
PLS-R	Partial Least Squares Regression
q-RT-PCR	Quantitative – Reverse Transcription – PCR
QSAR	Quantitative Structure Activity Relationship
REACH	Registration Evaluation Authorisation and Restriction of Chemicals
RSD	Relative Standard Deviation
SFG	Scope for growth
SIM	Single Ion Monitoring
SNR	Signal to Noise Ratio
SSAT	Spermidine/Spermine N-acetyltransferase
TSCA	Toxic Substances Control Act
TYH	Tyrosine hydroxylase
US-EPA	United States - Environmental Protection Agency

CHAPTER ONE:
General Introduction

1.1 Introduction

The impact of both natural and anthropogenic stressors on ecosystem health is an international issue. Linking the adverse effects of these impacts in individual animals to their ecosystem-level consequences is a key challenge in regulatory risk assessment (Moore *et al.* 2004). Section 1.2 provides an introduction to the current regulatory testing practices for assessing ecosystem health and the limitations of these approaches, particularly their high cost, the lack of confidence in extrapolating from the individual to higher levels of biological organisation, and their inability to provide information on modes of toxicity. The relatively recent emergence of ecotoxicogenomics (transcriptomics, proteomics and metabolomics) has considerable potential for addressing these issues and providing a better mechanistic understanding of the ecotoxicology of known and emerging toxicants (Snape *et al.* 2004). The application of ecotoxicogenomics in relation to regulatory toxicity testing is discussed in Section 1.3. This thesis focuses on one particular area of ecotoxicogenomics; metabolomics, which provides a relatively non-targeted assessment of toxicity, measuring potentially several hundred metabolites and multiple pathways in a single experiment. An overview of metabolomics and its potential for use in regulatory toxicity testing is given in Section 1.4, with particular focus on using metabolomics as a high-throughput screening tool for prioritisation of chemicals in a tiered testing approach. In this thesis, the metabolomics approach is being applied to *Daphnia magna*, a freshwater invertebrate with many attributes that make it an ideal test organism; these are discussed in Section 1.5. As such, this species is used extensively in current regulatory ecotoxicological testing and has great potential as a test organism for ecotoxicogenomic investigations. The small sample size afforded by using

Daphnia as a test organism brings with it further challenges and the correct analysis platform needs to be utilised to maximise the potential of using metabolomics for regulatory toxicity testing. Section 1.6 details the various platforms available and highlights direct infusion mass spectrometry as being the most appropriate tool for sensitive, accurate and high-throughput analysis of such small samples. The various approaches to the statistical analysis, both multivariate and univariate, of metabolomics data used in this thesis are discussed in Section 1.7, with the selection of which approach to use dependent on the overall objective of the study. The aims of this research are outlined in Section 1.8.

1.2 Ecotoxicology and selection of test species

Until recently, risk assessment procedures have been directed towards the protection of human health. Now it is widely acknowledged that such procedures must also ensure the protection of the complex biotic communities in natural ecosystems (Moore *et al.* 2004). Ecotoxicology is the integration of ecology and toxicology (Chapman 2002) typically defined as the study of the effects of anthropogenic toxicants on ecological systems (Truhaut 1977). The basic test principles of ecotoxicology come from toxicology with experimental studies resulting in dose response relationships and the estimation of effect concentrations (Van Straalen 2003). The influence of ecology can be seen in the design of these tests where environmentally relevant exposure concentrations need to be employed and tested on ecologically relevant test species (Chapman 2002).

In terms of ecological risk assessment the ideal would be to test millions of organisms across all environments that may become exposed to the chemical being assessed (Breitholtz *et al.*

2006). Since this is an impossibility, and in order to make more accurate predictions on toxicity and inform subsequent regulations on chemical use and disposal, the species selected for testing should be the equivalent of a keystone species for the trophic level being assessed (Chapman 2002). The Organisation for Economic Cooperation and Development (OECD) have defined a series of toxicity tests for ecological risk assessment utilising several different keystone species' of plant and animal of both aquatic and terrestrial origin. These include plants and animals such as algae, *Daphnia*, earthworms, bees, fish and birds; the OECD recommended species for aquatic toxicity tests are listed as part of Table 1.1. There is now a need to balance the growing requirement for ecotoxicity data with animal welfare, maximising the knowledge output from limited testing with lower vertebrates in order to help reduce the future level of vertebrate use in routine ecotoxicity testing (Snape *et al.* 2004). Furthermore, one of the major objectives of the registration, evaluation, authorisation and restriction of chemicals (REACH), a recent European Union directive, is to reduce all vertebrate testing in regulatory risk assessment (REACH 2006). The need for the reduction in vertebrate testing helped direct the selection of *Daphnia magna* as the test organism for this research, a keystone invertebrate species in the freshwater ecosystem, discussed in Section 1.5.

1.2.1 Current approaches in regulatory ecotoxicological testing

The ultimate aim of ecological risk assessment is to provide sufficient information for decision-making with the purpose of protecting the environment from unwanted effects of chemicals (Breitholtz *et al.* 2006). Society is faced with the enormous task to assess

numerous chemicals and complex chemical mixtures while protecting many different species in, and the diversity of, ecosystems (Escher and Hermens 2002). The need for improved safety data from ecological risk assessments is continually increasing; the effects of new and existing chemicals along with the threat of emerging pollutants, such as human and veterinary pharmaceuticals, are all increasing demand for regulatory testing for ecological effects (Ankley 2008). In Europe, REACH was introduced in June 2007 to redress the differences between the assessment and regulation of new and existing chemicals and to facilitate the replacement of existing dangerous chemicals with improved new ones (REACH 2006). The Chemical Acts, introduced in Europe at the start of the 1980s, required all manufacturers of chemicals that entered the market from 1981 to release information on their potential risks to both human health and the environment, however the testing strategies employed were inflexible and tended to relate to production volume rather than the risk of the chemical (Ahlers *et al.* 2008). With REACH, the responsibility for chemical testing was passed to industry rather than the authorities, with the overall scope of REACH being to ensure a high level of protection to human health and the environment whilst enhancing competitiveness and innovation in the market (REACH 2006). Both new and existing chemicals are subject to the testing requirements detailed in REACH and minimum regulatory data requirements must be reached, however the system is flexible in substituting standard tests for equivalent information and a weight of evidence based approach, allowing the use of all information while providing common standards for risk assessment (Ahlers *et al.* 2008). In the United States over 80,000 chemicals are currently listed in the Toxic Substances Control Act (TSCA) Inventory and the majority of them have not undergone

extensive toxicological testing. The US Environmental Protection Agency (US-EPA) now needs to make decisions regarding these chemicals such as prioritisation either for further testing or the decision that no further testing is required (US-EPA 2004). Currently, chemical prioritization may be determined by several factors including production volume, exposure information, persistence, and consideration of quantitative structure-activity relationships (QSARs) where the assumption is that similar molecules will have similar activities (US-EPA 2004). The decision as to whether the substance in question requires further evaluation or not can be considered as the first level in a tiered-testing system. The higher tiers then use a suite of standardised toxicity testing strategies for assessing the potential hazards of chemicals that may enter the environment. These can generally be split into two main types of test; acute (short-term) or chronic (long-term). The OECD provides guidelines for both acute and chronic tests designed to be relevant to various ecosystems; Table 1.1 summarises those tests used for assessing the threat to aquatic ecosystems. These conventional approaches for assessing the toxicity of chemicals utilise endpoints such as mortality, reproductive dysfunction, impaired growth and behavioural effects (Ankley 2008; De Coen and Janssen 2003).

Table 1.1 Summary of the OECD guidelines for toxicity testing in aquatic environments; highlighting the recommended test species and a brief outline of the aims and endpoints of each test (OECD 2009).

Guideline	Recommended test species	Summary of test
Test No. 201: Alga, Growth Inhibition Test	Green alga: <i>Pseudokirchneriella subcapitata</i> , <i>Desmodesmus subspicatus</i> Diatom: <i>Navicula pelliculosa</i> Cyanobacteria: <i>Anabaena flos-aquae</i> , <i>Synechococcus leopoliensis</i>	To determine the effects of a substance on the growth of freshwater microalgae and/or cyanobacteria. Typically a 72 h acute toxicity test.
Test No. 202: Daphnia sp. Acute Immobilisation Test	<i>Daphnia magna</i> (preferred) Other <i>Daphnia</i> species can be used	To determine the concentration of substance at which 50% (EC ₅₀) of <i>Daphnia</i> neonates (<24 h old) become immobilized. Typically a 24-48 h acute toxicity test.
Test No. 203: Fish, Acute Toxicity Test	<i>Danio rerio</i> – zebrafish <i>Pimephales promelas</i> – fathead minnow <i>Cyprinus carpio</i> – common carp <i>Oryzias latipes</i> – Japanese medaka <i>Poecilia reticulata</i> – guppy <i>Lepomis macrochirus</i> – bluegill <i>Oncorhynchus mykiss</i> – rainbow trout	To determine the concentration of substance at which 50% (LC ₅₀) of fish will die. Typically a 96 h acute toxicity test with mortality levels recorded at 24, 48, 72 and 96 h.
Test No. 204: Fish, Prolonged Toxicity Test: 14-Day Study	As for guideline No 203	To determine lethal, other observed effects (e.g. behavioural) and no effect levels at set time points through the duration of this test. Typically a 14 day chronic study, although can be extended.
Test No. 210: Fish, Early-Life Stage Toxicity Test	<i>Danio rerio</i> – zebrafish <i>Pimephales promelas</i> – fathead minnow <i>Oryzias latipes</i> – Japanese medaka <i>Oncorhynchus mykiss</i> – rainbow trout <i>Cyprinodon variegatus</i> - Sheepshead minnow	To determine the lethal and sub-lethal effects of chemicals on the early life stages of the species tested. Parameters measured include; fish weight and length, as well as the observations of abnormal appearance, abnormal behaviour, hatching and survival Typically a chronic test, begun by placing fertilised eggs in the test chambers and is continued at least until all the control fish are free-feeding

Test No. 211: <i>Daphnia magna</i> Reproduction Test	<i>Daphnia magna</i>	To determine the effects of a test substance on the reproductive capability of <i>Daphnia magna</i> . Mortality of parents and number of living offspring per brood should be reported. Typically a chronic toxicity test of 21 d duration
Test No. 212: Fish, Short-term Toxicity Test on Embryo and Sac-Fry Stages	<i>Danio rerio</i> – zebrafish <i>Pimephales promelas</i> – fathead minnow <i>Cyprinus carpio</i> – common carp <i>Oryzias latipes</i> – Japanese medaka <i>Oncorhynchus mykiss</i> – rainbow trout	To determine lethal and sublethal effects of test substance on embryo and sac fry stages of fish, mortality and parameters such as abnormal growth should be reported. Typically an acute toxicity test beginning with the fertilised egg and terminated at sac fry stage.
Test No. 215: Fish, Juvenile Growth Test	<i>Oncorhynchus mykiss</i> – rainbow trout	To determine the effects of prolonged exposure of juvenile fish to test substance, reportable parameters include fish weight at end of test and observation of growth or behavioural abnormalities. Typically a chronic toxicity test lasting 28 days
Test No. 229: Fish Short Term Reproduction Assay and Test No. 230: 21-day Fish Assay: A Short-Term Screening for Oestrogenic and Androgenic Activity, and Aromatase Inhibition	<i>Danio rerio</i> – zebrafish <i>Pimephales promelas</i> – fathead minnow <i>Oryzias latipes</i> – Japanese medaka	To determine the endocrine activity of the test substance. Measurement of vitellogenin and secondary sex characteristics are used as biomarkers for endocrine disruption, monitoring of fecundity throughout the test is reported and gonads are preserved for histopathology. Typically a chronic test of 21 days performed using pairs of sexually mature males and spawning females.

1.2.2 Limitations of current strategies

Whilst the highest credibility in ecotoxicological testing will be derived from tests which measure mortality and reproductive or growth effects, as these can more easily be predictive of population effects (Chapman 2002), these whole organism exposures are expensive in terms of both time and resources, particularly when moving from acute to chronic tests (Ankley 2008). The bias in toxicity databases for acute data (typically lethality tests) reflects this and any extrapolations to chronic endpoints are not as reliable as the data generated from the time and resource expensive chronic toxicity tests. Therefore extrapolations frequently add uncertainty to any toxicity assessment (Preston 2002). This trend for acute toxicity testing offers little more than a means of ranking and comparing the toxicity of substances (Moore *et al.* 2004) and is of little use to ecotoxicologists and risk assessors (Preston 2002). Furthermore, these methods do not take into account any sublethal effects of exposure and whilst stress-induced changes at the population, community and ecosystem levels are the primary concern, they are generally too complex and far removed from the causative events to be of much use in developing tools for the early detection and prediction of the consequences of exposure (Moore *et al.* 2004). Over the past few decades biomarker techniques have become more popular in ecotoxicology, specifically looking for biochemical, physiological or histological indicators of exposure to toxic chemicals and substantial efforts have been made to try to incorporate them into ecological risk assessment (De Coen and Janssen 2003; Forbes *et al.* 2006). Biomarkers can be considered as measures of the initial changes caused by toxic exposure starting at the subcellular level (e.g. interference with molecular pathways) and ultimately leading to adverse effects at higher levels of biological

organization (De Coen and Janssen 2003). In principle, these early warning biomarkers should be capable of predicting reduced performance, impending pathology and damage to health (Moore *et al.* 2004). Hence biomarkers should be able to identify those organisms that have been, or are being, exposed to certain chemicals or that those organisms are suffering, or will suffer, future impairments of ecological relevance (Forbes *et al.* 2006). In fact there has been some success in the use of biomarkers in regulatory ecotoxicology, the discovery that tributyltin (TBT) causes imposex in gastropod molluscs has led to legislation banning the use of this substance as the active ingredient in anti-biofouling paints, with imposex now being used as the biomarker for organotin (in particular TBT) exposure (Evans and Nicholson 2000; Forbes *et al.* 2006). One of the best known biomarkers is the significant elevation of vitellogenin caused by exposure to estrogenic compounds which were discovered to be the causal agents of intersex (feminisation of male fish) in UK wild fish populations (Jobling *et al.* 1998). The success of this biomarker in determining exposure to endocrine disrupting chemicals has meant that it has been adopted into some regulatory ecotoxicological studies, such as the OECD tests 229 and 230 (Table 1.1 (OECD 2009)) which aim to determine if the test substance has endocrine disrupting properties. However, whilst the use of sublethal endpoints, such as biomarkers of toxicity, have increased our ability to detect stress responses at low toxicant concentrations (Preston 2002) they have failed to demonstrate their usefulness, especially in predicting population to ecosystem level effects, as indicated by their minimal incorporation into national and international risk assessment protocols (Forbes *et al.* 2006). Indeed, even the vitellogenin biomarker of exposure to endocrine

disrupting chemicals is only recommended as a “signpost” in ecological risk assessment for directing chronic exposure studies (Hutchinson *et al.* 2006).

One of the greatest limitations of all of these testing strategies is that they are restricted to looking only at whole organism effects or changes in single biochemicals and subsequently provide no detailed data about the underlying biochemical mechanisms of toxicity (Snape *et al.* 2004; US-EPA 2004). Knowledge of mode of action (MOA) is fundamental to improve the scientific basis of risk assessment (Breitholtz *et al.* 2006), it will improve our understanding of the effects of pollutants on ecosystems and also be useful in setting up predictive models and avoiding pitfalls in applied ecological risk assessment of chemicals (Escher and Hermens 2002). However, with the current strategies, hypotheses need to be made on the mode of action (MOA) of the test substance to decide which tests may be applicable; at present QSARs typically tend to be used to do this (Escher and Hermens 2002; Moore *et al.* 2004). Testing costs will become enormous, particularly if there is a time limit on completion as there is for REACH, where approximately 30,000 existing chemicals need to be registered by 2018 (Ahlers *et al.* 2008), so a better knowledge-based approach is needed (US-EPA 2004). Ecological testing and screening programs need to be more thorough, less costly and able to be implemented rapidly and the incorporation of the omics into regulatory toxicity assessment could provide an answer (Ankley 2008).

1.3 The potential of omics in regulatory ecotoxicological testing

Toxicogenomics is the study of the global response of a genome to a chemical and has three distinct categories: transcriptomics (mRNA expression), proteomics (protein expression) and

metabolomics (metabolite profiling) (Ankley 2008). When these methods are applied to ecotoxicology this can then be termed as ecotoxicogenomics (Snape *et al.* 2004). Rapid advances in ecotoxicogenomics may have significant implications for risk assessment and regulatory decision making (US-EPA 2004), particularly as screens for regulatory decision making such as prioritisation in first tier testing (Ankley 2008). The US-EPA Genomics White Paper (US-EPA 2004) has evaluated these technologies as having great promise to provide more mechanistic, molecular-based data for risk-based prioritization of stressors. Thus offering more efficient, potentially high throughput, and low cost alternatives to the tests EPA currently relies on for prioritization. The most significant impact of ecotoxicogenomics on ecological risk assessment would be better definition of MOAs allowing for enhanced resource utilisation and reduced uncertainty in regulatory decision making (Ankley 2008). Knowledge of the MOA increases confidence in extrapolating toxicity data between species (Bundy *et al.* 2009). It should be noted that ecotoxicogenomics will not fundamentally alter the risk assessment process, but is expected to serve as a more powerful tool for evaluating the exposure to and effects of environmental stressors (US-EPA 2004). The application of transcriptomic, proteomic and metabolomic technologies allows the expression profile of hundreds to many thousands of genes, gene products and metabolites to be generated simultaneously, providing for the first time a broad impression of how organisms or cells respond to a given stimulus (Snape *et al.* 2004). This type of data may allow for the development of gene, protein, or metabolite profiles that can advance the screening of individual chemicals and allow faster and more accurate categorization into defined classes according to their MOA (US-EPA 2004). The inability of current strategies to elucidate MOA of

toxicants is one of the greatest limitations; therefore exploration of omics techniques that have this capability is essential for the future of regulatory toxicity testing. Moreover, basal cellular structures and functions measured by omics technologies are highly conserved biological entities; therefore, a large number of toxic effects that target these basal functions are universal in all organisms and target tissues allowing for cross-species extrapolation (Escher and Hermens 2002), another process in which there is little confidence when using the current approaches. Metabolomics in particular closely reflects the actual cellular environment (Schmidt 2004).

1.4 Metabolomics

Metabolomics is the study of endogenous, low molecular weight metabolites and can be used to examine biological systems at several levels, including cellular, tissue, organ, or even whole organism (Lin *et al.* 2006; Viant 2007). The metabolome, describes the composition of these low molecular weight metabolites at the time of sampling, and includes compounds such as lipids, sugars, and amino acids that can provide important clues about the individual's health and a functional measure of cellular status at that moment in time (Lin *et al.* 2006; Schmidt 2004). One of the greatest advantages of metabolomics is that the metabolome is often the first to respond to anthropogenic stressors, where in some cases no changes in the transcriptome and proteome occur (Viant 2007). Metabolomics investigations can be designed as targeted studies looking for specific metabolite changes, although this requires some prior knowledge on the metabolic action of whatever toxicant is being tested. An alternative metabolomic approach is where the global metabolome is analysed, although

constrained by the efficiency and sensitivity of the techniques used to extract and detect the metabolites. This method is a relatively non-targeted approach where there is little, if any, prior selection of which metabolic components to measure, thus, a similar study design can be used in both a screening mode and one of mechanistic exploration (Keun 2006) This research aims to investigate the use of both targeted and global metabolomics approaches for both of these applications and thus assess its future potential in first-tier regulatory ecotoxicological testing.

1.4.1 Metabolomics in ecotoxicology

To date metabolomics has had its greatest impact in the pharmaceutical industry, particularly in preclinical toxicology, and is now recognised as an independent and widely used technique for evaluating the toxicity of drug-candidate compounds (Nicholson *et al.* 2002; Robertson 2005; Robertson *et al.* 2007). However, the application of metabolomics in assessing environmental health is still in its infancy (Lin *et al.* 2006; Schmidt 2004). In the broader scope of environmental research, metabolomics has been applied in several areas. One area is in determining responses to environmental stressors such as temperature in a variety of organisms including arabidopsis (Kaplan *et al.* 2004), fruit flies (Malmendal *et al.* 2006) and fish (Turner *et al.* 2007; Viant *et al.* 2003b). Another area is disease monitoring, where metabolomics has been successfully utilised to characterise liver tumours in the flatfish *Limanda limanda* (Southam *et al.* 2008; Stentiford *et al.* 2005) and withering syndrome in red abalone (*Haliotis rufescens*) (Viant *et al.* 2003a).

In ecotoxicology, metabolomics can be used to characterize and understand the metabolic or biochemical responses of an organism to toxicant exposure and such information is of particular value for the risk assessment of chemicals in the environment (Lin *et al.* 2006). Recently there have been numerous studies applying metabolomic techniques to this area of research. In the terrestrial ecosystem there have been a few ecotoxicological metabolomics studies that use vertebrate test organisms. Griffin *et al.* (Griffin *et al.* 2001) used metabolomics to determine the effects of arsenic exposure on the renal tissue of the bank vole (*Clethrionomys glareolus*) and wood mouse (*Apodemus sylvaticus*) reporting that metabolic changes in the bank vole following arsenic exposure could be linked to the observed tissue damage; no effects were seen in the wood mouse. Earthworms have been widely used for studying environmental pollution and toxicity and have been employed in several ecotoxicological metabolomics studies (Bundy *et al.* 2009). The earthworm *Eisenia foetida* is the standard terrestrial invertebrate for toxicity testing and McKelvie *et al.* (McKelvie *et al.* 2009) determined significant metabolic changes in this species after exposure to dichlorodiphenyltrichloroethane (DDT) and endosulfan, highlighting alanine as a potential biomarker in this instance. Bundy *et al.* (Bundy *et al.* 2002) found toxicant induced metabolic changes in the earthworm, *Eisenia veneta*, exposed to three different xenobiotic compounds (4-fluoroaniline, 3,5-difluoroaniline and 2-fluoro-4-methylaniline). Jones *et al.* (Jones *et al.* 2008) determined alterations to the normal metabolic profiles of the earthworm, *Lumbricus rubellus*, following exposure to pyrene, a polycyclic aromatic hydrocarbon, and Bundy *et al.* (Bundy *et al.* 2007) determined a metabolic effect correlated to zinc exposure in this species, from multiple geographical sites.

In the aquatic environment metabolomics has been used to study of the toxic effects of pesticides, endocrine disrupting compounds and other xenobiotics on fish of differing life stages (Bundy *et al.* 2009). The metabolic effects of ethinylestradiol, a synthetic estrogen, exposure have been reported for several fish species (Ekman *et al.* 2008; Katsiadaki *et al.* 2009; Samuelsson *et al.* 2006) with responses in context with previous knowledge of the effects of estrogens on fish. The effects of pesticides on the metabolomes of various fish species have also been studied (Viant *et al.* 2005; Viant *et al.* 2006a; Viant *et al.* 2006b). To date there has been a single reported study using metabolomics in algae investigating the effects of the phytotoxin, prometryn, to a unicellular green alga (Kluender *et al.* 2009). Table 1.2 presents a summary of the key findings from these investigations, providing information on the species being investigated along with the type of tissue or biofluid analysed, the metabolomics analysis platform utilised and the data analysis approaches. These studies serve to highlight the potential of metabolomics for use in regulatory screening and potential biomarker discovery as in each case a toxicant induced metabolic effect could be determined. Yet, despite *D. magna* being one of the most widely utilised aquatic test species, no metabolomics studies have been reported, a knowledge gap that this research aims to redress.

Table 1.2 Summary of previously reported studies utilising metabolomics techniques in ecotoxicological studies of aquatic organisms.

Species and sample type	Toxicant exposure	Metabolomics analysis platform	Data analysis approaches	Key metabolomics findings	Reference
Fathead minnow (<i>Pimephales promelas</i>) Liver tissue	17 α -ethynylestradiol (EE ₂) 10 or 100 ngL ⁻¹ 8 day exposure with 8 day depuration	¹ H NMR spectroscopy (800 MHz)	PCA PLS-DA	Determined a greater impact on exposed male fish, with metabolic profiles resembling those of female fish. Biochemical changes in male livers included metabolites involved in energetics, hepatotoxicity and potentially vitellogenin synthesis. Response trajectories revealed males could compensate during exposure and partially recover following depuration	Ekman <i>et al.</i> , 2008
Three-spine Stickleback (<i>Gasterosteus aculeatus</i>) Liver tissue	Ethinyl-estradiol (EE ₂) 0.1- 100 ngL ⁻¹ 4 day exposure	¹ H NMR spectroscopy (500 MHz)	PCA ANOVA	Determined a weak dose-response relationship. Possible decrease in glutamate and alanine although not statistically significant.	Katsiadaki <i>et al.</i> , 2009
Rainbow trout (<i>Oncorhynchus mykiss</i>) Blood plasma and plasma lipid extracts	17 α -ethynylestradiol (EE ₂) 0.87 or 10 ngL ⁻¹ 2 week exposure	¹ H NMR spectroscopy (600 MHz)	PCA PLS-DA	Determined minor toxicant induced changes between control and high dose. Specific metabolite changes were increased phospholipids and decreased alanine and choloesterol levels.	Samuelsson <i>et al.</i> , 2006

Japanese Medaka (<i>Oryzias latipes</i>)	Dinoseb	¹ H NMR spectroscopy (500 MHz)	PCA	Determined a significant dose response effect and toxicant induced metabolic changes correlated with reduced growth and abnormal development. Specifically, significant decreases were found in the levels of ATP, phosphocreatine, alanine and tyrosine, as well as an increase in lactate.	Viant <i>et al.</i> , 2006a
Embryos	50 or 75 ppb		ANOVA		
	14, 62 and 110 h exposures	¹³ P NMR spectroscopy (200 MHz)			
		HPLC-UV			
Chinook salmon (<i>Oncorhynchus tshawytscha</i>)	Dinoseb, Diazinon and Esfenvalerate	¹ H NMR spectroscopy (500 MHz)	PCA	Revealed both dose-dependent and MOA specific metabolic changes induced by exposure to all three pesticides	Viant <i>et al.</i> , 2006b
Eggs and alevins	Varying concentrations (ppb)	HPLC-UV	ANOVA		
	96 h exposure				
Japanese Medaka (<i>Oryzias latipes</i>)	Trichloroethylene	¹ H NMR spectroscopy (500 MHz)	PCA	Determined metabolic perturbations at all exposure levels and PCA revealed a dose-response relationship and indicated an energetic cost to TCE exposure.	Viant <i>et al.</i> , 2005
Embryos	0-175 mgL ⁻¹		ANOVA		
	7 day exposure				
Unicellular green alga (<i>Scenedesmus vacuolatus</i>)	prometryn	GC-MS	PCA	Determined a clear toxicant induced effect. Metabolite changes suggest an impairment of energy metabolism and carbohydrate synthesis and an activation of catabolic processes	Kluender <i>et al.</i> , 2009
	0.1 μmolL ⁻¹				
Hydrophilic and lipophilic extracts	0-14 h exposure time course				

In mammalian toxicology, metabolomic studies have typically analysed biofluids such as blood, plasma or urine (Lindon *et al.* 2000). Biofluids are attractive to study as they represent a single largely cell-free compartment within an organism, quite different from the complexity of whole organism homogenates, and yet their composition is intimately linked to the cellular (dys)function of the organs which they perfuse. The use of biofluids could provide a unique insight into toxicant effect, particularly in those organisms that are too small in size for individual organ sampling, such as *Daphnia*, or when the mode of toxicity is unknown and therefore the target organ cannot be known ahead of time. Nevertheless, few ecotoxicology studies, particularly the investigation of terrestrial and aquatic invertebrates, have exploited the benefits of biofluids. Bundy *et al.* (Bundy *et al.* 2001) identified potential biomarkers of 3-fluoro-4-nitrophenol toxicity in the coelomic fluid of earthworms (*Eisenia veneta*) using nuclear magnetic resonance (NMR) spectroscopy based metabolomics. Phalaraksh *et al.* (Phalaraksh *et al.* 1999) used a similar technique to detect and quantify 19 endogenous metabolites in haemolymph from larval stages of the tobacco hornworm (*Manduca sexta*), and in a subsequent study determined changes in these metabolites during hornworm development (Phalaraksh *et al.* 2008). An investigative study into withering syndrome in red abalone (*Haliotis rufescens*) revealed metabolic biomarkers in haemolymph that could distinguish healthy, stunted and diseased animals (Viant *et al.* 2003a). With a demonstrated potential to provide biochemical insight into invertebrate responses to toxicant exposure, larval development and disease, together with the advantages of analyzing biofluids discussed above, metabolomics studies of haemolymph from *D. magna* are clearly warranted as a potentially powerful approach for toxicity testing. Therefore, the feasibility of using *D.*

magna haemolymph for metabolomics toxicity studies and its capability in discriminating toxic MOAs is investigated in this thesis.

It has been recognized for some time that metabolomics has enormous potential to identify novel biomarkers of toxicity, with arguably the most important endpoint being in elucidating a mode of toxicity (Robertson 2005). This has been successfully demonstrated by The Consortium on Metabonomic Toxicology (COMET) (Lindon *et al.* 2005) which built a database of the urinary metabolic responses of rats to 80 model toxicants and then confirmed the ability of these responses to predict the main organ of toxicity, either liver or kidney (Ebbels *et al.* 2007). In ecotoxicology, few studies have been published that have addressed the question of whether chemicals with differing MOAs can be discriminated. In a study of the earthworm, *Lumbricus rubellus*, reported by Guo *et al.* (Guo *et al.* 2009), a multiple toxicant study using cadmium chloride, atrazine and fluoranthene, confirmed that the metabolic responses to sub-lethal doses of these toxicants can be distinguished, consistent with their distinct MOAs. In the aquatic environment metabolomics has also successfully been used to determine the exposure effects of three pesticides to Chinook salmon (*Oncorhynchus tshawytscha*) eggs and alevins, reporting both dose-dependent and MOA specific changes to the metabolome induced by these toxicants (Viant *et al.* 2006b). Clearly more ecotoxicological studies are needed to investigate the capability of metabolomics in distinguishing toxicant MOA, not least in ecologically relevant species such as *D. magna*. Consequently, this research contains an investigation into the capability of metabolomics in discriminating toxicant MOAs in *D. magna*.

Following the recent success in applying metabolomics to ecotoxicological testing it is believed that metabolomics will have an important future role in ecological risk assessment, but exactly how this will be achieved is currently being debated (Ankley 2008). The most likely applications include: (i) as a screening tool within a tiered testing hierarchy, specifically as an early screening tool for chemicals that might cause adverse chronic effects and thus prioritization for more extensive testing; and (ii) as a tool to elucidate the MOA of a toxicant, at the metabolic level, as part of a comprehensive risk assessment (Bundy *et al.* 2009). The huge potential for utilising metabolomic techniques in regulatory toxicity testing is the main driving force behind this research and as such the overall aim of this thesis is to develop and apply metabolomics to toxicity testing in *Daphnia magna*, the OECD recommended freshwater invertebrate test species.

1.5 *Daphnia magna*

Given that invertebrates account for at least 95% of all known animal species and are critical to ecosystem structure and function (Verslycke *et al.* 2007), an ideal test organism for freshwater ecosystems is *Daphnia magna*, commonly known as the water flea (Figure 1.1). *Daphnia magna* are small (typically < 3 mm), freshwater filter-feeding crustaceans and can be found in almost any permanent body of water (LeBlanc 2007; Tatarazako and Oda 2007). They occupy a key position in the aquatic food web; they are highly abundant grazers of phytoplankton and provide a crucial link between primary and secondary production by being a major dietary component of fish and invertebrate predators (Dodson and Hanazato 1995; Martin-Creuzburg *et al.* 2007; Tatarazako and Oda 2007). Since *Daphnia* are such a

critical species in the aquatic food web any adverse effects on this species could cause community or ecosystem-level responses (Flaherty and Dodson 2005) making them model representatives of the zooplankton for any form of ecological testing (Dodson and Hanazato 1995).

Its small size, high fecundity and short lifecycle makes *D. magna* the ideal test species for laboratory controlled experiments of environmental stressors as they are easy to culture and their reproductive strategy (parthenogenesis) reduces biological variability (Barata *et al.* 2005). Parthenogenetic reproduction, where females asexually produce genetically identical female offspring, is a system which allows rapid expansion of daphnid populations in times of resource abundance and it is known that daphnids can switch to a sexual mode of reproduction in response to environmental stress (Olmstead and Leblanc 2002; Tatarazako and Oda 2007) (Figure 1.2). Occurrences such as reduced day length, decreased food availability, temperature changes and toxicant exposure can all cause daphnids to undergo a period of sexual reproduction generating dormant, resting eggs encased in a protective ephippium, which will then hatch when conditions become more favourable; this allows the species to survive in a habitat that may become inhospitable (Olmstead and Leblanc 2002, 2003). Typically this is an overwintering strategy, although these dormant eggs can remain viable for decades (Brendonck and De Meester 2003).

(a)



(b)

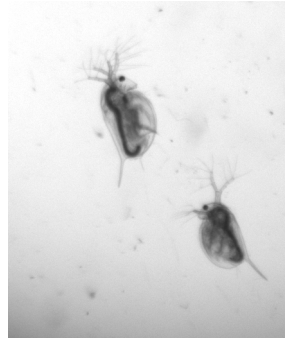


Figure 1.1 Images of (a) an adult female daphnid and (b) neonates from the *Daphnia* culture maintained at the University of Birmingham

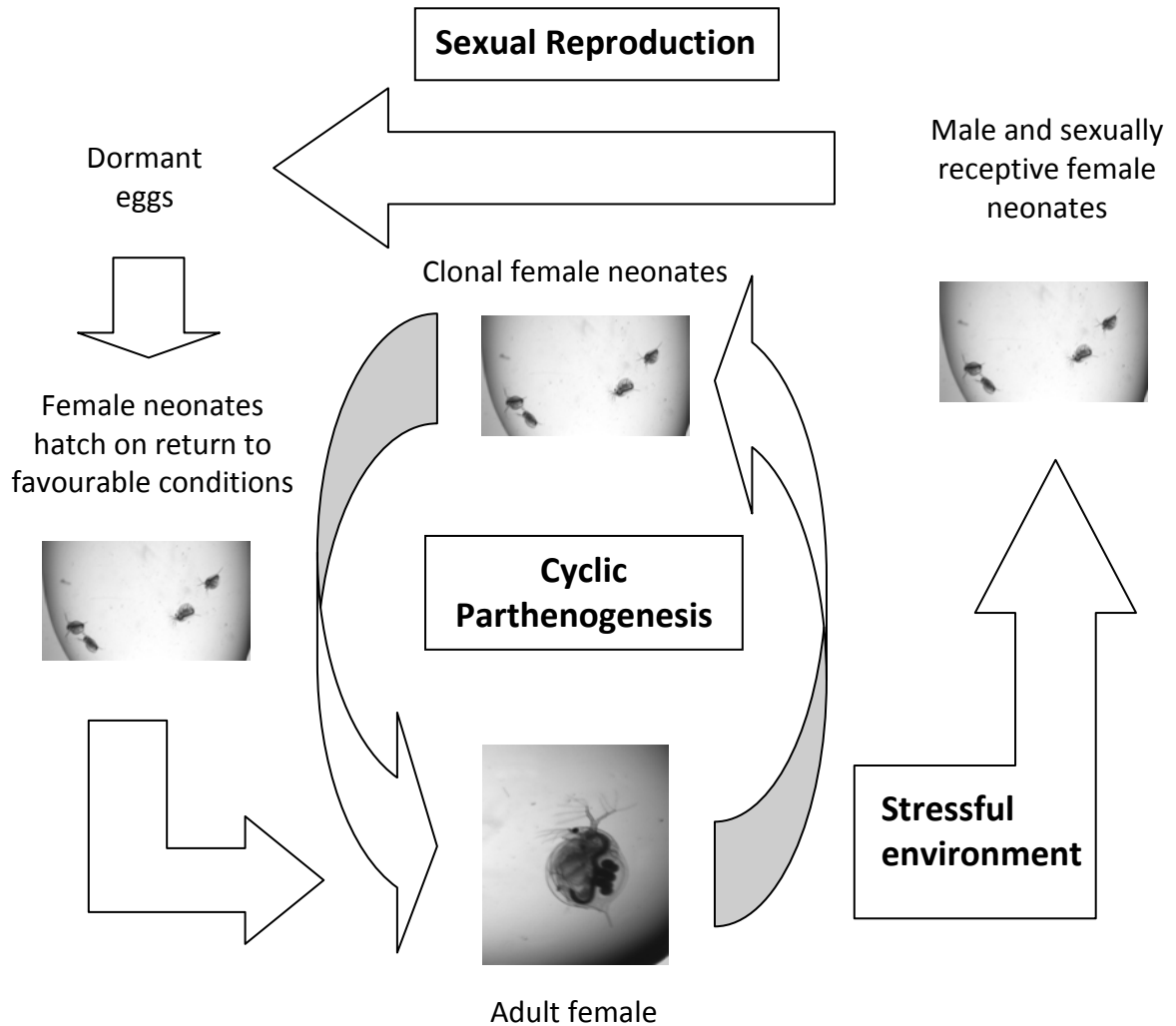


Figure 1.2 Graphical representation of parthenogenetic reproductive lifecycle of *Daphnia magna*. In favourable conditions *Daphnia* reproduce by cyclic parthenogenesis releasing genetically identical offspring. Under adverse conditions females release broods of males and sexually receptive females allowing for sexual reproduction, producing dormant eggs that will hatch when conditions return to normal.

1.5.1 *Daphnia magna* and regulatory toxicity testing

Water fleas have a long history in aquatic toxicity testing; they are known to be quite sensitive to many chemicals (Tatarazako and Oda 2007) and with their ease of handling in the laboratory, several methods using *D. magna* exist for regulatory toxicity testing (Tatarazako and Oda 2007). *D. magna* is the recommended test species for the OECD (OECD 1998, 2004) in their chemical testing guidelines and the current ecotoxicological requirements of directive 79/831/EEC for all new industrial chemicals are that acute toxicity tests must be carried out using fish and *Daphnia* (Sandbacka *et al.* 2000). It is an extensively used test species that has been found to be markedly more sensitive to a larger variety of stressors in toxicity tests than fish (Martins *et al.* 2007; Sandbacka *et al.* 2000) and has been used to evaluate the toxicity of many toxicants including heavy metals (Arambasic *et al.* 1995; Knops *et al.* 2001; Smolders *et al.* 2005) and pharmaceuticals (Flaherty and Dodson 2005). However, the majority of studies use the standard endpoints of acute and chronic toxicity discussed earlier and to date relatively few studies have been reported that utilise *D. magna* with ecotoxicogenomic approaches.

1.5.2 *Daphnia magna* and ecotoxicogenomics

Of the few studies reported that have utilised ecotoxicogenomic techniques with *D. magna* all of them have used transcriptomics, employing DNA microarrays to characterise changes in gene expression following exposure of *D. magna* to toxicants. Poynton *et al.* (Poynton *et al.* 2007) used a custom cDNA microarray to identify distinct expression profiles of *D. magna* in response to sublethal exposures of copper, cadmium and zinc, which supported the known

MOAs of these toxicants. Further microarray studies investigating the effects of short-term cadmium exposure on *D. magna* have also determined cadmium induced changes in gene expression and that these changes could potentially be linked to altered population growth rate (Connon *et al.* 2008; Soetaert *et al.* 2007b). Watanabe *et al.* (Watanabe *et al.* 2007) exposed *D. magna* to several different compounds finding chemical-specific patterns of gene expression which indicated that *Daphnia* DNA microarrays could be used for classification of toxicants. Other transcriptomic studies into the effects of ibuprofen (pharmaceutical) (Heckmann *et al.* 2008), propiconazole (pesticide) (Soetaert *et al.* 2006) and fenarimol (fungicide) (Soetaert *et al.* 2007a) on *D. magna* have all reported toxicant induced changes in gene expression profiles. In general, the goals were to reveal insight into the MOA, to discover biomarkers for hazard characterisation, and to classify toxicants using characteristic profiles of gene expression. Collectively these studies illustrate the emerging value of ecotoxicogenomics for toxicity testing and risk assessment and it is surprising that despite the importance of *Daphnia* in the freshwater ecosystem and the numerous advantages of ecotoxicogenomics techniques over standard test methods that so few studies have been reported. What's more, given the importance of the metabolome, it's even more surprising that at the beginning this research and at the time of writing this thesis no metabolomics studies (aside from those at the University of Birmingham) using *D. magna* had been reported.

1.6 Metabolomics analysis platforms

The key requirement in metabolomics is for analytical methods that can provide comprehensive metabolite profiles from complex biological samples (Lenz and Wilson 2007) and any technique capable of generating comprehensive metabolite measurements could, in theory, be used (Robertson 2005). Lenz and Wilson (Lenz and Wilson 2007) list criteria for the ideal analytical platform as needing to be: able to be performed directly on the samples, i.e. without the need for sample pre-processing; should be high-throughput and unbiased in respect to metabolite class; would be both highly and equally sensitive to all components in the samples; needs to be robust and reproducible with a wide dynamic range; and all this should be combined with enough information to allow the identification of key metabolites following post analysis multivariate statistics. In reality there is not a platform currently available that can provide all of these properties and there is a trade-off between technologies and objectives (Figure 1.3). Reproducibility is one of the key attributes required, therefore, the most useful techniques should be highly reproducible, this can be affected by variation introduced by sample preparation and analysis techniques so the platform used must generate data where this introduced variation is less than that found in the normal population of interest thus ensuring any significant metabolic changes are due to the biological status of the organism (Keun 2006; Robertson *et al.* 2007).

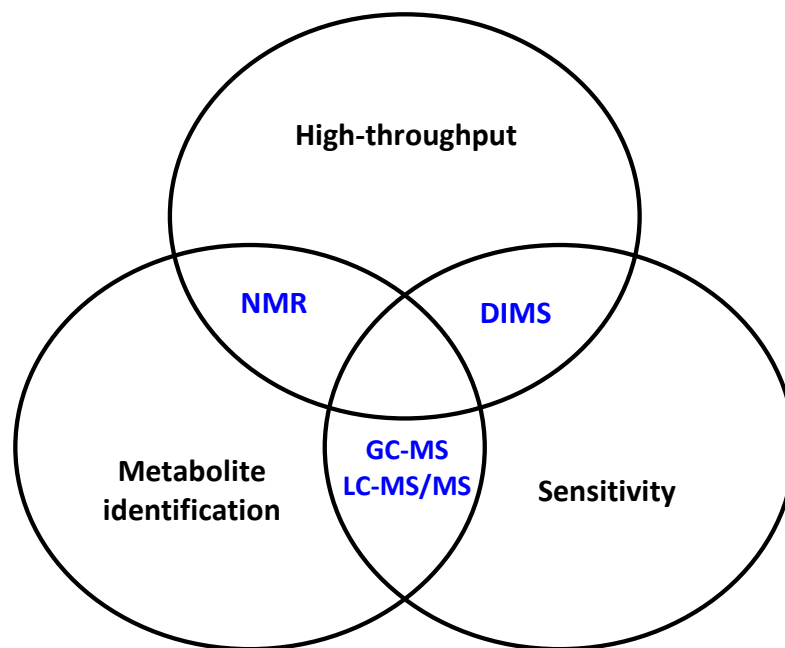


Figure 1.3 The trade-off between analytical platforms and the objectives of metabolomics, adapted from Dunn *et al.* (Dunn *et al.* 2005)

A successful metabolomics study should result in a high quality data set reflecting a biochemical snapshot of the state of an organism through its endogenous metabolites (Robertson *et al.* 2007); dependent on the objective of the study, it need not be a completely resolved and assigned survey of composition (Keun 2006). In fact, this is the simplest way to treat metabolomics data, producing a metabolic fingerprint that reflects the changes in metabolites without necessarily identifying the components that are changing (Robertson *et al.* 2007) allowing for rapid, high-throughput, unbiased sample analysis that can be used for screening purposes comparing and discriminating between samples of different biological status or origin (Dunn and Ellis 2005; Lin *et al.* 2006). The ultimate goal is to identify discriminating metabolites and a more powerful interpretation of metabolomics data is metabolic profiling, where a comprehensive (although this can be a targeted approach looking for pre-selected metabolites), and hopefully quantitative, list of metabolites can be identified in order to gain mechanistic information of biological processes and determine potential biomarkers of toxicity and disease (Dettmer *et al.* 2007; Lin *et al.* 2006; Robertson *et al.* 2007). Since this research aims to utilise metabolomics for both toxicity screening purposes and to elucidate information on modes of toxic action then a platform that can produce information for both applications is required. There are relatively few techniques capable of providing this required level of detail and currently the two most widely used platforms for metabolomics analysis are nuclear magnetic resonance (NMR) spectroscopy and mass spectrometry (MS) based methods, not least because both these techniques are able to detect a wide range of metabolites and provide a wealth of metabolic information

with relatively high reproducibility and sensitivity (Lin *et al.* 2006; Miller 2007; Robertson *et al.* 2007).

1.6.1 NMR spectroscopy

High-resolution (field strengths of 400MHz and higher) NMR spectroscopy has historically been the platform of choice for metabolomics studies; it is a cost-effective, robust and highly reproducible technique that can quantitatively report on a few to several tens of compounds in a single measurement with little or no sample preparation (Keun *et al.* 2002; Lenz and Wilson 2007). NMR works on the principle that certain atomic nuclei have the property of spin and magnetic moment; exposure to a strong magnetic field leads to splitting of their energy levels and absorption of radio frequency radiation that can be correlated with molecular structure (Skoog *et al.* 1998). Individual signals are dispersed dependent on the chemical environment of the source nuclei making NMR spectra rich in structural information and there are NMR visible isotopes for most chemical elements including ^1H , ^{13}C , ^{31}P and ^{15}N (Keun 2006). To date the most commonly used technique for generating metabolic profiles is ^1H NMR since hydrogen atoms are ubiquitous in organic molecules making this approach non-biased to particular metabolites, and with a natural abundance of 99.98% gives the highest relative sensitivity of all naturally occurring spin-active nuclei (Dunn and Ellis 2005; Keun 2006; Lenz and Wilson 2007). For these reasons ^1H NMR has become, and likely will continue to be, one of the primary choices in analytical platforms for metabolomics studies despite the fact that it is a relatively insensitive technique (Robertson *et al.* 2007). However, this lack of sensitivity means NMR requires larger sample sizes in order for metabolites of

interest to be within its limits of detection so is not the most appropriate tool for use with small organisms such as *D. magna*.

1.6.2 Mass Spectrometry

The major advantage of mass spectrometry techniques over NMR as a means of metabolic profiling is its vastly greater sensitivity (Keun 2006). MS platforms are able to achieve low detection limits enabling the detection of low abundance metabolites that are beyond the capabilities of NMR (Dettmer *et al.* 2007), and as such is the platform of choice for metabolomics studies that utilise small sample sizes and complex matrices (Brown *et al.* 2005). These attributes mean that MS technologies are the more appropriate choice of analytical platform for this research into metabolomics toxicity testing of *D. magna*, a small freshwater invertebrate. MS operates by separation and detection of ions according to their mass to charge (m/z) ratio and has the ability to provide rapid, sensitive and selective qualitative and quantitative analyses with the potential to identify metabolites (Dunn and Ellis 2005).

MS is often employed using front-end separation techniques such as gas chromatography (GC-MS) and liquid chromatography (LC-MS) (Robertson *et al.* 2007 1056) to enable better metabolite separation (and consequently identification and quantification) (Dunn *et al.* 2005). GC-MS detects volatile, low molecular weight metabolites by first separating them by GC then detecting the eluting compounds traditionally using electron-impact mass spectrometers, although the majority of metabolites, such as sugars and amino acids, need to be made volatile and thermally stable prior to analysis and such sample preparation can

introduce variability (Dunn and Ellis 2005; Lenz and Wilson 2007). LC-MS is simpler in terms of sample preparation as it does not require sample volatility; LC is the separation technique typically followed by electrospray ionisation (ESI) of the sample for MS detection (Dunn and Ellis 2005). However, metabolite detection by a mass spectrometer using ESI is limited by the ability of the metabolites to be ionised. Despite the benefits for metabolite identification, the use of hyphenated MS techniques increases preparation and analysis time per sample, making this a less cost effective technique particularly in terms of a high-throughput screening tool. Since one of the main objectives of this research is to evaluate the potential of using metabolomics as a potential first-tier screening tool for regulatory toxicity testing then a high-throughput method is an essential, thus making hyphenated MS techniques unsuitable for this purpose.

Direct injection mass spectrometry (DIMS) has been proposed as the answer to this problem; here crude samples are injected directly in to the ESI source of a mass spectrometer with no prior separation method, resulting in a mass spectrum representative of the composition of the sample being analysed (Lenz and Wilson 2007). This is a high-throughput approach with samples processed in typically a few minutes, the short analysis time potentially increasing sample reproducibility and improving the accuracy of subsequent data analysis (Dettmer *et al.* 2007). As with LC-MS, the ability of metabolites to be ionised determines the proportion of the metabolome that can be detected, but ESI can be conducted in both positive and negative ion modes to obtain the most comprehensive profile possible (Dunn and Ellis 2005; Lenz and Wilson 2007). Alongside this, ion suppression, which occurs when all components of the sample are introduced simultaneously into the ionisation source, has been greatly

decreased by the introduction of nano-electrospray ionisation (nESI) which reduces the flow rate at which the sample enters the ionisation source (Dettmer *et al.* 2007), though it should be noted that this does not completely remove the issue of ion suppression. The drawback with ESI techniques, however, is that metabolite identification is more time intensive; tandem MS (MS/MS) can be employed where fragmentation of molecular ions allows structural identification of metabolites from interpretation of fragment ions and fragmentation patterns (Dunn and Ellis 2005), yet this reduces the capability of DIMS to be useful as a high-throughput method. The use of high resolution instruments which allow accurate mass determination and are capable of fully resolving detected peaks for accurate calculation of their empirical formula can overcome this problem (Dunn and Ellis 2005; Keun 2006). Fourier transform ion cyclotron resonance mass spectrometry (FT-ICR MS) is one of the few techniques capable of the necessary mass resolution and accuracy required for this (Dunn *et al.* 2005).

1.6.3 FT-ICR MS

FT-ICR MS is a DIMS technique ideal for high-throughput analysis of complex mixtures; its performance characteristics include ultra-high mass resolution (values over 1,000,000 are possible but routinely 100,000), and high mass accuracy with average errors generally < 1 ppm (Brown *et al.* 2005; Dunn and Ellis 2005). Mass accuracy is simply the difference between the theoretical and measured mass of any peak relative to the theoretical mass of that peak. Mass resolution refers to the resolution of a single peak, expressed as the m/z value of that peak divided by the width of that peak at half its height, meaning that peaks

differing by the mass resolution yield distinguishable peaks (Breitling *et al.* 2006). In basic terms, this means that with a mass resolution of 1,000,000 the m/z value of an individual peak can be given to six decimal places, and peaks separated by this mass can be distinguished by the instrument. It should be noted that the higher the resolution, the larger the data files that subsequently need to be analysed (Breitling *et al.* 2006). This high-resolving power reduces the need for time consuming and costly chromatographic separations prior to MS analysis (Brown *et al.* 2005) and in principle would allow the resolution of millions of peaks, although the dynamic range of the instruments can prevent such performance (Breitling *et al.* 2006). Until recently the maximum reported dynamic range of FT-ICR MS platforms was 10,000, meaning components < 0.01% abundant, compared to the most abundant components, will not be observed (Brown *et al.* 2005). Southam *et al.* (Southam *et al.* 2007) developed an analysis method which increases dynamic range (to 16,000) whilst achieving a high mass accuracy (0.18 ppm). This approach collects multiple, narrow, overlapping spectra (termed windows), the windows are analysed by single ion monitoring (SIM) and then “stitched” together to form a complete “SIM-stitched” spectrum with a greater dynamic range, enabling the detection of both low and highly abundant metabolites. The high mass accuracy capabilities of FT-ICR MS means that metabolites can often be putatively identified by determining their elemental composition, i.e. $C_cH_hN_nO_oP_pS_s$ (Brown *et al.* 2005; Dettmer *et al.* 2007). If only the most common biological elements are permitted (carbon, hydrogen, oxygen, nitrogen, sulfur, and phosphate), only a finite number of combinations of atoms will give a match to an observed mass with a given degree of accuracy, although for larger molecules more alternatives

become chemically possible (Breitling *et al.* 2006). FT-ICR MS, and other high resolution MS platforms, have an important future in high-throughput metabolomics investigations (Dunn and Ellis 2005). FT-ICR MS is the analytical platform that has been selected for use in this research, coupled with the SIM stitching approach developed by Southam *et al.* (Southam *et al.* 2007), to maximise its potential in metabolite detection and therefore its ability to determine toxicant induced effects on the daphnid metabolome.

1.7 Metabolomics data analysis

Metabolomics data is intrinsically multivariate so typically necessitates multivariate analysis. The statistical tools chosen for metabolomics data analysis need to be selected according to the objectives of the study (Dettmer *et al.* 2007). If the aim of the study is sample classification (e.g. can control samples be distinguished from exposed samples) unsupervised methods such as principal components analysis (PCA) can be used (Dettmer *et al.* 2007). PCA has been widely used in metabolomics studies; it allows inherent clustering behaviour of samples to be ascertained with no *a priori* knowledge of sample class (Coen *et al.* 2008). Given that PCA does not use class information in construction of the model, it just attempts to describe the overall variation in the data (Wise *et al.* 2006). PCA breaks down the data into scores and loadings, scores reflect the relationship between individual samples whereas loadings indicate the relationships between the variables (peaks) (Robertson 2005; Wise *et al.* 2006). Principal components (PCs) describe decreasing amounts of variance in the data; that is PC1 accounts for the greatest variance, followed by PC2 then PC3 and so on (Robertson 2005). The number of PCs included in the PCA model is dependent on how best

to represent the variance in the dataset. All PC analyses use score plots (typically PC1 against PC2) to visually determine if there are any natural clusters (Robertson *et al.* 2007); these clusters allow for rapid identification of similar and dissimilar samples, indicating a common effect or mechanism (Keun 2006). Whilst scores plots visually highlight the similarities and differences between individual samples they give no mechanistic insight into their molecular basis (Robertson 2005).

If the aim of the study is to discover characteristic biomarkers between groups (e.g. peaks that distinguish between exposed and control groups), supervised classification methods such as partial least squares discriminant analysis (PLS-DA) can also be used (Dettmer *et al.* 2007). PLS-DA uses prior knowledge of sample class to maximise separation and derive predictive models based on the original data (Nicholson *et al.* 2002) and hence can be used to determine variables that directly discriminate between classes (Wise *et al.* 2006). Latent variables (LVs), which are similar to the PCs obtained from PCA, can be depicted as scores plots with LV1 representing the highest variation that discriminates between the sample classes, and the PLS-DA weightings (akin to PCA loadings) can be used as a feature selection tool for identifying discriminating peaks (Baldovin *et al.* 1996). As this is a supervised analysis, specifically looking for differences between the sample classes, the model must be cross-validated in order to prevent over-fitting of the data and allow accurate prediction of sample class. Cross-validation eliminates one or more samples (forming the test set) from the data, building the predictive model with the remaining samples (the training set), this model is then used for the classification of the samples in the test set; with the predictive capability of the model assessed by determining a classification error rate using the difference between

the true and predicted values of the test set (Baldovin *et al.* 1996). Alongside the cross validation, it is recommended that permutation testing is also performed. Here the data is randomly permuted, mixing up the class labels, which should then create models with a much higher classification error rate than the true models (i.e. those built using the correctly labelled data) and thus giving confidence in the predictive capabilities of the true models, if indeed they are robust. Examination of the loadings or weightings data can then determine which peaks are responsible for any separation seen in the scores plots but it is important not to interpret these as having any univariate significance (Robertson *et al.* 2007).

However, although metabolomics is in its nature multivariate, it is possible to utilise univariate analysis with the right approaches. Standard statistical p -tests (e.g. ANOVA, t-test) can be used to screen for peaks that change significantly, although due to the large size of the datasets generated by metabolomics, the measurement of multiple variables will induce a large number of false positives (Robertson *et al.* 2007). This means that when using a significance value of 0.05 that chance alone means 5% of peaks could be wrongly assigned as changing significantly (Benjamini and Hochberg 1995; Robertson *et al.* 2007). This false discovery rate (FDR) needs to be accounted for, which can be achieved by calculating a corrected significance level as described in Benjamini and Hochberg (Benjamini and Hochberg 1995). For an FDR of 5% the following calculation: $0.05 \times (p\text{-value of the peak}/\text{total number of peaks})$, creates an adjusted p -value; the peak is still considered to be changing significantly if the original p -value is smaller than the FDR adjusted p -value. Both multivariate classification techniques and FDR-corrected univariate statistics are employed in this thesis.

Finally, if the aim of the study is to relate the metabolic data to another set of measured variables (e.g. reproductive output) then multivariate regression analysis can be employed (Wise *et al.* 2006). Partial least squares regression (PLS-R) can be used to analyse metabolomics data, whilst simultaneously modelling another response variable; the metabolomics data are classed as predictors whereas the other measured variable(s) are classed as responses (Wold *et al.* 2001). PLS-R attempts to find factors that both capture the variance in the metabolomics data and achieve correlation with the response variable (Wise *et al.* 2006). Again, cross validation needs to be employed as with PLS-DA to prevent overfitting of the data (Wold *et al.* 2001). The quality of the regression model can be assessed after cross validation by comparing the measured and predicted values of the response variable (e.g. reproductive output); this generates an R^2 value that is indicative of how well the model might predict the response variable of unknown samples (Wise *et al.* 2006; Wold *et al.* 2001). To determine which metabolites are correlated to (i.e. predictive of) changes in the response variable a regression vector can be generated, and the highlighted metabolites can then, in theory, be putatively identified (Wise *et al.* 2006). Multiregression analyses are also employed in this thesis, for discovering molecular markers that are predictive of *D. magna* reproductive fitness

1.8 Research aims

Overall, the primary objective of this thesis research is to evaluate the potential of FT-ICR mass spectrometry based metabolomics for use in first-tier, regulatory toxicity testing using *Daphnia magna*; the specific aims of my research are:

1. To optimise an FT-ICR mass spectrometry based metabolomics approach using whole organism homogenates of *D. magna* and to validate the technique using copper as a model toxicant.
2. To optimise an FT-ICR mass spectrometry based metabolomics approach using *D. magna* haemolymph and to validate the technique using cadmium as a model toxicant.
3. To develop robust multivariate models that can discriminate toxicant modes of action in *D. magna* acute toxicity tests, utilising four model toxicants, and to evaluate whether the haemolymph or whole organism metabolome is better at discriminating toxicant mode of action.
4. To discover metabolic markers in individual *D. magna* exposed to model toxicants that are predictive of higher level biological effects, specifically reproductive output.

These aims are addressed in Chapters 3, 4, 5 and 6 respectively.

CHAPTER TWO:
Materials and Methods

2.1 Culturing of *Daphnia magna*

In accordance with OECD guidelines (OECD 1998, 2004), *D. magna* were cultured at a density of 20 animals per 1200 mL media (OECD-recommended ISO test media for exposures, including 0.002 mgL⁻¹ sodium selenite; Table 2.1) in a 16:8 hr light:dark photoperiod and temperature of 20 ± 1°C. Media was renewed twice weekly and supplemented with an organic seaweed extract: Marinure (Wilfrid-Smith Limited, Oakley Hay, UK). Cultures were fed on suspensions of unicellular green alga, *Chlorella vulgaris*, and supplemented by a daily amount of dried bakers yeast (Sigma-Aldrich, UK), described below. All cultures were initiated using third or fourth brood neonates aged <24 h old. Original animals were obtained from the University of Reading, having originated from the National Institute for Applied Chemical Research (IRCHA), France, and categorised as IRCHA Clone Type 5.

2.1.1 Preparation of nutritional supplement Marinure

To obtain a stock solution of Marinure, approximately 12 mL of Marinure was added to 1 L of deionised water and shaken vigorously until fully dissolved. A 1:10 dilution of this stock should measure an optical density of 0.800 ± 5% at 400nm; either more water or Marinure is added to the stock solution until this OD (1:10) is achieved. The prepared stock solution is then used in the culturing of *D. magna* and was replaced every 6 months. Marinure was supplemented with each media renewal in an age-dependent amount (3 mL <7 days old, 4 mL >7 days old).

2.1.2 Culture of *Chlorella vulgaris* algal stock

Chlorella vulgaris was cultured in Bolds Basal Medium (BBM) in an aerated system under photosynthetic light. A minimum of two *C. vulgaris* stocks were active at any time. BBM was prepared as detailed in Table 2.2, and autoclaved prior to use. Algal suspensions were alternately removed from these stock vessels in order to prepare as food for the daphnid cultures and the volume taken replenished with BBM.

2.1.3 Preparation of *Chlorella vulgaris* algal feed

A known volume of *C. vulgaris* was taken from one of the main culture vessels, in order to obtain the correct density of algae for the daphnids the OD (1:10) at 440nm required is 0.800. The algae was spun at 3000 rpm for 30 min at room temperature, the supernatant discarded and the algae resuspended in the calculated volume of deionised water to achieve the required density:

$$\text{Resuspension volume} = (\text{measured OD (1:10)} \times \text{volume of algae}) / 0.800$$

Algal feed suspensions were stored at 4 °C and kept for a maximum of two weeks before replacing with a fresh suspension. *D. magna* were fed daily with varying volumes of algae depending on age: <2 days old: 1 mL; 3-7 days old: 1.5 mL; >7 days old: 2 mL per culture vessel.

2.1.4 Preparation of Baker's Yeast

10 mg of dried baker's yeast was added to 100 mL of distilled water and dissolved using a magnetic stirrer. This was stored at 4 °C and replaced every two weeks. A volume of 0.5 mL per culture vessel was added daily to the daphnids.

Table 2.1 Media for *Daphnia magna* culturing and exposure, modified from OECD guidelines (OECD 1998, 2004).

Stock solutions		To prepare media add the following volumes of stock solutions to 1 litre water *
Substance	Concentration	
Calcium chloride CaCl ₂ ·2H ₂ O	11.76 gL ⁻¹	25 mL
Magnesium sulphate MgSO ₄ ·7H ₂ O	4.93 gL ⁻¹	25 mL
Sodium bicarbonate NaHCO ₃	2.59 gL ⁻¹	25 mL
Potassium chloride KCl	0.23 gL ⁻¹	25 mL
Sodium selenite Na ₂ SeO ₃	40 µgmL ⁻¹	50 µL

* Water of suitable purity with conductivity not exceeding 10 µScm⁻¹

Table 2.2 Bolds Basal Medium (BBM) for culturing of *Chlorella vulgaris*.

Stock solutions			Volume required to make up 1 litre BBM *
Substance	Weight	Volume	
di-potassium hydrogen orthophosphate (K ₂ HPO ₄)	1.875 g	250 mL	10 mL
Potassium di-hydrogen orthophosphate (KH ₂ PO ₄)	4.375 g	250 mL	10 mL
Magnesium sulphate (MgSO ₄ .7H ₂ O)	1.875 g	250 mL	10 mL
Sodium Nitrate (NaNO ₃)	6.250 g	250 mL	10 mL
Calcium chloride (CaCl ₂ .2H ₂ O)	0.625 g	250 mL	10 mL
Sodium Chloride (NaCl)	0.625 g	250 mL	10 mL
EDTA tetrasodium salt (EDTA - Na ₄) + Potassium hydroxide (KOH)	5.000 g 3.100 g	100 mL	1 mL
Ferrous sulphate (FeSO ₄ 7H ₂ O) Sulphuric acid conc. (H ₂ SO ₄)	0.498 g 0.1 mL	100 mL	1 mL
Boric acid (H ₃ BO ₃)	1.142 g	100 mL	1 mL
Zinc sulphate (ZnSO ₄ .7H ₂ O)	0.353	25 mL	0.1 mL
Manganese chloride (MnCl ₂ .4H ₂ O)	0.058	25 mL	0.1 mL
Copper sulphate (CuSO ₄ .5H ₂ O)	0.063	25 mL	0.1 mL
Cobaltous nitrate (Co(NO ₃) ₂ .6H ₂ O)	0.020	25 mL	0.1 mL
Sodium molybdate (Na ₂ MoO ₄ .2H ₂ O)	0.048	25 mL	0.1 mL

* After making up to 1 litre with deionised water pH must be 6.7 ± 0.3

2.2 Toxicity exposures and animal capture

Exposure to toxicants is described for each individual study in each Chapter. Capture of animals following exposures was dependent on the sample type to be analysed. For those experiments where whole organism homogenates were to be analysed capture of exposed animals was via filtration through a fine mesh gauze and then quickly transferred into a Precellys™ homogenisation tube containing ceramic beads (CK14; Stretton Scientific Ltd, UK), immediately frozen in liquid nitrogen, and transferred to storage at -80 °C prior to metabolite extraction (Section 2.3.1). This whole process took ca. 30-45 s per sample. Capture of exposed animals where haemolymph samples were to be analysed involved the immediate extraction of the haemolymph at the end of the exposure period; this is as detailed in Section 2.3.2.

2.3 Metabolite extraction

2.3.1 Whole organism homogenates

Metabolites were extracted from whole *D. magna* using the two step methanol:water:chloroform (2:2:1.8 final solvent ratio) protocol as described previously (Wu *et al.* 2008). Since the *D. magna* samples were of such low mass some modifications were made; all samples were assumed to weigh 10 mg wet mass and solvent volumes were increased. Each sample was homogenised in 320 µL methanol and 128 µL water (both HPLC grade) using a Precellys-24 ceramic bead-based homogeniser (Stretton Scientific Ltd, UK). Samples were then transferred to 1.8 mL glass vials before adding 320 µL chloroform (pesticide analysis grade) and 160 µL water, keeping the final solvent ratio as previously

described (Bligh and Dyer 1959; Wu *et al.* 2008). The biphasic mixture was centrifuged (1,500-g) and the upper (polar) and lower (non-polar) fractions were removed, each split into two equal volumes, and aliquotted into two 1.5 mL microcentrifuge tubes (polar fraction) and two 1.8 mL glass vials (non-polar fraction). Samples were then dried in a centrifugal concentrator (Thermo Savant, Holbrook, NY, USA) and stored at -80° C until FT-ICR analysis. For each individual experiment an “extract blank” was also prepared using identical methods except that no biological material was added to the solvents.

2.3.2 Haemolymph

Extraction of haemolymph from individual adult daphnids was as described in Mucklow and Ebert (Mucklow and Ebert 2003). Immediately following the end of exposure, each daphnid was placed on a clean microscope slide, rinsed with deionised water to remove any algae, then carefully blotted dry. Next the haemolymph of the daphnid was sampled by pricking the carapace close to the heart with a 21 gauge needle and collecting approximately 1 µL of the haemolymph that immediately seeped out using a micropipette (Mucklow and Ebert 2003). The haemolymph sample was immediately transferred to a microcentrifuge tube and stored at -80° C until metabolite extraction. Metabolite extraction occurred the evening prior to FT-ICR analysis. Due to the very small volume of haemolymph obtained only negative ion mass spectrometry analysis could be undertaken, so metabolite extraction was by the addition of 30 µL 80:20 methanol:water (both HPLC grade) containing 20 mM ammonium acetate to the sample and allowing for precipitation of proteins in the solvent overnight at -20° C. As for the

whole organism homogenate samples, for every study an extract blank was also prepared with no addition of haemolymph.

2.4 FT-ICR mass spectrometry

Dried polar extracts from the whole organism homogenate samples were resuspended in 30 μ L 80:20 methanol:water (both HPLC grade) containing 0.25% formic acid for positive ion analysis, or in 30 μ L 80:20 methanol:water containing 20 mM ammonium acetate for negative ion analysis. The non-polar extracts were not used in this research. The haemolymph samples were simply removed from the -20° C freezer on the day of analysis following overnight metabolite extraction (Section 2.3.2). All samples were then centrifuged at 5,000g for 10 minutes and 5 μ L aliquots of each sample were loaded into a 96-well plate in triplicate, covered with 20 μ m easy-pierce heat-sealing foil and sealed using a Thermo-sealer (Agbene, Epsom, UK). Samples were analyzed using a hybrid 7-T Fourier transform ion cyclotron resonance mass spectrometer (LTQ FT, Thermo Scientific, Bremen, Germany) equipped with a chip-based direct infusion nanoelectrospray ionisation assembly (Triversa, Advion Biosciences, Ithaca, NY). Nanoelectrospray conditions comprised of a 200 nL/min flow rate, 0.3 psi backing pressure, and +1.7 or -1.7 kV electrospray voltage (for positive and negative ion analysis, respectively), controlled by ChipSoft software (version 8.1.0, Advion Biosciences). Samples were analysed in triplicate using the SIM-stitching FT-ICR method from m/z 70 to 500, as reported previously (Southam *et al.* 2007). Parameters included an automatic gain control setting of 1×10^5 (to control the number of ions entering the FT-ICR detection cell) and a mass resolution of 100,000, and data was recorded for 5.5 min per

replicate analysis using Xcalibur software (version 2.0, Thermo Scientific). The “extract blanks” were also analysed in triplicate using identical methods.

2.5 Data pre-processing

Transient data from the FT-ICR detector (i.e., in the time-domain) were processed as described previously (Southam *et al.* 2007), including averaging of transients, Hanning apodisation, zero filling once, and application of a fast Fourier transformation, all using custom-written code in MATLAB (version 7, The MathWorks). Next, the SIM-stitching algorithm was applied (version 2.10, custom-written MATLAB code; (Southam *et al.* 2007)), which stitched together multiple SIM windows, rejected all peaks with a signal-to-noise ratio (SNR) below 3.5, and then internally calibrated each mass spectrum using a pre-defined calibrant list of known metabolites, listed in Tables 2.3 (haemolymph) and 2.4 (whole organism homogenates). At this stage of processing each replicate analysis (i.e., of a total of three per biological sample) consisted of a single list of peaks characterised by specific m/z and intensity values. A novel two-stage peak filtering algorithm was then applied to the dataset (Payne *et al.* 2009). The first stage, referred to as the “replicate filter”, retained only those peaks which appeared in at least 2 out of the 3 technical replicate mass spectra to help reject noise. Peaks were considered to arise from the same metabolite if they occurred within a 1.5 ppm spread along the m/z axis. This generated a single peak list per biological sample. Next, peaks in these lists that also occurred in the “extract blank” mass spectrum were either removed or retained if they were more intense in the “extract blank” versus biological sample dependent on a pre-defined ratio. The second stage of the peak filtering

algorithm, termed the “sample filter”, was used to further eliminate noise from the spectra and also to reduce the problem of missing values. Using the peak lists from the replicate filter (one per biological sample), the sample filter retained only those peaks which appeared in a defined percentage of the biological samples in the dataset (e.g., in at least 50% of all samples), using a defined (e.g. 2 ppm) spread along the m/z axis for defining unique peaks. This results in a matrix of peak intensities, where each row corresponds to a unique sample and each column to a unique peak, thus allowing for data comparison and the discovery of differentially expressed metabolites (Dettmer *et al.* 2007).

Inevitably the matrix resulting from the two-stage peak filtering algorithm has entities missing due to peaks only needing to be present in a pre-defined percentage of samples (typically 50%). Therefore a similar strategy as Sangster *et al.* (Sangster *et al.* 2007) was employed to replace the missing values by re-examining the original spectral data and selecting features (typically below the initial SNR threshold of 3.5) that occurred at the location of each missing peak. To minimise the impact of the variability of high intensity peaks, data normalisation and transformation was employed (Dettmer *et al.* 2007). Spectra were normalised using probabilistic quotient normalisation (PQN) where all peaks are individually assessed, allocated a normalisation scaling factor, and the median scaling factor is then used to normalise the entire spectra thus avoiding the use of highly variable peaks (Dieterle *et al.* 2006). Transformation of the data is intended to reduce the intrinsic variability of high intensity peaks relative to low intensity ones (Dettmer *et al.* 2007). Technical variation caused by sample preparation and detection means that the absolute intensity changes of highly abundant peaks are larger than those of lower abundance peaks and are

hence seen as more important in subsequent multivariate statistical analysis. Here we used a generalised-log (g-log) transformation to stabilise (i.e. “normalise”) technical variance across the peaks by reducing the intensity of highly abundant peaks and increasing the intensity of lower abundance peaks, effectively evening out technical variation across the samples and preventing highly abundant peaks from dominating any multivariate analysis (Parsons *et al.* 2007). The g-log transformation parameter, λ , was optimised using six technical replicate mass spectra of one biological sample (six adults individually extracted and then pooled to obtain enough biological material) in order to estimate technical variance and select an appropriate λ value for both positive and negative ion analysis (Parsons *et al.* 2007). The λ values calculated and used in this thesis were 5.8365×10^{-9} for positive ion data and 7.3097×10^{-11} for negative ion data. All of these data pre-processing steps result in the production of a final processed data matrix that can be used for statistical analysis.

Table 2.3 The empirical formula, ion form (i.e. molecular ion or adduct), and exact mass of each internal calibrant used to calibrate the negative ion (23 peaks) SIM-stitched spectra of *D. magna* haemolymph extracts.

Empirical formula	Ion form	Theoretical exact mass (Da)
C ₃ H ₇ NO ₂	[M-H] ⁻	88.04040
C ₃ H ₆ O ₃	[M-H] ⁻	89.02442
CH ₂ O ₂	[M+Ac] ⁻	105.01933
C ₂ H ₄ O ₂	[M+Ac] ⁻	119.03498
C ₅ H ₁₀ N ₂ O ₃	[M-H] ⁻	145.06187
C ₆ H ₉ N ₃ O ₂	[M-H] ⁻	154.06220
C ₉ H ₁₁ NO ₂	[M-H] ⁻	164.07170
C ₆ H ₁₂ O ₆	[M-H] ⁻	179.05611
C ₁₁ H ₁₂ N ₂ O ₂	[M-H] ⁻	203.08260
C ₉ H ₁₁ NO ₃	[M+ ³⁵ Cl] ⁻	216.04330
C ₆ H ₁₂ O ₆	[M+Ac] ⁻	239.07724
C ₁₆ H ₃₂ O ₂	[M-H] ⁻	255.23295
C ₉ H ₁₂ N ₂ O ₆	[M+ ³⁵ Cl] ⁻	279.03894
C ₁₀ H ₁₃ N ₅ O ₄	[M+ ³⁵ Cl] ⁻	302.06616
C ₁₈ H ₃₅ NO	[M+ ³⁵ Cl] ⁻	316.24127
C ₁₈ H ₃₅ NO	[M+ ³⁷ Cl] ⁻	318.23832
C ₁₈ H ₃₅ NO	[M+Ac] ⁻	340.28572
C ₂₂ H ₄₃ NO	[M+ ³⁵ Cl] ⁻	372.30387
C ₂₂ H ₄₃ NO	[M+ ³⁷ Cl] ⁻	374.30092
C ₂₂ H ₄₃ NO	[M+Ac] ⁻	396.34832
C ₂₂ H ₂₆ O ₆	[M+ ³⁵ Cl] ⁻	421.14234
C ₂₂ H ₂₆ O ₆	[M+ ³⁷ Cl] ⁻	423.13939
C ₂₂ H ₂₆ O ₆	[M+Ac] ⁻	445.18679

Table 2.4 The empirical formula, ion form (i.e. molecular ion or adduct), and exact mass of each internal calibrant used to calibrate the positive (27 peaks) and negative ion (22 peaks) SIM-stitched spectra of *D. magna* whole organism homogenate extracts.

Empirical formula	Ion form	Theoretical exact mass (Da)
Positive ion		
C ₃ H ₇ NO ₂	[M+H] ⁺	90.05495
C ₅ H ₉ NO ₂	[M+H] ⁺	116.07060
C ₅ H ₁₁ NO ₂	[M+H] ⁺	118.08625
C ₆ H ₁₃ NO ₂	[M+H] ⁺	132.10190
C ₅ H ₁₀ N ₂ O ₃	[M+H] ⁺	147.07642
C ₆ H ₁₄ N ₂ O ₂	[M+H] ⁺	147.11280
C ₅ H ₉ NO ₄	[M+H] ⁺	148.06043
C ₅ H ₁₁ NO ₂ S	[M+H] ⁺	150.05833
C ₆ H ₁₃ NO ₂	[M+Na] ⁺	154.08384
C ₆ H ₉ N ₃ O ₂	[M+H] ⁺	156.07675
C ₉ H ₁₁ NO ₂	[M+H] ⁺	166.08625
C ₆ H ₁₄ N ₄ O ₂	[M+H] ⁺	175.11895
C ₉ H ₁₁ NO ₃	[M+H] ⁺	182.08117
C ₁₁ H ₁₂ N ₂ O ₂	[M+H] ⁺	205.09715
C ₁₂ H ₂₄ O ₃	[M+H] ⁺	217.17982
C ₁₂ H ₂₄ O ₃	[M+Na] ⁺	239.16177
C ₁₂ H ₂₄ O ₃	[M+ ³⁹ K] ⁺	255.13570
C ₁₈ H ₃₆ O ₂	[M+H] ⁺	284.29479
C ₁₈ H ₃₆ O ₂	[M+Na] ⁺	306.27674
C ₁₂ H ₂₂ O ₁₁	[M+Na] ⁺	365.10543
C ₂₂ H ₂₆ O ₆	[M+H] ⁺	387.18021
C ₂₄ H ₃₈ O ₄	[M+H] ⁺	391.28429
C ₂₂ H ₂₆ O ₆	[M+Na] ⁺	409.16216

C ₂₄ H ₃₈ O ₄	[M+Na] ⁺	413.26623
C ₂₂ H ₂₆ O ₆	[M+ ³⁹ K] ⁺	425.13609
C ₂₄ H ₃₈ O ₄	[M+ ³⁹ K] ⁺	429.24017
C ₂₄ H ₄₇ NO ₇	[M+Na] ⁺	484.32447

Negative ion

CH ₂ O ₂	[M+ ³⁵ Cl] ⁻	80.97488
C ₃ H ₇ NO ₂	[M-H] ⁻	88.04040
C ₃ H ₆ O ₃	[M-H] ⁻	89.02442
CH ₂ O ₂	[M+Ac] ⁻	105.01933
C ₂ H ₄ O ₂	[M+Ac] ⁻	119.03498
C ₅ H ₁₀ N ₂ O ₃	[M-H] ⁻	145.06187
C ₅ H ₉ NO ₄	[M-H] ⁻	146.04588
C ₆ H ₁₂ O ₆	[M-H] ⁻	179.05611
C ₁₁ H ₁₂ N ₂ O ₂	[M-H] ⁻	203.08260
C ₆ H ₁₂ O ₆	[M+Ac] ⁻	239.07724
C ₁₆ H ₃₂ O ₂	[M-H] ⁻	255.23295
C ₁₀ H ₁₃ N ₅ O ₄	[M+ ³⁵ Cl] ⁻	302.06616
C ₈ H ₂₀ NO ₆ P	[M+Ac] ⁻	316.11668
C ₁₈ H ₃₅ NO	[M+ ³⁵ Cl] ⁻	316.24127
C ₁₈ H ₃₅ NO	[M+ ³⁷ Cl] ⁻	318.23832
C ₁₈ H ₃₅ NO	[M+Ac] ⁻	340.28572
C ₂₂ H ₄₃ NO	[M+ ³⁵ Cl] ⁻	372.30387
C ₂₂ H ₄₃ NO	[M+ ³⁷ Cl] ⁻	374.30092
C ₂₂ H ₄₃ NO	[M+Ac] ⁻	396.34832
C ₂₂ H ₂₆ O ₆	[M+ ³⁵ Cl] ⁻	421.14234
C ₂₂ H ₂₆ O ₆	[M+ ³⁷ Cl] ⁻	423.13939
C ₂₂ H ₂₆ O ₆	[M+Ac] ⁻	445.18679

2.6 Putative identification of empirical formulae and metabolites

Between zero and many potential empirical formulae ($C_C H_H N_N O_O P_P S_S$) were calculated for each of the experimentally detected peaks in the data matrix described above. This was achieved using a custom-written elemental composition calculator (Weber and Viant submitted) in which the number of occurrences of each element were restricted as follows: $^{12}C = 0-34$, $^1H = 0-72$, $^{14}N = 0-15$, $^{16}O = 0-19$, $^{31}P = 0-4$ and $^{32}S = 0-3$ (Kind and Fiehn 2007). In addition, since the observed peaks correspond to charged molecular ions or adducts of the neutral metabolites, the masses of the seven most common positive or negative ion adducts were effectively added to the elemental composition calculator. In practice, the calculation was conducted seven times for each positive ion peak (i.e. allowing for $[M-e]^+$, $[M+H]^+$, $[M+Na]^+$, $[M+^{39}K]^+$, $[M+^{41}K]^+$, $[M+2Na-H]^+$, $[M+2^{39}K-H]^+$) or seven times for each negative ion peak (i.e. allowing for $[M+e]^-$, $[M-H]^-$, $[M+^{35}Cl]^-$, $[M+^{37}Cl]^-$, $[M+Na-2H]^-$, $[M+^{39}K-2H]^-$, $[M+Ac]^-$, where Ac=acetate). Only those empirical formulae with an absolute mass error of <0.75 ppm were recorded, and then all potential formulae were filtered using four heuristic rules reported by Kind and Fiehn (Kind and Fiehn 2007), specifically: (1) restricted number of atoms per element, (2) Lewis and Senior rules, (3) H/C ratio, and (4) elemental ratio of N, O, P, and S versus C. Note that these rules were applied to the neutral metabolites following subtraction of the adduct; e.g. applied to $[C_5H_9NO_2]$ not to $[C_5H_9NO_2+Na]^+$. In some cases, the ^{13}C isotope of $C_C H_H N_N O_O P_P S_S$ was identified, allowing the approximate determination of the number of carbon atoms in the molecule based upon the intensity ratio of the ^{12}C and ^{13}C peaks.

The putative metabolite identity of each of the observed peaks was determined based upon accurate mass measurements, which was achieved using custom-written script (in Python and MySQL; by Ralf Weber, Centre for Systems Biology, University of Birmingham) and the Kyoto Encyclopedia of Genes and Genomes (KEGG) database (Kanehisa *et al.* 2006). First the KEGG LIGAND database was downloaded and the exact mass of each entry was re-calculated based on the associated empirical formula; this served to increase the mass accuracy to 6 decimal places. Then the exact mass of each entry (neutral compound) was modified to allow for the formation of all 14 adduct ions listed above. For example, the database record glucose (KEGG ID C00031, m/z 180.063390) was extended by different adduct masses such as m/z 203.052611 for $[\text{glucose}+\text{Na}]^+$, m/z 215.032792 for $[\text{glucose}+^{35}\text{Cl}]^-$, etc. Next the m/z values of all the experimentally observed peaks were compared to the modified KEGG data and matches with an absolute mass error of <0.75 ppm.

2.7 Statistical analysis

2.7.1 Multivariate statistics

For all multivariate statistics the metabolic data matrix used had previously been normalised and g-log transformed. PCA and PLS-DA were both employed in this thesis as multivariate classification techniques, using the PLS_Toolbox (v 4.21) in Matlab (Eigenvector Research, USA). PCA was used as an unbiased analysis to visually depict whether there was any separation between sample classes in each study. The number of PCs included in each model typically accounted for at least 60% of the total variance of the dataset. Scores plots were generated depicting two PCs plotted against each other (typically PC1 against PC2) allowing

rapid identification of clusters that indicate inherent similarities within the samples (Nicholson *et al.* 2002).

PLS-DA was used to maximise separation and derive predictive models based on the original data (Nicholson *et al.* 2002). A Y matrix was constructed containing sample class information, consisting of one variable for each class in the model, a value of 1 if the sample belongs to a class, or 0 if not (Coen *et al.* 2008; Keun 2006). By regressing against the Y matrix, latent variables (LVs) can be derived that separate the classes (Keun 2006). Cross-validation was employed to test the stability of the model (Rubingh *et al.* 2006) using a method known as venetian blinds. Here a pre-defined number of samples (square root of the total number of samples) were left out when building the model and then used to generate a classification error rate for each sample class. To determine the robustness of the predictive models, random permutations of the class labels (n=1000) were used to generate a mean permuted classification error for comparison with the real classification error. The number of LVs used in the model accounted for at least 50% of the total variation, and the scores plots (typically LV1 against LV2) allowed visualisation of similarities and differences between samples. Weightings data was used as a feature selection tool, in order to elucidate those peaks that discriminated between sample classes (Baldovin *et al.* 1996). For one investigation a multivariate regression technique, PLS-R, was used to link changes in reproductive output to metabolic changes and this is detailed in Chapter 6.

2.7.2 Univariate Statistics

The metabolomics data used for univariate statistical analysis were normalised but not g-log transformed. For each dataset either a Student's t-test or ANOVA, depending on the number of sample classes in the study, were applied to determine if any peaks were changing significantly. Due to the large number of tests being carried out a FDR of 5% was utilised to correct for any false positive results (Benjamini and Hochberg 1995). Following this the fold changes (between control and exposed groups) of these putatively identified significant peaks were calculated.

CHAPTER THREE:

**Optimisation and validation of FT-ICR MS based
metabolomics using whole organism homogenates of
Daphnia magna[†]**

[†]The contents of this Chapter, including the figures have been published in *Metabolomics*: Taylor, N. S.; Weber, R. J. M.; Southam, A. D.; Payne, T. G.; Hrydziuszko, O.; Arvanitis, T. N.; Viant, M. R. A new approach to toxicity testing in *Daphnia magna*: Application of high throughput FT-ICR mass spectrometry metabolomics. *Metabolomics*. **2009**, *5* (1), 45-58.

3.1 Introduction

Currently there is a surge of interest in developing toxicogenomic techniques, including transcriptomics, proteomics and metabolomics, to advance the screening of individual chemicals, allowing more rapid and accurate categorisation into defined classes according to their MOA, and thereby help to prioritise chemicals for further evaluation (Benson *et al.* 2007; US-EPA 2004). Furthermore, within the framework of tiered toxicity testing, toxicogenomic techniques may better direct the focus of resources within the higher tier tests (Ankley 2008).

As discussed in Chapter 1, *Daphnia magna* is a keystone species in the freshwater ecosystem that is extensively used as a toxicity test species and recently, several toxicogenomic studies of this species have been reported (Connon *et al.* 2008; Heckmann *et al.* 2008; Poynton *et al.* 2007; Soetaert *et al.* 2007a; Soetaert *et al.* 2007b; Watanabe *et al.* 2007). Although metabolomics is also recognised to be a powerful tool for investigating toxicity (Coen *et al.* 2008; Nicholson *et al.* 2002; Robosky *et al.* 2002), including in the field of aquatic toxicology (Ekman *et al.* 2008; Viant 2007; Viant *et al.* 2005; Viant *et al.* 2006b), no metabolomics studies of utilising *D. magna* have been reported.

This Chapter describes the application of FT-ICR MS based metabolomics for assessing toxic responses in *D. magna*. Specifically, the approach is a nESI DIMS technique that utilises the SIM spectral stitching method, which has been shown to detect over 3000 peaks in a liver extract of dab (*Limanda limanda*), a marine flatfish (Southam *et al.* 2007). FT-ICR is widely accepted to be one of the most powerful tools for the analysis of complex mixtures of

metabolites since it offers the highest mass accuracy and resolution of all mass spectrometers (Breitling *et al.* 2006; Breitling *et al.* 2008; Brown *et al.* 2005; Han *et al.* 2008). Here the effectiveness of DI FT-ICR MS metabolomics for toxicity testing in *D. magna* is evaluated. The initial aim was to optimise the daphnid biomass to extract and analyse by nanoelectrospray MS in order to detect a large number of metabolites with high reproducibility. This was optimised for both neonatal and adult *D. magna* since both life stages are used in OECD toxicity testing (OECD 1998, 2004). The second aim was to validate the metabolomics approach using copper as a model toxicant in an OECD 24-h acute toxicity test. The overall goal was to conduct the first steps in evaluating the effectiveness of high throughput, ultrahigh resolution mass spectrometry based metabolomics as a tool for screening and prioritising chemicals within tiered risk assessment.

3.2 Materials and Methods

3.2.1 Biomass optimisation study

To determine the optimal biomass of *D. magna* for FT-ICR mass spectrometry, varying numbers of adults (1, 2 and 5 animals) and neonates (10, 20 and 50) were analysed (n=3 replicates per group size). All animals were obtained from the *D. magna* culture, adults aged 14 days, and third brood neonates < 24 h old. Animals were captured and flash frozen as described in Chapter 2 and samples were stored at -80°C prior to metabolite extraction. The aim was to determine what biomass of *D. magna* was required to generate high quality mass spectra with a large number of peaks and low technical variation (i.e., high reproducibility) across the three replicate analyses of each biological sample.

3.2.2 Copper toxicity testing

To determine the appropriate copper concentrations for the acute toxicity study, an initial range-finding experiment was performed. Groups of 30 neonates (<24 h old) in 250 mL of clean media were exposed to increasing concentrations of $\text{CuSO}_4 \cdot 5\text{H}_2\text{O}$ (calculated as Cu^{2+} ions) for 24 h. Nominal concentrations of 0, 5, 10, 25, 50, 75 and $100 \mu\text{gL}^{-1}$ were used (n=5 test beakers per concentration). No food or supplements were provided during this exposure and any mortality after 24 h was recorded.

Subsequently, a more extensive acute copper exposure study was undertaken. Groups of 30 neonates (<24 h old) in 250 mL of clean media were exposed to nominal copper concentrations of 0, 5, 10, 25 and $50 \mu\text{gL}^{-1}$ for 24 h (n=6 per concentration). During the method optimisation studies it was discovered that the number of animals analysed by FT-ICR per exposure beaker must be kept constant (refer to Section 3.3.1). Since dead animals were not retained on the mesh gauze during filtering and therefore were not analysed, it was necessary to set up an additional exposure beaker for the highest concentration group ($50 \mu\text{gL}^{-1}$) to guarantee that at final sampling each of the six replicates comprised of 30 live neonates. Animals were captured and stored as described in Chapter 2.

3.2.3 Metabolite extraction and FT-ICR mass spectrometry

Metabolites were extracted from whole *D. magna* using the two-step methanol:water:chloroform protocol as detailed in Chapter 2. The dried polar extracts were resuspended in 30 μL of 80:20 methanol:water with the addition of either 0.25% formic acid for positive ion analysis or 20mM ammonium acetate for negative ion MS analysis. All

biological samples and extract blanks were analysed in triplicate in each ionisation mode by DI FT-ICR MS, utilising the SIM-stitching method, as described in Section 2.4.

3.2.4 Data processing and peak identification

The positive and negative ion MS data were treated as two separate datasets. As described in Section 2.5, data was processed, missing values filled in and then normalised and the g-log parameter applied. For the two stage filtering algorithm, the sample filter parameters consisted of peaks being retained if they occurred in 50% of all spectra using a 2 ppm spread along the m/z axis; i.e., the sample filter was applied across the entire dataset in an unbiased manner. Peaks that occurred in the extract blank were retained only if they were at least twice as intense in biological samples. Putative identification of peaks was as detailed in Section 2.6

3.2.5 Statistical analysis

Unsupervised multivariate analyses (PCA) were used to assess the metabolic similarities and differences between samples, and supervised analyses (PLS-DA) with cross validation (in a leave-5-out approach) were used to identify those peaks that tended to discriminate groups. To determine if any peaks were changing significantly, univariate analyses were employed (ANOVA across the 5 dose groups) with FDR <0.05.

3.3 Results and Discussion

3.3.1 Biomass optimisation study

The initial aim was to determine what biomass of *D. magna* was required to generate high quality mass spectra with a large number of peaks and low technical variation (i.e., high reproducibility) across the three replicate analyses of each biological sample. The dry mass of a single neonate ($7.46 \pm 0.27 \mu\text{g}$) and adult *D. magna* ($301 \pm 18 \mu\text{g}$) were determined. The group sizes of 10, 20 and 50 neonates and 1, 2 and 5 adults therefore corresponded to dry masses of 74.6, 149, 373, 301, 602 and 1505 μg , respectively. An FT-ICR analysis (in positive ion mode only) of these 6 group sizes, with n=3 replicate samples per group size was conducted. The mass spectra were processed using a 2 out of 3 replicate filter (for the 3 technical replicates per biological sample) followed by a sample filter that retained only those peaks that occurred in at least 66% of the samples (for each group size independently) generating a single peak list for each group. Representative FT-ICR mass spectra of the polar extracts from whole *D. magna* neonates, in positive and negative ion modes, are shown in Figure 3.1a and b respectively.

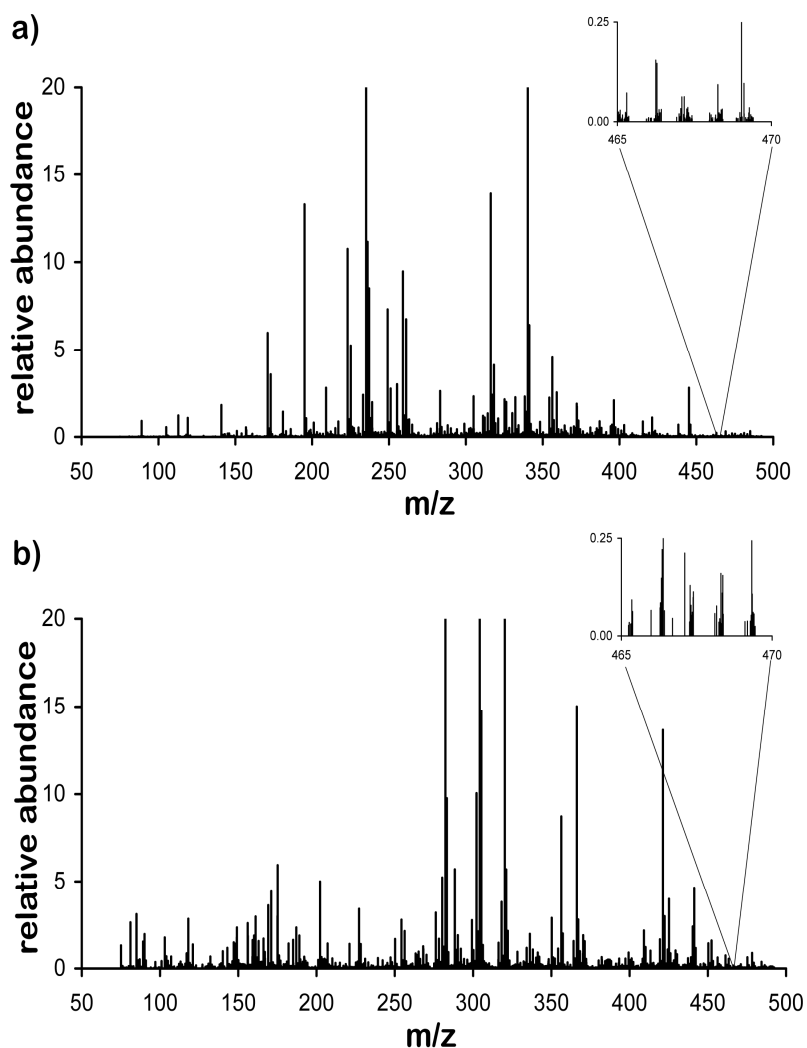


Figure 3.1 Representative FT-ICR mass spectra of whole-organism extracts of the water flea, *D. magna* (30 neonates, <24 h old): (a) SIM-stitched positive ion spectrum, in centroid mode, between m/z 70 and 500, and (b) corresponding negative ion spectrum of the same sample. These spectra were normalized to the largest peak (corresponding to 100% intensity). The insets show the mass range between m/z 465 and 470 using a 400-fold zoom on the intensity axis.

A software tool was developed (by Olga Hrydziusko, Centre for Systems Biology, University of Birmingham) to visualise which peaks were common (or not) across the extract blank and multiple biological mass spectra using the peak lists generated from the sample filter (Figure 3.2a). The peaks in the extract blank likely include contaminants from the air and compounds such as plasticisers that may leach from the plastic sample preparation tubes.

From Figure 3.2a it is evident that the majority of peaks occurring in the extract blank spectrum were suppressed as soon as biological metabolites from the daphnid extracts were present and able to compete for charge during nanoelectrospray ionisation. This is a clear demonstration of the finite dynamic range of the mass spectrometric detector.

Further examination of Figure 3.2a shows that as the biomass increased, up to a maximum of 5 pooled adults in a single extract, additional unique peaks were detected but at the expense of losing some peaks detected in the lower mass groups. To summarise this more clearly, Figure 3.2b shows the total peak count for each group size (with all extract blank peaks removed), as well as a measure of spectral reproducibility.

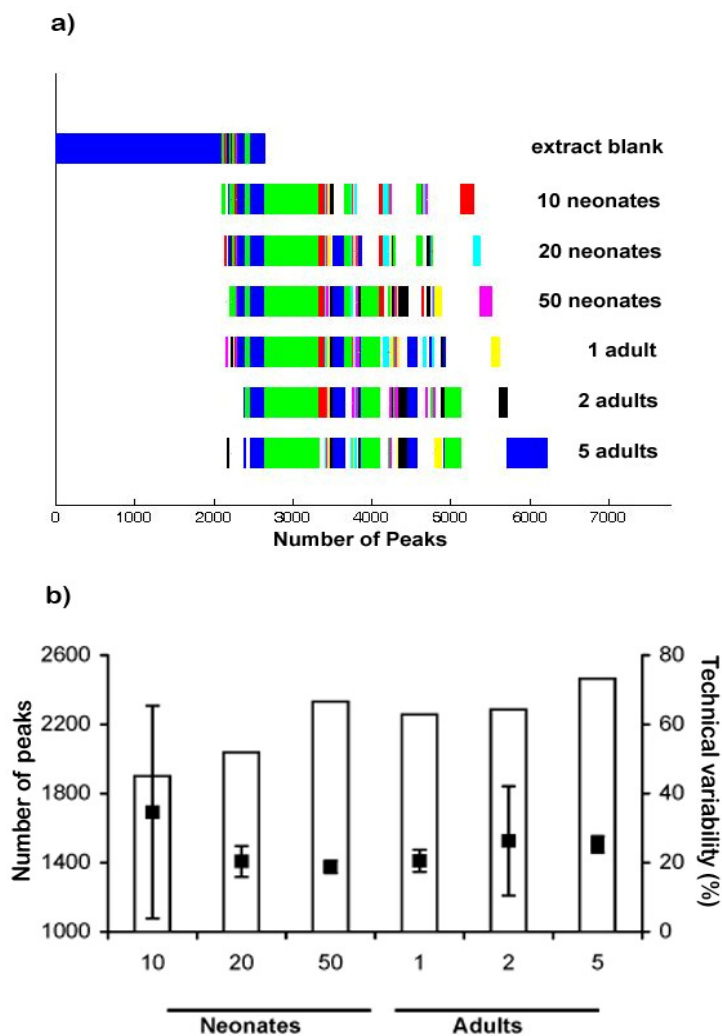


Figure 3.2 Summary of peaks detected in positive ion FT-ICR mass spectra of *D. magna* extracts in the biomass optimisation study. (a) Graphical depiction of the occurrence of each of the >6000 unique peaks that were detected by the FT-ICR analyses, i.e., whether the peaks occurred in the extract blank only (peaks 0 to ca. 2000 on the x-axis), in the extract blank and biological samples, or in the biological samples only. The shading is used to highlight which peaks are common to which samples. Peaks depicted in this figure are those which were present after a sample filter of 66%. (b) Total number of peaks detected in the six group sizes (with all blank peaks removed as described in main text). The secondary y-axis summarises the technical variability associated with each of the group sizes, specifically the mean \pm standard deviation, across the 3 biological replicates per group, of the median spectral RSD values (the calculation of RSD values is described in main text).

The reproducibility was determined by first calculating the relative standard deviations (RSDs) of the intensities of all the peaks that appeared in 3 out of 3 technical replicates per sample. The median RSD value was then used to represent the reproducibility for that mass spectrum, a parameter recently proposed as a valuable benchmark in metabolomics (Parsons *et al.* 2009). Figure 3.2b shows the mean of the 3 median RSD values (one RSD value per biological replicate). Considering the total peak counts, group sizes of 10 and 20 pooled neonates resulted in an apparent reduction in the number of peaks detected, whereas 50 neonates and 1, 2 or 5 adults yielded greater and more consistent numbers of peaks. The spectral reproducibility appeared largely independent of biomass analysed, with a single 10-neonate sample and 2-adult sample having unusually poor reproducibility, generating large error bars.

The biomass optimisation data was further analysed using PCA to visualise any metabolic differences between the 10, 20 and 50 neonate and 1, 2 and 5 adult group sizes. The scores plot (Figure 3.3) highlights three significant points. First, the three biological replicates per group size are relatively well clustered, as would be anticipated, providing a degree of validation to the FT-ICR metabolomics data acquisition and processing strategies. Second, there is separation of the neonatal and adult *D. magna* along the PC1-PC3 axis (t-test on PC1-PC3 scores, $p=5.95 \times 10^{-9}$), which is not surprising given the difference in developmental stages. This separation could also be affected by the gut contents of the adult daphnids at the time of sampling, whereas the neonates were not exposed to food prior to sampling. Third, and most importantly, the separation along PC1 (which accounts for 41% of the variance in the dataset) correlates well with the mass of *D. magna* that was extracted and

analysed. For example, 10 neonates (74.6 μg) have the largest PC1 score, the approximately equivalent masses of 50 neonates (373 μg) and 1 adult (301 μg) both have a PC1 score close to zero, and 5 adults (1505 μg) have the most negative PC1 score. The separation along PC1 is a highly statistically significant (ANOVA, $p=1.66\times 10^{-11}$, followed by a Tukey-Kramer post-hoc test that revealed significant differences between all combinations of the six group sizes except between 1 adult and 50 neonates, and between 10 and 20 neonates). This clearly illustrates that varying the biomass induces a noticeable change in the FT-ICR metabolic profile, as suggested by Figure 3.2a, and highlights the critical need to standardise the biomass per sample within a metabolomics study.

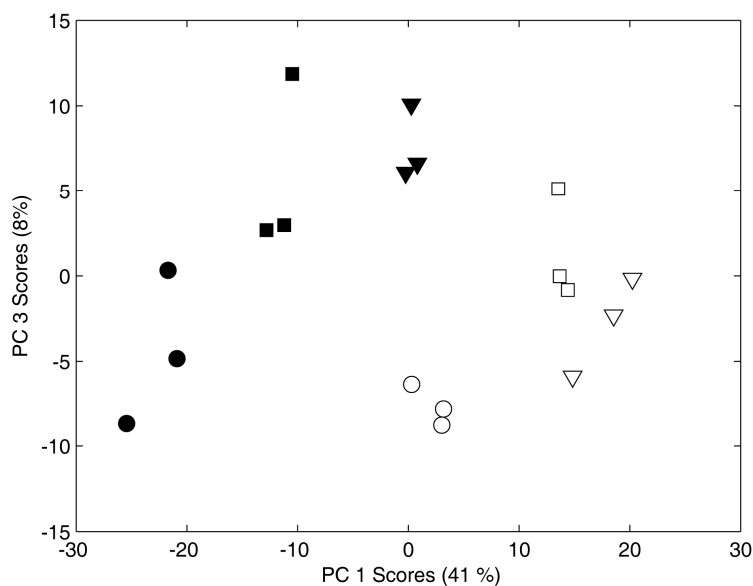


Figure 3.3 PCA scores plot from analysis of the positive ion FT-ICR mass spectra from the *D. magna* biomass optimisation study. Polar extracts from varying numbers of animals were analysed, each in triplicate: 10 neonates (∇), 20 neonates (\square), 50 neonates (\circ), 1 adult (\blacktriangledown), 2 adults (\blacksquare), and 5 adults (\bullet).

Considering all these results it was concluded that a *D. magna* sample of dry mass ca. 300 µg can be extracted and analysed in triplicate, yielding high quality spectra with a large number of peaks and low technical variation.

However, a practical requirement for high throughput toxicity testing is to minimise the number of animals per exposure group, in order to minimise the culture volumes and total number of daphnids required. Therefore all subsequent studies using *D. magna* neonates were conducted using 30 animals per sample and those studies using *D. magna* adults were conducted using a single individual per sample.

3.3.2 Acute copper range-finding study

An acute 24-h toxicity test of *D. magna* neonates (<24 h old) to increasing concentrations of copper was conducted in order to select appropriate exposure concentrations for the subsequent metabolomics study. The onset of mortality occurred at 50 µgL⁻¹ enabling an LC₅₀ of between 50 and 75 µgL⁻¹ to be determined (Figure 3.4). In order to minimise lethality, 50 µgL⁻¹ was selected as the highest dose for the metabolomics study.

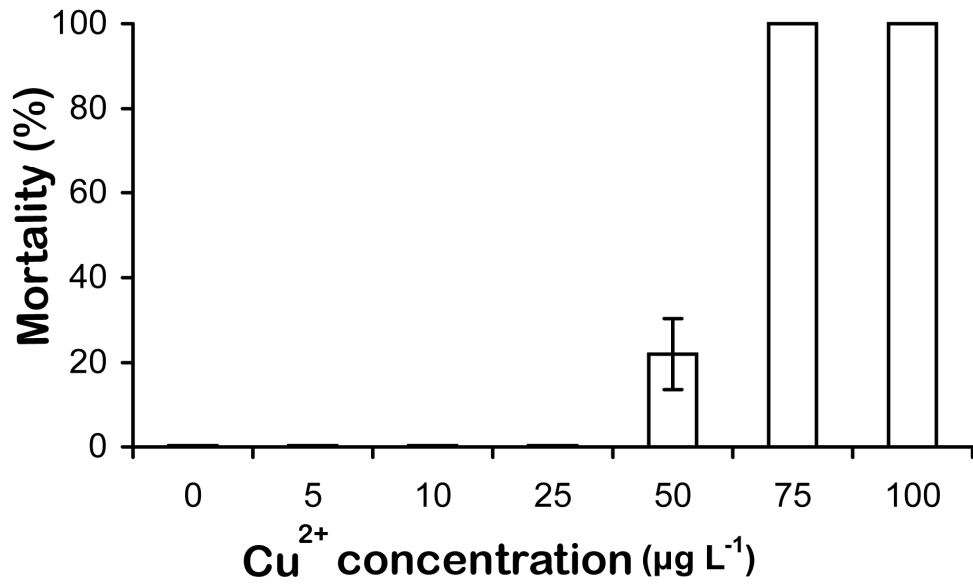


Figure 3.4 Dose-mortality relationship determined from an acute exposure of <24-h old *D. magna* neonates to waterborne copper. Data shows nominal metal concentrations.

3.3.3 Acute copper toxicity metabolomics study

Based upon the range-finding study, doses of 0, 5, 10, 25 and 50 μgL^{-1} were selected (n = 6 beakers, each containing 30 neonates, per dose). Additionally, since it was demonstrated in Section 3.3.1 that samples analysed by FT-ICR should have a similar biomass, an additional exposure beaker was added for the highest dose group so that there were sufficient animals for 30 live *D. magna* per sample. After 24 h, 7% mortality was observed at 50 μgL^{-1} (the dead animals were discarded, replaced with similarly-exposed live ones, and samples rapidly frozen) while no mortality was observed at 25 μgL^{-1} or below. FT-ICR analysis was conducted on all 30 samples, in positive and negative ion modes, and the spectra were processed as described. The total number of peaks comprised 1848 for positive ion and 3599 for negative ion mode (Table 3.1), giving a total of 5447 peaks.

Table 3.1 Summary of the total number of peaks in positive and negative ion datasets of *D. magna* neonate extracts, and the number of those peaks that could be assigned empirical formulae and putative metabolite identities.

Number of peaks	Negative ion	Positive ion	Total
Total (after replicate & sample filters)	3599	1848	5447
Assigned to ≥ 1 empirical formulae	3290	1478	4768
Assigned to unique empirical formula	231	675	906
Assigned to ≥ 1 KEGG LIGAND ID ^a	734	283	1017

^a Following removal of assignments in which the match was a non-endogenous metabolite such as a drug, plasticiser or pesticide.

PCA was then used to visualise any metabolic differences between the FT-ICR metabolic profiles of control and exposed animals. The PC scores plots for negative (Figure 3.5a) and positive (Figure 3.5b) ion data were consistent, both showing the 0, 5 and 10 μgL^{-1} exposed *D. magna* tending to cluster together, while the 25 and 50 μgL^{-1} groups occurred at higher PC scores. One sample did not fit this trend (sample 24, 5 μgL^{-1} group), which was evident in both the positive and negative ion analyses. The overall differences between the metabolic profiles were confirmed to be significant via ANOVAs of the PC scores. Specifically, significant separation of exposure groups occurred along PC1 ($p=8.94\times 10^{-3}$) and PC1+PC2 ($p=7.76\times 10^{-6}$) for the negative ion data (Figure 3.5a), and along PC2 ($p=3.08\times 10^{-2}$) and PC2+PC3 ($p=9.06\times 10^{-4}$) for the positive ion data (Figure 3.5b). Subsequent post-hoc tests (Tukey-Kramer) performed on both the negative (PC1+PC2) and positive (PC2+PC3) ion data identified that there was a significant difference between the 0, 5 and 10 μgL^{-1} doses compared to the 25 and 50 μgL^{-1} doses, but no significant differences within these two groupings.

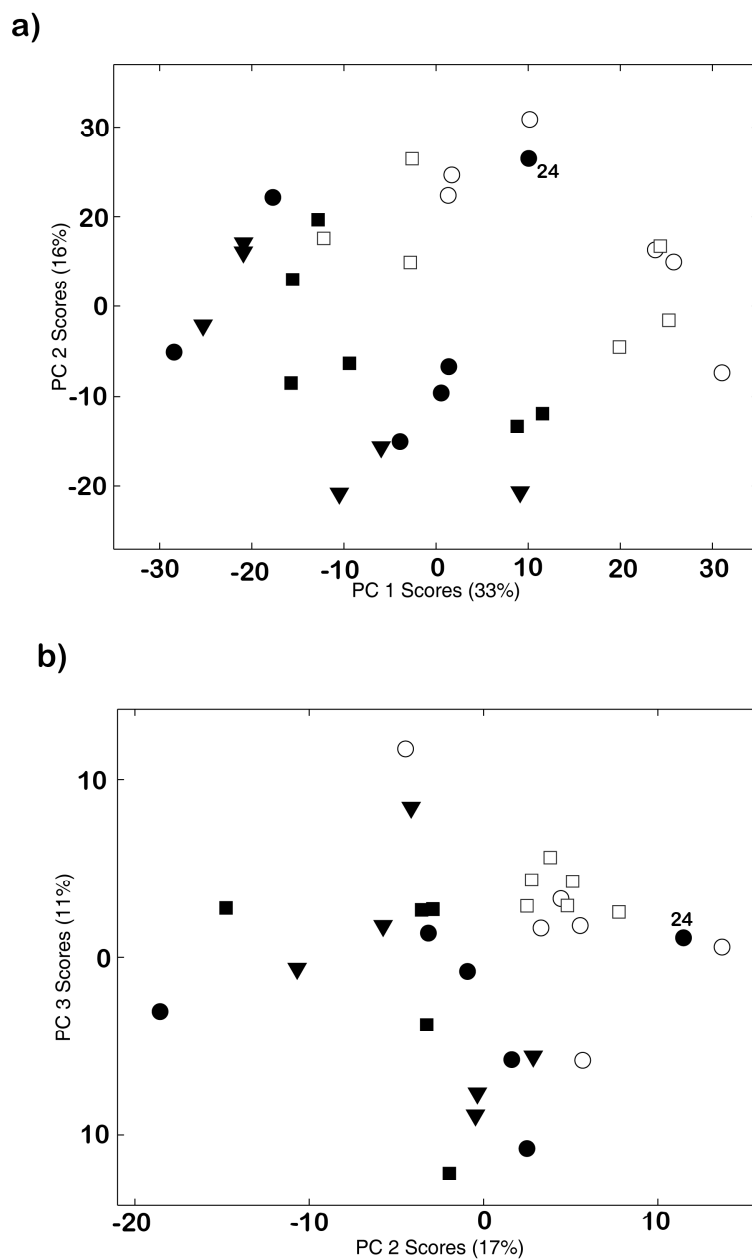


Figure 3.5 PCA scores plots from analysis of (a) negative ion, and (b) positive ion FT-ICR mass spectra of whole organism extracts of *D. magna* neonates that were exposed to a series of copper concentrations: 0 (\blacktriangledown), 5 (\bullet), 10 (\blacksquare), 25 (\circ) and 50 (\square) μgL^{-1} . Both scores plots show a dose-dependent metabolic response to copper along the diagonal axis, from the bottom left to top right. Sample 24 consistently appears as an outlier in both datasets.

The next step was to discover which peaks were responsible for the separation in multivariate space. Therefore, based upon the results of the post-hoc tests, the treatments were reclassified: the 0, 5 and 10 μgL^{-1} treatments termed as “no effect” and the 25 and 50 μgL^{-1} treatments termed as “effect”, then conducted PLS-DA on this 2-class dataset (n=18 and 12 in “no effect” and “effect” classes, respectively). This strategy was used since the existing 5-class dataset, with n=6 per class, would be highly susceptible to over-fitting in a supervised analysis. Even with sample sizes of n=18 and 12 there is the potential for over-fitting. As expected, the separation of the “no effect” and “effect” classes in the PLS scores plots (Figure 3.6) improved upon the PCA results, though this alone provides relatively little new information (Westerhuis *et al.* 2008). However, the PLS models were internally cross-validated, achieving classification error rates of 6.94% and 2.78% for positive and negative ion data, respectively. Furthermore, when the class labels were randomly permuted the classification error rates increased to between 40 and 65%, giving us still greater confidence in the real PLS models. Note that the aim was not so much to build predictive models of copper toxicity, but rather to use PLS as a feature selection tool to find those peaks that distinguished the “no effect” and “effect” classes (Baldovin *et al.* 1996).

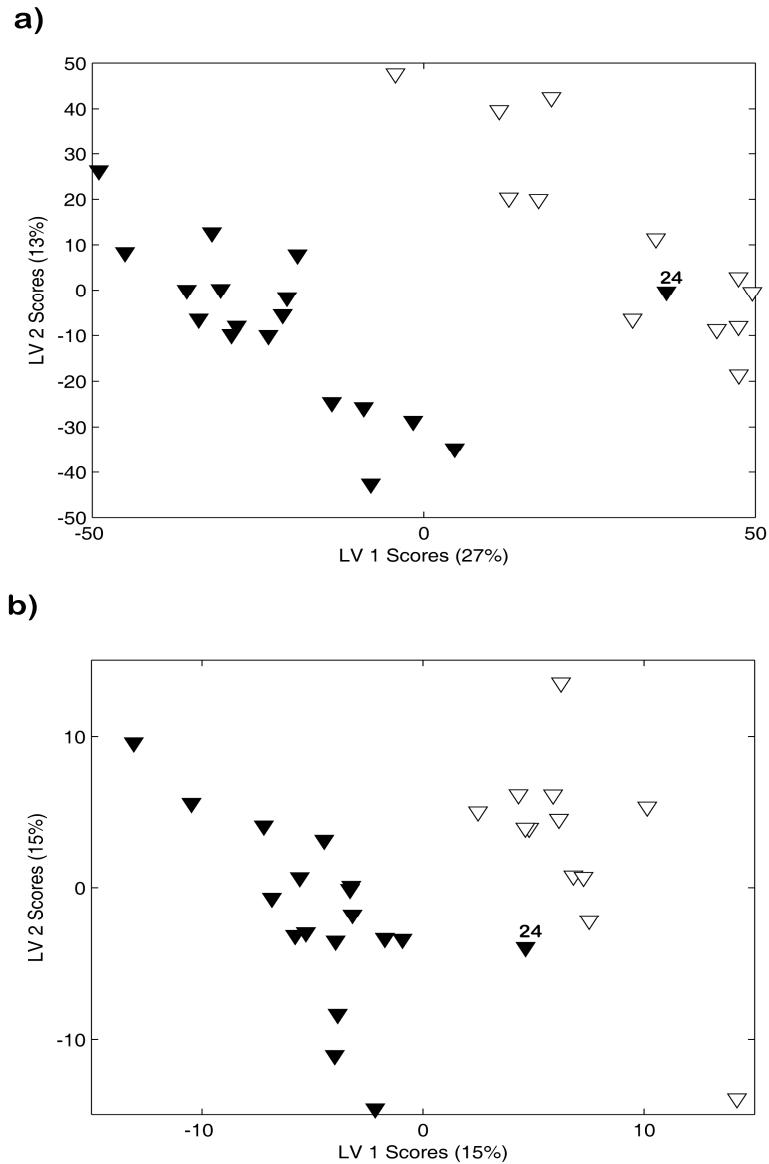


Figure 3.6 PLS-DA scores plots from analysis of (a) negative ion, and (b) positive ion FT-ICR mass spectra of whole organism extracts of *D. magna* neonates that were exposed to a series of copper concentrations. Based upon statistically significant findings from unsupervised PCA of the same data, the 5 concentration groups were re-categorised as either “no effect” (▼; 0, 5 and 10 μgL^{-1}) or “effect” (▽; 25 and 50 μgL^{-1}). Both scores plots show a dose-dependent metabolic response to copper along the LV1+LV2 diagonal axis, and the cross-validated PLS models yielded classification error rates of 6.94% and 2.78% for positive and negative ion data, respectively. Sample 24 consistently appears as an outlier in both datasets.

Next the absolute values of the LV1 weightings were ranked for both the positive ion and negative ion analyses. In addition, to check that these top weighted peaks did in fact change intensity in response to copper toxicity, all 1848 peaks in the positive ion dataset and 3599 peaks in the negative ion data were examined using univariate statistics. Ten of the top 12 LV1 weightings from the positive ion dataset corresponded to peaks that changed significantly with copper exposure. Similarly, for the negative ion data, 10 of the top 16 LV1 weightings were significant. The top weighted peaks that were also significant (with $FDR < 0.05$) are listed in Table 3.2, for positive and negative ion data, along with their associated p-value and fold-change between the control ($0 \mu\text{gL}^{-1}$) and highest dose ($50 \mu\text{gL}^{-1}$) groups. To justify the use of these supervised analyses in this study, even when some separation of classes was evident in the unsupervised PCA, we compared the peaks with the top LV weightings with those with the top PC loadings (from the PLS-DA and PCA models described above, respectively). Table 3.3 shows that the two approaches found similar peaks for the negative ion data, but that this was not the case for the positive ion data for which the PLS-DA found many more highly ranked significant peaks.

Table 3.2 Summary of the top weighted peaks following PLS-DA for both positive and negative ion analyses of *D. magna* neonate extracts exposed to copper.

Observed peak (<i>m/z</i>)	p-value ^a	Fold change ^b	No. of C atoms	Potential empirical formulae	Absolute mass error (ppm)	Ion form	Putative metabolite identification
Positive ion							
398.37427	1.41×10 ⁻⁵	6.843	27.0±5.1	C ₂₃ H ₄₇ N ₃ O ₂	0.418	[M+H] ⁺	M1 (¹² C)
399.37761	3.45×10 ⁻⁵	6.640	27.0±5.1	C ₂₃ H ₄₇ N ₃ O ₂	0.106	[M+H] ⁺	M1 (¹³ C)
275.06259	5.66×10 ⁻⁶	0.236	-	C ₁₀ H ₁₇ N ₂ OP ₃	0.230	[M+H] ⁺	?
				C ₅ H ₁₄ N ₈ OS	0.671	[M+ ⁴¹ K] ⁺	
				C ₁₀ H ₁₀ N ₆ O	0.674	[M+2Na-H] ⁺	
182.08119	2.86×10 ⁻⁷	0.393	9.3±0.5	C ₉ H ₁₁ NO ₃	0.108	[M+H] ⁺	tyrosine (¹² C)
463.35321	1.33×10 ⁻³	0.573	25.7±3.0	C ₂₃ H ₅₀ N ₃ O ₄ P	0.294	[M-e] ⁺	M2 (¹² C)
				C ₂₇ H ₄₆ N ₂ O ₄	0.379	[M+H] ⁺	
188.17572	1.72×10 ⁻⁵	2.948	-	C ₉ H ₂₁ N ₃ O	0.098	[M+H] ⁺	N-acetyl-spermidine
183.08454	4.29×10 ⁻⁷	0.412	-	C ₉ H ₁₁ NO ₃	0.160	[M+H] ⁺	tyrosine (¹³ C)

293.07333	1.03×10^{-5}	0.235	-	C ₁₀ H ₁₉ N ₂ O ₂ P ₃	0.381	[M+H] ⁺	?
				C ₁₁ H ₁₃ N ₆ PS	0.169	[M+H] ⁺	
				C ₅ H ₁₅ N ₆ O ₅ P	0.165	[M+Na] ⁺	
				C ₁₂ H ₂₀ N ₂ P ₂	0.012	[M+ ³⁹ K] ⁺	
				C ₁₀ H ₁₂ N ₆ O ₂	0.035	[M+2Na-H] ⁺	
447.35868	2.82×10^{-3}	0.598	24.2±3.2	C ₂₃ H ₅₀ N ₃ O ₃ P	0.556	[M-e] ⁺	M3 (¹² C)
				C ₂₄ H ₄₉ N ₄ P	0.280	[M+Na] ⁺	
182.07968	6.73×10^{-5}	0.425	-	no matches	-	-	?
Negative ion							
245.08530	1.90×10^{-9}	0.079		C ₉ H ₁₇ N ₃ OP ₂	0.259	[M+e] ⁻	?
				C ₁₁ H ₁₈ O ₄ S	0.023	[M-H] ⁻	
				C ₉ H ₁₄ O ₂ S	0.023	[M+Ac] ⁻	
479.17125	5.97×10^{-4}	0.089	29.4±17.3	31 possibilities c	-	-	?
238.10012	3.27×10^{-6}	0.143	10.7±0.7	no matches	-	-	M4 (¹³ C)
237.09675	4.06×10^{-6}	0.139	10.7±0.7	no matches	-	-	M4 (¹² C)
237.10765	3.75×10^{-6}	0.136	-	C ₇ H ₁₇ N ₄ O ₃ P	0.538	[M+e] ⁻	M5 (¹³ C)
237.10520	3.44×10^{-6}	0.140	16.4±11.8	C ₉ H ₂₁ NO ₂ P ₂	0.437	[M+e] ⁻	?
				C ₁₀ H ₁₅ N ₅ S	0.698	[M+e] ⁻	
				C ₁₄ H ₁₈ O	0.141	[M+ ³⁵ Cl] ⁻	
				C ₁₅ H ₂₀	0.394	[M+ ³⁹ K-2H] ⁻	

441.14374	1.12×10^{-4}	0.130	-	30 possibilities c	-	-	?
309.03351	5.10×10^{-4}	0.145	-	7 possibilities ^c	-	-	?
293.05961	1.22×10^{-3}	0.146	-	C ₁₁ H ₂₁ NP ₂ S ₂	0.026	[M+e] ⁻	?
				C ₁₉ H ₇ N ₃ O	0.510	[M+e] ⁻	
				C ₁₅ H ₁₁ N ₄ OP	0.555	[M-H] ⁻	
				C ₉ H ₈ N ₁₀	0.620	[M+ ³⁷ Cl] ⁻	
				C ₉ H ₂₁ O ₅ PS	0.704	[M+Na-2H] ⁻	
236.10430	6.09×10^{-6}	0.161	-	C ₇ H ₁₇ N ₄ O ₃ P	0.329	[M+e] ⁻	M5 (¹² C)

^a Determined from ANOVA of peak intensities across all 5 dose groups (0, 5, 10, 25 and 50 μgL^{-1} copper).

^b Fold change between the control (0 μgL^{-1}) to highest dose (50 μgL^{-1}) groups.

^c Not listed explicitly because of limited space.

Table 3.3 Comparison of the PLS weightings and the PCA loadings from the multivariate analyses of the copper toxicity study, including the univariate ANOVA results. (a) Negative ion data, showing that the peaks associated with the top PLS and PCA loadings are similar (i.e. they have similar ranking and also a similar number of peaks that are significant based upon univariate statistical tests with FDR correction). (b) Positive ion data, showing that the peaks associated with the top PLS and PCA loadings are quite different, with most of the peaks in the top PLS weightings being significant and most of the peaks in the top PCA loadings being non-significant. Shading denotes those peaks that were significantly different across the 5 dose groups, determined from ANOVA of peak intensities following FDR correction at <0.05.

(a) Negative ion data

p value	LV1 weightings	PC1+PC2 loadings	
	from PLS-DA	from PCA	p value
0.0000	245.08530	387.01969	0.2574
0.0006	479.17125	306.07654	0.1132
0.1325	371.17447	371.17447	0.1325
0.0063	426.18041	245.08530	0.0000
0.0293	471.21002	426.18041	0.0063
0.0000	238.10012	479.17125	0.0006
0.0000	237.09675	367.20618	0.3602
0.0000	237.10765	441.14374	0.0001
0.0000	237.10520	238.10012	0.0000
0.2574	387.01969	237.09675	0.0000
0.0105	333.07832	237.10520	0.0000
0.1132	306.07654	237.10765	0.0000
0.0001	441.14374	328.05862	0.1392
0.0005	309.03351	409.13340	0.0060
0.0012	293.05961	355.2425	0.3229
0.0000	236.10430	236.10430	0.0000

0.0000	236.10037	→	236.10037	0.0000
0.0000	235.10091	↘	353.22679	0.3651
0.0130	415.08111	→	235.10091	0.0000
0.0070	431.19424		411.27537	0.4845

(b) Positive ion data

p value	LV1 weightings		PC2+PC3 loadings	p value
	from PLS-DA		from PCA	
0.0000	398.37427	→	398.37427	0.0000
0.0270	160.18087	↘	424.27344	0.2899
0.0040	281.07949	↘	160.18087	0.0270
0.0000	399.37761	↘	177.13463	0.6523
0.0000	275.06259	↘	456.26349	0.1399
0.0000	182.08119	↘	319.25921	0.0379
0.0013	463.35321	↘	399.37761	0.0000
0.0000	188.17572	↘	470.31513	0.2435
0.0000	183.08454	↘	182.08119	0.0000
0.0000	293.07333	↘	425.27693	0.2800
0.0028	447.35868	↘	281.07949	0.0040
0.0001	182.07968	↘	412.23729	0.2540
0.0010	464.35647	↘	421.33996	0.8899
0.0324	490.27992	↘	329.18200	0.0000
0.0001	343.04971	↘	183.08454	0.0000
0.0009	307.08869	↘	421.33250	0.6533
0.4345	366.22711	↘	422.34338	0.8603
0.0075	88.07569	↘	487.32685	0.0918
0.0011	463.22226	↘	441.30886	0.9582
0.9139	322.23670	↘	209.97431	0.2254

3.3.4 Identification of empirical formulae and metabolites

One of the greatest challenges in metabolomics is the annotation of the thousands of peaks detected, in particular for non-mammalian species for which novel metabolites may occur (Ankley 2008). Here employed two strategies were employed: first, the assignment of empirical formulae to the peaks using an elemental composition calculator with appropriate constraints. The number of matches per peak ranged from zero to many potential formulae, summarised in Table 3.1. The second strategy utilised the high mass accuracy of the FT-ICR measurements to match the observed m/z values of the peaks to putative metabolite identities in a modified KEGG LIGAND database, as described in Section 2.6. Note that none of the metabolite assignments reported in this study can be regarded as unambiguous since they depend only on accurate mass and therefore do not fulfil the Metabolomics Standards Initiative criteria for metabolite identification (Sumner *et al.* 2007). Table 3.1 summarises the number of metabolites that have been putatively identified in *D. magna* extracts, and all 1017 of these assignments are listed on the Supplementary Information CD (Tables SI1 and SI2).

The same two strategies were employed to identify the top weighted peaks from the PLS models, listed in Table 3.2. In addition, in cases where carbon isotope patterns were detected, the $^{12}\text{C}/^{13}\text{C}$ ratio was used to calculate the approximate number of carbon atoms in the metabolite. Seventeen of the top 20 significant peaks could be assigned one or more empirical formulae. The 3 remaining “no matches” likely arise due to the presence of isotopes (not included in our elemental composition calculator) or alternative adducts (not included in our algorithm). Putatively identified metabolites included tyrosine (^{12}C and ^{13}C

isotopes) and N-acetylspermidine, and a further five unidentified metabolites with ^{12}C and ^{13}C peaks were detected, labelled M1-M5 (note that for two of these metabolites the ^{13}C isotopes were outside of the top weighted peaks). What is particularly reassuring is the consistency between the isotope pairs; e.g., the ^{12}C and ^{13}C isotopes of tyrosine show 0.393- and 0.412-fold changes following copper exposure, with associated p -values of 3×10^{-7} and 4×10^{-7} . Furthermore the number of carbon atoms derived from the $^{12}\text{C}/^{13}\text{C}$ intensity ratio is 9.3 ± 0.5 , consistent with the actual empirical formula of $\text{C}_9\text{H}_{11}\text{NO}_3$.

Having putatively identified tyrosine as undergoing a highly significant decrease in concentration in response to copper toxicity, attention was then focussed on the other amino acids. Table 3.4 lists those amino acids that also changed concentration significantly following copper exposure (with $\text{FDR} < 0.05$). Again, the fold-changes and associated p -values for the multiple observations of each metabolite are consistent; e.g., arginine is detected as four positively charged and four negatively charged ions, arising from various combinations of adducts and ^{13}C isotopes, with fold changes between 0.367 to 0.697 and with 7 of the 8 p -values statistically significant. The consistency across the positive and negative ion data is particularly reassuring since these datasets were acquired independently, i.e., the final stages of sample preparation, FT-ICR data collection and all stages of spectral processing including the two-stage peak filtering, normalisation and \log transformation were conducted separately for positive and negative ion data. What is also noteworthy is that the mean of the absolute mass error for the 57 peaks in Table 3.4 is only 0.10 ppm, and the maximum error is 0.40 ppm, which is consistent with earlier studies on liver extracts (rms error of 0.18 ppm, and maximum error of 0.48 ppm; (Southam *et al.* 2007). The results presented here clearly

show a significant decrease in the concentrations of several amino acids. In addition a search was made for the classic biomarker of heavy metal induced oxidative stress, glutathione (Gaetke and Chow 2003; Stohs and Bagchi 1995), as well as a recently reported analogue of this tri-peptide called ophthalmic acid, which is an alternative marker of oxidative stress (Soga *et al.* 2006). Peaks corresponding to their empirical formulae were detected, with GSH showing a large but non-significant >10-fold depletion after 50 μgL^{-1} copper exposure, and ophthalmic acid showing a statistically significant 1.5-fold depletion in the high dose group versus controls.

Table 3.4 Summary of significantly changing amino acids as well as key metabolic indicators of oxidative stress in *D. magna* neonates following exposure to copper.

Empirical formula	Putative metabolite identification	Ion form	Absolute mass error (ppm)	Fold change ^a	p-value ^b
Amino acids					
C ₄ H ₉ NO ₃	Threonine	[M+H] ⁺	0.007	0.629	7.51×10 ⁻⁵ (*)
C ₅ H ₉ NO ₂	Proline	[M+H] ⁺	0.047	0.759	5.21×10 ⁻⁵ (*)
		[M-H] ⁻	0.114	0.689	9.51×10 ⁻² (*)
C ₅ H ₉ NO ₄	Glutamic acid	[M+H] ⁺	0.042	0.787	8.51×10 ⁻²
		[M+Na] ⁺	0.050	0.775	1.97×10 ⁻¹
		[M+ ³⁹ K] ⁺	0.090	0.611	1.56×10 ⁻²
		[M-H] ⁻	0.012	0.646	8.19×10 ⁻³
		[M(¹³ C)-H] ⁻	0.352	0.841	3.61×10 ⁻²
		[M+ ³⁵ Cl] ⁻	0.056	0.544	1.04×10 ⁻³ (*)
C ₅ H ₁₁ NO ₂ S	Methionine	[M+H] ⁺	0.043	0.570	1.76×10 ⁻⁴ (*)
		[M+Na] ⁺	0.006	0.694	1.49×10 ⁻¹
		[M-H] ⁻	0.030	0.497	5.84×10 ⁻⁵ (*)
C ₆ H ₉ N ₃ O ₂	Histidine	[M+H] ⁺	0.240	0.801	1.58×10 ⁻¹
		[M+Na] ⁺	0.184	0.807	8.44×10 ⁻²
		[M+ ³⁹ K] ⁺	0.131	0.636	1.23×10 ⁻¹
		[M-H] ⁻	0.068	0.584	4.55×10 ⁻³ (*)
		[M+ ³⁵ Cl] ⁻	0.045	0.288	1.74×10 ⁻⁴ (*)
C ₆ H ₁₃ NO ₂	Leucine/Isoleucine	[M+H] ⁺	0.036	0.673	2.11×10 ⁻³ (*)
		[M+Na] ⁺	0.061	0.806	1.69×10 ⁻¹
		[M+ ³⁹ K] ⁺	0.014	0.634	5.28×10 ⁻³

C ₆ H ₁₄ N ₂ O ₂	Lysine	[M+H] ⁺	0.110	0.588	7.76×10 ⁻⁴ (*)
		[M(¹³ C)+H] ⁺	0.228	0.666	1.76×10 ⁻²
		[M+Na] ⁺	0.009	0.671	2.17×10 ⁻¹
		[M+ ³⁹ K] ⁺	0.072	0.645	7.07×10 ⁻²
		[M-H] ⁻	0.012	0.586	5.00×10 ⁻³
		[M+ ³⁵ Cl] ⁻	0.109	0.336	1.95×10 ⁻³ (*)
		[M+Ac] ⁻	0.092	0.717	8.13×10 ⁻³
C ₆ H ₁₄ N ₄ O ₂	Arginine	[M+H] ⁺	0.104	0.591	9.28×10 ⁻⁶ (*)
		[M(¹³ C)+H] ⁺	0.010	0.575	3.70×10 ⁻⁶ (*)
		[M+Na] ⁺	0.271	0.697	7.98×10 ⁻³
		[M+ ³⁹ K] ⁺	0.398	0.478	1.16×10 ⁻³ (*)
		[M-H] ⁻	0.002	0.578	6.20×10 ⁻⁵ (*)
		[M+ ³⁵ Cl] ⁻	0.106	0.385	5.80×10 ⁻⁴ (*)
		[M(¹³ C)+ ³⁵ Cl] ⁻	0.053	0.390	2.66×10 ⁻⁸ (*)
		[M+ ³⁷ Cl] ⁻	0.058	0.367	5.33×10 ⁻⁴ (*)
C ₉ H ₁₁ NO ₂	Phenylalanine	[M+H] ⁺	0.092	0.502	4.73×10 ⁻⁴ (*)
		[M(¹³ C)+H] ⁺	0.208	0.531	1.55×10 ⁻³ (*)
		[M+Na] ⁺	0.103	0.497	9.44×10 ⁻⁴ (*)
		[M+K] ⁺	0.061	0.445	5.10×10 ⁻⁵ (*)
		[M-H] ⁻	0.045	0.445	2.06×10 ⁻⁴ (*)
		[M+ ³⁵ Cl] ⁻	0.003	0.431	1.49×10 ⁻²
C ₉ H ₁₁ NO ₃	Tyrosine	[M+H] ⁺	0.114	0.393	2.86×10 ⁻⁷ (*)
		[M(¹³ C)+H] ⁺	0.160	0.412	4.29×10 ⁻⁷ (*)
		[M+Na] ⁺	0.275	0.570	4.90×10 ⁻²
		[M+K] ⁺	0.309	0.558	8.34×10 ⁻³
		[M-H] ⁻	0.016	0.348	6.85×10 ⁻⁵ (*)
		[M(¹³ C)-H] ⁻	0.040	0.369	1.10×10 ⁻⁵ (*)
		[M+Ac] ⁻	0.014	0.350	1.68×10 ⁻⁴ (*)

C ₁₁ H ₁₂ N ₂ O ₂	Tryptophan	[M+H] ⁺	0.018	0.521	1.08×10 ⁻⁵ (*)
		[M(¹³ C)+H] ⁺	0.212	0.538	2.63×10 ⁻⁵ (*)
		[M+Na] ⁺	0.139	0.584	1.61×10 ⁻³ (*)
		[M-H] ⁻	0.041	0.410	2.24×10 ⁻⁶ (*)
		[M(¹³ C)-H] ⁻	0.302	0.668	2.99×10 ⁻³ (*)
		[M+Ac] ⁻	0.034	0.590	6.87×10 ⁻⁴ (*)
Biomarkers of oxidative stress					
C ₁₀ H ₁₇ N ₃ O ₆ S	Glutathione	[M-H] ⁻	0.029	0.079	1.13×10 ⁻¹
C ₁₁ H ₁₉ N ₃ O ₆	Ophthalmic acid	[M-H] ⁻	0.141	0.652	9.26×10 ⁻³
		[M+H] ⁺	0.384	0.701	2.86×10 ⁻⁵ (*)

^a Fold change between the control (0 µgL⁻¹) to highest dose (50 µgL⁻¹) groups.

^b Determined from ANOVA of peak intensities across all 5 dose groups (0, 5, 10, 25 and 50 µgL⁻¹ copper).

(*) Significant following FDR correction at <0.05

3.3.5 Biochemical interpretation

Copper is an essential trace element for *D. magna*, at low levels it is likely to be utilised for normal biochemical processes, with toxicity occurring only at higher concentrations. Although normally bound to proteins, copper may be released and become free to catalyse the formation of highly reactive hydroxyl radicals and initiate oxidative damage or interfere with important cellular events (Bopp *et al.* 2008; Gaetke and Chow 2003; Linder and Hazegh-Azam 1996). Copper induced cellular toxicity is thought to be caused by the participation of copper ions in the formation of reactive oxygen species (ROS) (Gaetke and Chow 2003; Stohs and Bagchi 1995). The protective effect of GSH has been attributed to its ability to stabilise copper in its Cu²⁺ oxidised state, preventing redox cycling and the generation of free radicals (Stohs and Bagchi 1995). This is consistent with our observed >10-fold decrease in GSH concentration at the highest exposure dose, an effect that has also been observed in a copper toxicity study on rats (Gaetke and Chow 2003). Consequently, this could explain the observed significant reduction in the GSH analogue, ophthalmic acid, as it is speculated to act in the role of GSH for some cellular functions following the depletion of GSH due to oxidative stress (Soga *et al.* 2006). In addition to ROS depleting antioxidants such as GSH, they will also oxidise amino acids. The amino acids listed in Table 2, that significantly decreased concentration at the highest copper dose, are among those listed as most susceptible to oxidation (Berlett and Stadtman 1997). A further reason for the observed decrease in amino acids is likely because of a general depletion of the amino acid pool in response to induction of defence and repair mechanisms, such as the synthesis of stress proteins and DNA repair enzymes (Knops *et al.* 2001; Smolders *et al.* 2005). A previously reported metabolomics study

using earthworms (*Lumbricus rubellus*) exposed to copper determined a decrease (at 10 and 40mgKg⁻¹ of copper) in several of the amino acids that were found to decrease in this investigation, including leucine/isoleucine, phenylalanine, tyrosine and tryptophan (Bundy *et al.* 2008). Bundy *et al.* (Bundy *et al.* 2008) also determined changes to the levels of several nucleosides following exposure, including a decrease in adenosine and uridine at concentrations of 10mgKg⁻¹, putative identifications of these metabolites (in various ion forms) in our investigation has also found fold changes of ca. 0.4-0.6 in both of these metabolites. Though generally these are not significant, the deprotonated form of uridine was determined to be a significant fold change and these findings indicate that copper exposure may cause a metabolic perturbation to the nucleotide sugar metabolism pathway.

The significant increase in N-acetylspermidine in response to copper exposure was unexpected and this observation has not previously been reported. However, a viable rationalisation of this discovery can be proposed. Polyamines, including spermidine, are small abundant molecules found ubiquitously in all living organisms (Coffino and Poznanski 1991). In mammalian cells they are thought to have several roles in cell growth and differentiation, and the intracellular concentrations of these polycations are highly regulated (Casero and Pegg 1993). Spermidine/spermine N-acetyltransferase (SSAT) is the rate limiting enzyme in the degradation of intracellular polyamines, forming N-acetylspermidine/spermine (Casero and Pegg 1993). This enzyme's activity is known to increase in response to numerous toxic stimuli, including radical-producing agents such as paraquat (Casero and Pegg 1993). Furthermore, mouse liver cells exposed to free radical inducing lipopolysaccharides exhibited an increase in N-acetylspermidine, presumably as a result of increased SSAT activity

(Sugimoto *et al.* 1991). We hypothesise that the known induction of ROS due to copper exposure also increases the activity of SSAT in *D. magna*, resulting in the observed increase in N-acetylspermidine.

The biochemical interpretation of particular aspects of our metabolomics data has identified metabolic changes that are consistent with previously known responses of organisms to copper exposure; note that a comprehensive biochemical analysis of this data was not the primary aim of the study. However, the ability to determine these metabolic changes has huge potential in the future of ecotoxicogenomics research, especially as sequencing of the genome of *D. magna* is now underway (Colbourne *et al.* 2005). This interpretation provides some validation for the first application of the SIM-stitching FT-ICR method in a metabolomics study. Furthermore, the approach has uncovered a potentially novel marker for copper toxicity in N-acetylspermidine. This highlights the potential of FT-ICR mass spectrometry for metabolic biomarker discovery, and as a tool for providing detailed mechanistic insight into the MOA of toxicants, discussed further below.

3.3.6 Applicability of SIM-stitching DI FT-ICR for metabolomics

Measuring a complete cellular or organismal metabolome is impossible to achieve with current technologies as many metabolites occur at low concentration. However, mass spectrometry remains the technology of choice for the measurement of metabolites at small sample sizes in complex matrices (Brown *et al.* 2005). FT-ICR mass spectrometry currently provides the highest resolving power and mass accuracy of all commercial mass

spectrometers which, in theory, should enable the detection and identification of a large number of metabolites even when a complex mixture is directly infused into the ion source. This removes the need for time consuming chromatographic separation prior to ionisation and produces a multivariate dataset with extremely high reproducibility along the independent axis (i.e., m/z), and is increasingly being used in metabolomics (Breitling *et al.* 2006; Breitling *et al.* 2008; Brown *et al.* 2005; Dunn 2008; Southam *et al.* 2007; Takahashi *et al.* 2008). Furthermore, Han *et al.* (Han *et al.* 2008) have recently demonstrated that ultrahigh-field FT-ICR mass spectrometry shows great promise for quantitative metabolomics and reported that comparable quantitation accuracies were achieved by DI FT-ICR and LC/MS, however the former analysis consumed much less sample and was significantly faster. A potential disadvantage of FT-ICR mass spectrometry is that in order to achieve a high dynamic range, and detect both low and high concentration metabolites, the necessarily high number of ions within the ICR detector cell will undergo space-charge interactions which reduces the mass accuracy (Zhang *et al.* 2005). However, this problem can be solved with a SIM-stitching approach, which has been demonstrated to yield a rms mass error of only 0.18 ppm and a dynamic range of 16,000 (Southam *et al.* 2007). These values should be contrasted with more “traditional” DI FT-ICR mass spectrometry metabolomics approaches, for example Han *et al.* (Han *et al.* 2008) reported a mass error of ≤ 1 ppm and a dynamic range of 750, and also with other FT mass spectrometry analysers such as the LTQ Orbitrap, where a mass accuracy of between 0.48 to 5 ppm and a dynamic range of 5000 have been reported (Makarov *et al.* 2006; Olsen *et al.* 2005). Furthermore, the SIM-stitching approach, after a two-stage peak filtering algorithm to remove noise, yielded a total of 5447 peaks from

D. magna extracts (positive and negative ion modes combined). This is surprisingly large considering that the extracts are directly infused and are therefore susceptible to ion suppression. In fact this value greatly exceeds other FT-ICR mass spectrometry metabolomic studies, such as by Takahashi *et al.* (Takahashi *et al.* 2008) where only 220 ions were detected using negative ion mode, 72 of which were assigned to candidate metabolites, and by Han *et al.* (Han *et al.* 2008) who reported 570 metabolite features, 250 of which could be assigned a rational empirical formula and 100 given a possible metabolite identification. Collectively, these results highlight the excellent sensitivity, mass accuracy and dynamic range of the SIM-stitching DI FT-ICR method for metabolomics.

3.4 Conclusion

In this study we have optimised and then confirmed the effectiveness of SIM-stitching DI FT-ICR mass spectrometry metabolomics for toxicity testing in *D. magna*. It has been demonstrated that the approach is sensitive by detecting more than 5000 peaks, as described above. In addition the approach has high resolution, not only from a spectral perspective of narrow peak widths but also in terms of the processing of the m/z measurements; i.e., each peak is treated as unique, which avoids the problem of “binning” multiple peaks into the same variable prior to statistical analysis. Of course each peak could still comprise of more than one metabolite as isomers will not be separated by the DI FT-ICR approach. This is also the first successful application of the g-log transform to mass spectrometry data. These results confirm that the entire approach, including the toxicity testing, metabolite extraction, mass spectrometric analysis and spectral processing, has

sufficient reproducibility (both technical and biological) to allow the classification of different life stages of *D. magna* as well as the classification of differing degrees of copper toxicity. Furthermore, all aspects of the approach are highly scalable which would enable screening of multiple chemicals with high sample throughput. This is particularly true of the culturing and toxicity testing components since *D. magna* are easy to culture and have a short generation time, and therefore it is rapid and low cost to generate the single adult or 30 neonates required per sample. Based upon the copper toxicity results, we conclude that the combination of toxicity testing, DI FT-ICR mass spectrometry and multivariate classification methods is ideal for high throughput first-tier screening of chemicals in *D. magna*. Furthermore, this combination of methods coupled with a more detailed and unbiased investigation of the metabolic mechanism of toxicity will be of particular value for a more comprehensive chemical risk assessment.

Having confirmed in this investigation that using FT-ICR MS, coupled with the SIM-stitching approach, is an effective method of high-throughput toxicity testing; I next evaluate the feasibility of utilising this approach with *D. magna* haemolymph.

CHAPTER FOUR:

**Optimisation and validation of FT-ICR MS based
metabolomics using *Daphnia magna* haemolymph[†]**

[†]The contents of this Chapter, including the figures, have been submitted to *Environmental Science and Technology*: Poynton, H. C.; Taylor, N. S.; Hicks, J.; Colson, K.; Chan, S.; Clark, C.; Scanlan, L.; Louginov, A. V.; Vulpe, C.; Viant, M. R. Integration of metabolomics and transcriptomic signatures offers a coordinated model of cadmium toxicity in *Daphnia magna*.

4.1 Introduction

Metabolomics is increasingly becoming a valuable tool in molecular and eco-toxicology (Bundy *et al.* 2009; Coen *et al.* 2008; Viant 2007, 2008). The measurement of the small molecule compounds in a biological sample enables a non-biased investigation into the metabolic responses to toxic stress. As previously stated, given the importance of *Daphnia magna* in the freshwater ecosystem and its widespread use as a test organism, no metabolomics studies have been conducted that utilise this species. The findings from the studies discussed in Chapter 3 have determined that FT-ICR MS-based metabolomics studies using *D. magna* are a viable tool for high-throughput toxicity testing and thus further studies are required to realise the full potential of this technique.

Metabolomics studies in mammalian toxicology often use biofluids such as blood, plasma and urine to detect significant metabolic responses to toxicants. In biofluids, metabolites are in dynamic equilibrium with those inside cells and tissues and, consequently, abnormal cellular processes in tissues of the whole organism following toxicant exposure will be reflected in altered biofluid compositions (Lindon *et al.* 2000). Consequently the use of biofluids could provide a “cleaner” biological sample for detecting significant metabolic changes when compared to whole organism homogenates that could mask subtle toxicant induced effects. In environmental metabolomics, in particular in terrestrial and aquatic invertebrates, few studies have taken advantage of the benefits of using biofluids. As detailed in Chapter 1, there have been two studies reported using the haemolymph of the tobacco hornworm (*Manduca sexta*) (Phalaraksh *et al.* 1999; Phalaraksh *et al.* 2008), one using the coelomic fluid of the earthworm (*Eisenia veneta*) (Bundy *et al.* 2001), and one utilising the haemolymph of

red abalone (*Haliotis rufescens*) (Viant *et al.* 2003a). All four of these studies, and the majority of mammalian biofluid metabolomics investigations (Lindon *et al.* 2000), use NMR spectroscopy based metabolomics. However, if the ultimate aim of metabolomics is to detect every small-molecule metabolite and xenobiotic in a biofluid, then MS has a huge advantage in terms of sensitivity over NMR spectroscopy (Griffin 2003), and this technique has yet to be exploited in ecotoxicological metabolomic investigations.

Since our previous work (Chapter 3) has shown whole organism homogenates of *D. magna* to be compatible with FT-ICR MS-based metabolomics, the first objective of this study was to assess the feasibility of sampling ca. 1 μL of haemolymph from individual adult *D. magna* and then measuring high quality metabolic fingerprints from small pools of these samples using this same technique. Following this, the second objective was to apply these metabolomic investigations of haemolymph to examine the toxicity of the model toxicant, cadmium, to *D. magna*. These metabolomics studies were done in conjunction with transcriptomic studies on additional *D. magna* samples, conducted by Dr Helen Poynton (National exposure Research Laboratory, US-EPA, Cincinnati, USA), allowing a combined omics investigation into the toxicity of cadmium to *D. magna*.

4.2 Materials and Methods

4.2.1 *Daphnia magna* exposures and haemolymph extraction

The exposure of *D. magna* to cadmium and the subsequent haemolymph extraction was carried out at UC Berkeley, California, USA. Briefly, adult daphnids (10-14 d old, immediately after release of second brood) were exposed to 18 $\mu\text{g}\text{L}^{-1}$ of cadmium sulfate for 24 h. This

corresponded to 10% of the LC₅₀, a previously determined sublethal concentration of cadmium that resulted in impaired reproduction in chronic exposures (Poynton *et al.* 2008). A zero concentration control was performed alongside each cadmium exposure. Following exposure, haemolymph was extracted as described in Mucklow and Ebert (Mucklow and Ebert 2003) by pricking the heart of the *Daphnia* and collecting ca. 1 µL of haemolymph from the body cavity. Haemolymph was then rapidly frozen in liquid nitrogen and stored at -80 °C, including during shipping to our laboratory at Birmingham.

4.2.2 FT-ICR MS metabolomics

4.2.2.1 Initial haemolymph study

A total of 20 cadmium exposed haemolymph samples and 19 control haemolymph samples from *D. magna* were delivered to Birmingham University on dry ice; these were then stored at -80 °C prior to extraction analysis. To determine the feasibility of using FT-ICR based metabolomics for analysing *Daphnia* haemolymph it was decided that 3 individual samples would be pooled for an initial MS investigation in order to obtain sufficient material for analysis. At this stage two cadmium exposed samples and one control sample (total of ca. 3 µL) were pooled; metabolite extraction (with corresponding extract blank), FT-ICR analysis and data processing were all as described in Chapter 2.

4.2.2.2 Cadmium toxicity study

Since the initial haemolymph study proved successful (see Section 4.3.1) the remaining haemolymph samples (18 cadmium exposed and 18 control) were pooled as 3 haemolymph

samples per biological replicate, resulting in 6 biological replicates per group; again an extract blank was also prepared. Metabolites were extracted by methanol precipitation as described in Section 2.3.2. FT-ICR MS analysis (negative ion), data processing and metabolite identification were all as detailed in Chapter 2. The data pre-processing parameters consisted of a 2 out of 3 replicate filter, a sample filter retaining peaks that occurred in at least 50% of all samples using a 1.8ppm spread along the m/z axis for defining unique peaks, and blank peaks were retained only if twice as intense in the biological sample. PCA was used to assess metabolic similarities and differences between the samples while univariate statistics (Student's t-test across the 2 groups) were used to examine the significance of these metabolic changes, with p-values adjusted for a False Discovery Rate (FDR) of 5% (Benjamini and Hochberg 1995).

4.2.3 Transcriptomics (conducted by Dr Helen Poynton, US-EPA)

For the transcriptomic analysis 6 replicate exposures, each containing 12 individual adult *D. magna*, were conducted. These analyses were performed on a different batch of exposed daphnids to the metabolomics investigation, and used whole organism samples rather than haemolymph. RNA was extracted from each of the 12 daphnids and pooled resulting in 6 biological replicates. In brief, the extracted RNA was labelled and hybridised to a custom 44k *D. magna* array (eArray AMADID# 020720; Agilent Technologies, Santa Clara, CA). The arrays were scanned and the resulting data analysed to determine any differentially expressed genes. Quantitative Reverse Transcription PCR (q-RT-PCR) of five genes was used to confirm differential expression.

4.3 Results and Discussion

4.3.1 Initial metabolomics study

The initial aim was to determine if high quality mass spectra, distinguishable from blank samples, could be achieved from the pooled haemolymph of 3 individual adult daphnids; i.e. 3 μL of haemolymph. An FT-ICR MS analysis was conducted on this sample and on the corresponding extract blank in triplicate and the data was SIM-stitched and subjected to a two out of three replicate filter giving a single peak list each for the haemolymph sample and the extract blank. A representative mass spectrum of *D. magna* haemolymph is shown in Figure 4.1. The peak lists generated from the replicate filter were then compared using a visualization software tool (see Section 3.3.1) to compare the commonality of the peaks between the haemolymph sample and the extract blank (Figure 4.2). As with the whole organism *D. magna* samples in Chapter 3, the presence of biological material competing for charge during nano-electrospray ionisation causes suppression of the peaks in the “blank” revealing over 2000 peaks unique to *D. magna* haemolymph. There is clearly an overlap of ca. 1000 peaks between the sample and the extract blank, however, further investigation of these common peaks revealed that over 50% were at least twice as intense in the haemolymph sample and would be classed as biological peaks in a FT-ICR MS metabolomics study. It was therefore determined that 3 μL of *D. magna* haemolymph could produce distinguishable, high quality mass spectra using FT-ICR MS and would be suitable for a metabolomics study into cadmium toxicity.

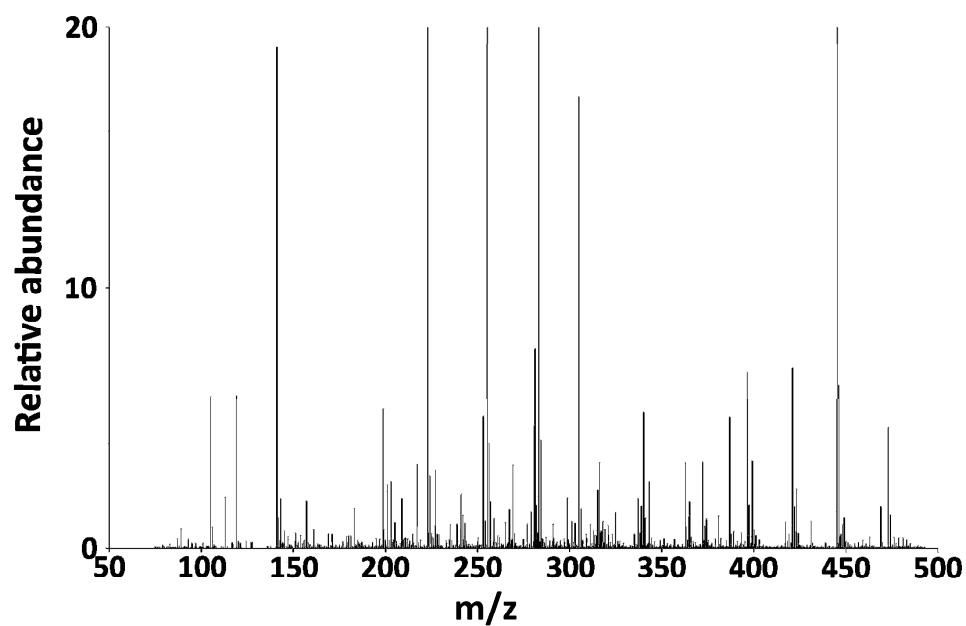


Figure 4.1 A representative FT-ICR mass spectra of pooled haemolymph extracts of the water flea, *D. magna*: a SIM-stitched spectrum, in centroid mode, between m/z 70 and 500. This spectrum was normalised to the largest peak (corresponding to 100% intensity).

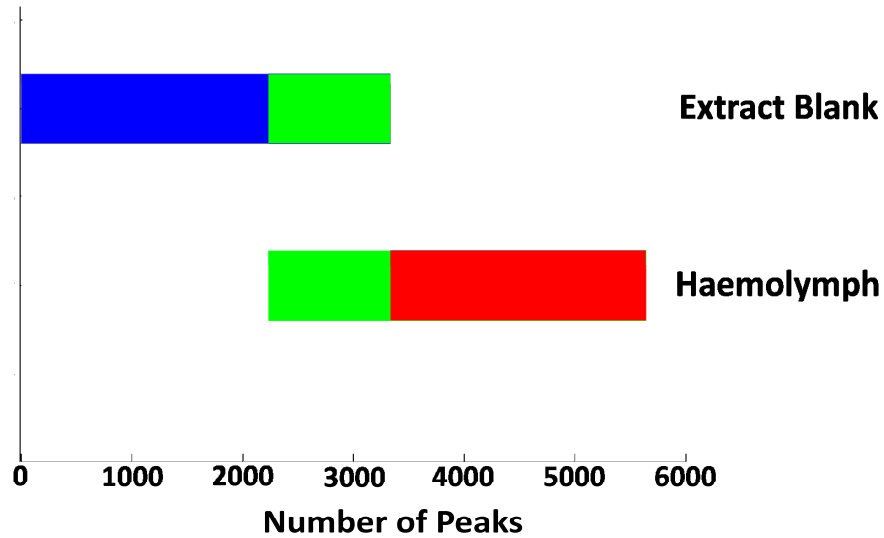


Figure 4.2 Graphical depiction of the peaks detected in an FT-ICR mass spectrum of pooled *D. magna* haemolymph extracts. Shows the occurrence of each of the >5000 unique peaks that were detected by the FT-ICR analyses, i.e., whether the peaks occurred in the extract blank only (blue), in the extract blank and the haemolymph sample (green), or in the haemolymph sample only (red). The peaks depicted in this figure are those which were present following a 2 out of 3 replicate filter.

4.3.2 Metabolomics cadmium toxicity study

FT-ICR MS was conducted in negative ion mode (as described in Chapter 2) and detected a large number of signals in *D. magna* haemolymph arising from ionised, low molecular weight metabolites including various ion forms (e.g. deprotonated metabolites, chlorine adducts, etc) and naturally occurring isotopes. The signals detected are summarised in Table 4.1, with the findings comparable to the reported signals found in the negative ion dataset of *D. magna* whole organism homogenates (see Chapter 3). Here the haemolymph dataset comprised of 3921 peaks and 883 of these could be putatively assigned one or more metabolite name, similar to the 3599 peaks found in the whole organism homogenates where 734 peaks could be putatively assigned one or more metabolite name.

Table 4.1 Summary of the total number of peaks in the dataset of *D. magna* haemolymph extracts, and the number of those peaks that could be assigned empirical formulae and putative metabolite identities.

Number of peaks	
Total (after replicate & sample filters)	3921
Assigned to ≥ 1 empirical formulae	3583
Assigned to unique empirical formula	245
Assigned to ≥ 1 KEGG LIGAND ID ^a	883

^a Following removal of assignments in which the match was a non-endogenous metabolite such as a drug, plasticiser or pesticide.

PCA was used to visualise any differences between the control and exposed samples and the PCA scores plot (Figure 4.3) shows a clear separation between the two groups, indicative of a cadmium induced metabolic response. This separation was confirmed to be significant following a t-test of the PC scores, specifically along the PC1 axis ($p=3.19\times 10^{-3}$) and the PC1+PC2 axis ($p=2.24\times 10^{-3}$). The samples in the control group are more tightly clustered relative to the cadmium exposed samples which show considerable metabolic variability.

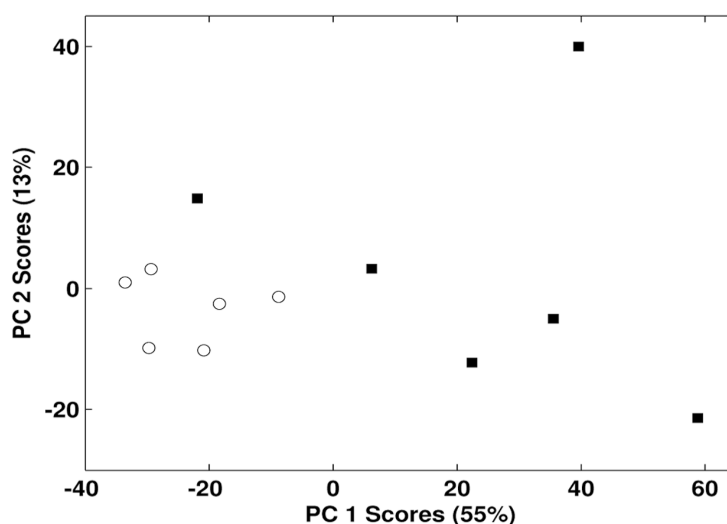


Figure 4.3 PCA scores plot from analysis of FT-ICR mass spectra of haemolymph extracts of *D. magna*: control (○) and cadmium exposed (■). The scores plot shows a cadmium induced metabolic response along the PC1 axis and the diagonal axis from bottom left to top right (PC1+PC2).

Univariate analysis of the 3921 peaks detected by FT-ICR MS revealed that 126 of these peaks (representing 3.2% of the total peaks) changed significantly following exposure of *D. magna* to cadmium (at FDR <0.05). Putative identifications of several of these metabolites are listed in Table 4.2 where it can be seen that metabolites were often detected as ^{12}C and ^{13}C containing forms, enabling the calculation of the number of carbon atoms in the metabolite from the $^{12}\text{C}/^{13}\text{C}$ intensity ratio. Alongside this, the consistency of the fold changes and associated *p*-values for the various adducts and isotope forms of each metabolite provide increased confidence in the identification of the empirical formulae. It should be noted that the mean mass error of the peaks identified in Table 4.2 is 0.34 ppm with the maximum error at 0.94 ppm. These values are higher than those found in the *D. magna* whole organism study, where the mean mass error was only 0.10 ppm (see Chapter 3) but still depict the high mass accuracy found in FT-ICR MS studies (Brown *et al.* 2005). A selected region of a representative FT-ICR mass spectrum of *D. magna* haemolymph (*m/z* 220-295, equivalent to ca. 7% of the total spectrum) is shown in Figure 4.4, and includes signals from three putatively identified metabolites, inosine ($\text{C}_{10}\text{H}_{12}\text{N}_4\text{O}_5$), uridine ($\text{C}_9\text{H}_{12}\text{N}_2\text{O}_6$) and palmitic acid ($\text{C}_{16}\text{H}_{32}\text{O}_2$), all of which change concentration significantly in response to cadmium exposure as indicated in the inset bar charts. These results from the FT-ICR MS metabolomics investigation successfully achieved the objective of determining a toxicant induced effect in the haemolymph of *D. magna* following exposure to cadmium.

Table 4.2 Summary of peaks detected by FT-ICR MS that change significantly upon cadmium exposure for which putative metabolite names could be assigned.

Observed peak (m/z)	Theoretical exact mass (m/z)	Empirical formula	Putative metabolite identification	Ion form	Number of C atoms	Absolute mass error (ppm)	Fold change ^a	p-value ^b
148.04377	148.043774	C ₅ H ₁₁ NO ₂ S	Methionine	[M-H] ⁻	-	0.031	0.345	1.22×10 ⁻³ (*)
154.06219	154.0622	C ₆ H ₉ N ₃ O ₂	Histidine	[M-H] ⁻	5±1	0.069	0.471	6.21×10 ⁻⁵ (*)
155.06555	155.0656	C ₆ H ₉ N ₃ O ₂	Histidine	[M(¹³ C)-H] ⁻	5±1	0.326	0.512	1.45×10 ⁻⁴ (*)
164.07169	164.071703	C ₉ H ₁₁ NO ₂	Phenylalanine	[M-H] ⁻	11±2	0.077	0.479	8.31×10 ⁻⁴ (*)
165.07503	165.075103	C ₉ H ₁₁ NO ₂	Phenylalanine	[M(¹³ C)-H] ⁻	11±2	0.440	0.617	1.66×10 ⁻²
173.10437	173.1044	C ₆ H ₁₄ N ₄ O ₂	Arginine	[M-H] ⁻	-	0.171	0.246	3.29×10 ⁻⁷ (*)
203.0826	203.082602	C ₁₁ H ₁₂ N ₂ O ₂	Tryptophan	[M-H] ⁻	13±4	0.008	0.411	1.79×10 ⁻⁵ (*)
204.08597	204.086002	C ₁₁ H ₁₂ N ₂ O ₂	Tryptophan	[M(¹³ C)-H] ⁻	13±4	0.155	0.534	5.50×10 ⁻³
207.11574	207.1157316	C ₁₀ H ₂₀ O ₂	Decanoic acid	[M+ ³⁵ Cl] ⁻	-	0.041	0.606	3.79×10 ⁻⁵ (*)
209.0811	209.081078	C ₆ H ₁₄ N ₄ O ₂	Arginine	[M+ ³⁵ Cl] ⁻	-	0.107	0.537	5.21×10 ⁻⁵ (*)
211.07811	211.078128	C ₆ H ₁₄ N ₄ O ₂	Arginine	[M+ ³⁷ Cl] ⁻	-	0.083	0.428	1.04×10 ⁻⁵ (*)
220.09391	220.0938956	C ₇ H ₁₅ N ₃ O ₅	1-Guanidino-1-deoxy-scyllo-inositol	[M-H] ⁻	-	0.065	2.372	5.12×10 ⁻⁴ (*)

243.06231	243.06226	C ₉ H ₁₂ N ₂ O ₆	Uridine	[M-H] ⁻	-	0.199	0.407	6.20×10 ⁻⁵ (*)
255.23295	255.232954	C ₁₆ H ₃₂ O ₂	Palmitic acid	[M-H] ⁻	-	0.017	0.558	1.14×10 ⁻²
267.07355	267.073493	C ₁₀ H ₁₂ N ₄ O ₅	Inosine	[M-H] ⁻	11±1	0.207	0.460	4.66×10 ⁻⁵ (*)
	267.0736346	C ₁₁ H ₁₉ O ₃ P	c	[M+ ³⁷ Cl] ⁻	11±1	0.317		
268.07696	268.076893	C ₁₀ H ₁₂ N ₄ O ₅	Inosine	[M(¹³ C)-H] ⁻	11±1	0.248	0.518	1.92×10 ⁻⁴ (*)
	268.0771256	C ₁₀ H ₁₇ NO ₅	c	[M+ ³⁷ Cl] ⁻	-	0.618		
	268.0770346	C ₁₁ H ₁₉ O ₃ P	c	[M(¹³ C)+ ³⁷ Cl] ⁻	11±1	0.279		
279.0392	279.038938	C ₉ H ₁₂ N ₂ O ₆	Uridine	[M+ ³⁵ Cl] ⁻	8±1	0.939	0.386	7.85×10 ⁻⁶ (*)
280.0425	280.042338	C ₉ H ₁₂ N ₂ O ₆	Uridine	[M(¹³ C)+ ³⁵ Cl] ⁻	8±1	0.058	0.422	7.56×10 ⁻⁵ (*)
281.03622	281.035988	C ₉ H ₁₂ N ₂ O ₆	Uridine	[M+ ³⁷ Cl] ⁻	-	0.825	0.428	1.04×10 ⁻⁵ (*)
	281.0362756	C ₁₀ H ₁₂ N ₄ O ₂ P ₂	c	[M-H] ⁻	-	0.198		
	281.0363376	C ₁₁ H ₆ N ₈ S	c	[M-H] ⁻	-	0.418		
	281.0364156	C ₁₁ H ₁₉ P ₃	c	[M+ ³⁷ Cl] ⁻	-	0.696		
291.20989	291.209633	C ₁₆ H ₃₂ O ₂	Palmitic acid	[M+ ³⁵ Cl] ⁻	19±6	0.884	0.388	1.29×10 ⁻³ (*)
292.2132	292.213033	C ₁₆ H ₃₂ O ₂	Palmitic acid	[M(¹³ C)+ ³⁵ Cl] ⁻	19±6	0.573	0.451	1.12×10 ⁻³ (*)
293.20691	293.206683	C ₁₆ H ₃₂ O ₂	Palmitic acid	[M+ ³⁷ Cl] ⁻	21±7	0.776	0.426	1.30×10 ⁻³ (*)
294.21024	294.210083	C ₁₆ H ₃₂ O ₂	Palmitic acid	[M(¹³ C)+ ³⁷ Cl] ⁻	21±7	0.535	0.488	2.11×10 ⁻³
	294.2104586	C ₁₆ H ₃₀ N ₃ P	c	[M-H] ⁻	-	0.743		

305.04741	305.047221	C ₁₀ H ₁₂ N ₄ O ₅	Inosine	[M+ ³⁷ Cl] ⁻	-	0.614	0.434	3.19×10 ⁻⁵ (*)
	305.0474016	C ₆ H ₁₄ N ₂ O ₁₂	c	[M-H] ⁻	-	0.028		
	305.0475086	C ₁₁ H ₁₂ N ₆ OP ₂	c	[M-H] ⁻	-	0.323		

^a Fold change between the control and cadmium exposed groups.

^b Determined from t-test of peak intensities across control and cadmium exposed groups

^c No metabolite name in KEGG matching this formula

(*) Significant following FDR correction at <0.05

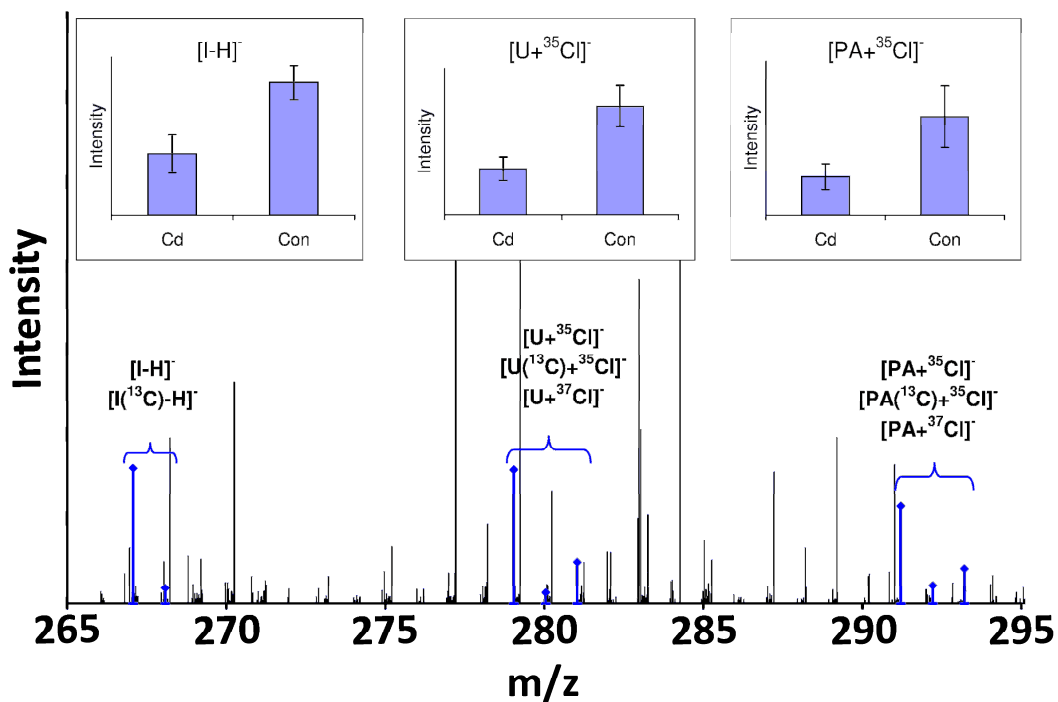


Figure 4.4 Section of a representative negative ion FT-ICR mass spectrum of *D. magna* haemolymph highlighting the putatively identified signals from inosine (I), uridine (U) and palmitic acid (PA), each detected as various adduct forms and naturally-occurring isotopes. Inset bar charts show the levels of these significantly effected metabolites in control versus cadmium exposed daphnids. Error bars represent the standard deviation.

4.3.3 Key findings from transcriptomic cadmium toxicity study

The transcriptomic studies and subsequent analysis were performed by Dr Helen Poynton (US-EPA National Exposure Laboratory) and the key findings from this work are as follows. Affected genes included those involved in digestion, immune function, xenobiotic metabolism and growth and development; with the microarray and q-RT-PCR results being strongly correlated. Specifically; there was an up-regulation of genes involved in embryonic development (2.9 to 4.5-fold increases), including vitellogenin and egg-shell proteins; a down-regulation of carboxypeptidase A (an enzyme involved in protein digestion; 2-fold decrease); these changes in gene expression are linked to the metabolomics data and are discussed in the next Section. An up-regulation in oxidative stress response genes (2.2 to 2.6-fold increases), including cytochrome P450, glutathione-S-transferase (GST) and metallothionein (MT); and an up-regulation of cuticle proteins (up to 3.7-fold increases) were also determined from the transcriptomic analysis.

4.3.4 Relevance of findings to cadmium toxicity

As this was a combined omics study into the toxicity of cadmium to *D. magna*, the key findings from both the metabolomics and transcriptomic studies have been integrated into Figure 4.5 giving an overview of the physiological processes affected by cadmium exposure. However, the focus of this discussion is on the findings of the metabolomics investigation into the effects of cadmium on the daphnid haemolymph metabolome, summarised in Table 4.2.

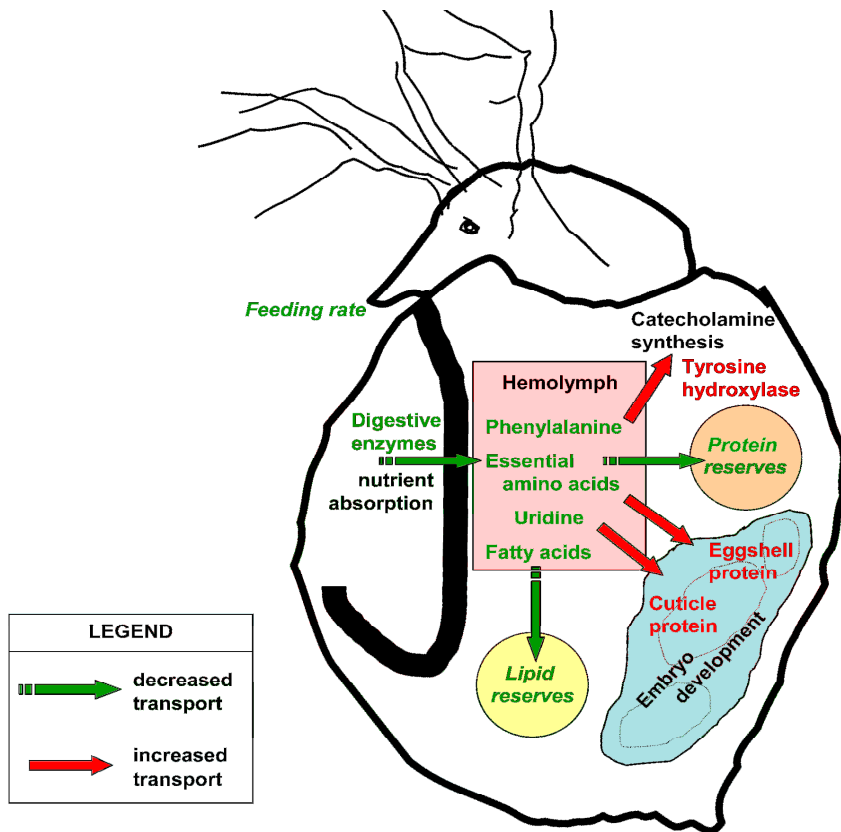


Figure 4.5 Summary model of sub-lethal cadmium toxicity in *D. magna*. Processes, metabolites and genes affected by cadmium exposure are shown in red (increases) or green (decreases). Those revealed in this study shown in plain text, those found in other studies are italicised. Decrease in feeding rate and digestive enzyme activity was shown by De Coen and Janssen (1998) (De Coen and Janssen 1998), while decreases in digestive enzyme expression level were described by Poynton *et al.* (Poynton *et al.* 2007). Decreases in protein and lipid reserves were described by Soetaert *et al.* (Soetaert *et al.* 2007b).

Cadmium is a toxic non-essential metal with no reported biological function (Connon *et al.* 2008). It is known to cause oxidative tissue damage, increased lipid peroxidation and DNA damage (Stohs and Bagchi 1995) and has been reported to significantly decrease survival, growth and reproduction in *D. magna* (Smolders *et al.* 2005). The significant decrease in several amino acids is comparable to the findings from the whole organism study into copper toxicity (Chapter 3) and could again be a consequence of depletion of the amino acid pool following induction of defence and repair mechanisms in response to cadmium stress (Smolders *et al.* 2005). Interestingly, all the amino acids found to be changing significantly are essential amino acids (methionine, histidine, phenylalanine, arginine and tryptophan) and are therefore only obtainable via absorption from food. This suggests that an effect on food uptake or digestive capabilities could account for these changes in metabolite concentration. Following exposure of *D. magna* to cadmium, De Coen and Janssen (De Coen and Janssen 1998) observed a drastic reduction in ingestion activity and an initial reduction of digestive enzyme activity which then recovered. Another study by De Coen and Janssen (De Coen and Janssen 1997a) found an increase in digestive enzyme activity of *D. magna* in response to cadmium stress, and a transcriptomic investigation by Soetaert *et al.* (Soetaert *et al.* 2007b) determined an up-regulation of genes involved in digestive processes. It is likely that a decrease in essential amino acids is the result of reduced feeding capability and an increase in digestive enzyme activity is reflecting an increased efficiency in food assimilation to compensate for reduced food intake (De Coen and Janssen 1997b) and the increased energy demand required for dealing with the toxicant (Connon *et al.* 2008). These responses would

all contribute to a depleted pool of amino acids that the daphnids are unable to replenish due to inhibition of feeding activity.

Another reason for the significant decrease in phenylalanine could be due to its role in catecholamine synthesis. Phenylalanine can be converted to tyrosine, a precursor for catecholamines, in particular dopamine, which has been shown to be increased in aquatic invertebrates in response to stress (Lansing *et al.* 1993). The present transcriptomic study found an increase in tyrosine hydroxylase (TYH). This enzyme catalyses the initial step in the conversion of tyrosine into dopamine, suggesting the decrease in the metabolite phenylalanine could also be due to it being shuttled into the synthesis of dopamine.

As with the decrease in essential amino acids, the reduction in food intake could also explain the significant decrease in two putatively identified fatty acids, palmitic acid and decanoic acid, found in the haemolymph of cadmium exposed *D. magna*. A decrease in feeding rate could cause decreased absorption of fatty acids, and with previous transcriptomic studies reporting down-regulation of fatty acid binding proteins and reduced lipid reserves (Poynton *et al.* 2007; Soetaert *et al.* 2007b) this could contribute to decreased levels of fatty acids in the haemolymph.

The metabolomics investigation also determined a significant decrease in two nucleosides, uridine and inosine, in the haemolymph of *D. magna* in response to cadmium exposure. Uridine is a pyrimidine nucleoside found in RNA and is a precursor for the pyrimidine nucleosides in DNA, while inosine is a precursor for the purine ribonucleotides. The up-regulation of genes involved in embryonic development in this present study would explain

the decrease in these nucleosides as they are utilised for the synthesis of nucleotides required for embryonic growth.

4.4 Conclusion

This study has demonstrated for the first time the feasibility of FT-ICR MS metabolomics on small volumes of *D. magna* haemolymph, showing that it is a sensitive approach, detecting thousands of unique signals. We have reported that significant cadmium induced toxic effects can be determined using the haemolymph metabolome of *D. magna*, specifically decreases in amino acids, fatty acids and nucleic acids. The concurrent transcriptomic study has enabled us to integrate both metabolomics and transcriptomic signatures into a model of cadmium toxicity, where a depletion of both lipid and protein reserves would likely result in decreased fitness and survival during prolonged exposure.

Having confirmed here that FT-ICR MS analysis of haemolymph is a feasible approach for determining toxicant induced effects in *D. magna*; I next evaluate the capabilities of both haemolymph and whole organism homogenates of *D. magna* in discriminating between toxicant MOAs.

CHAPTER FIVE:

**Discriminating toxicant modes of action via changes in the
daphnid metabolome[†]**

[†]The contents of this Chapter, including the figures, have been submitted to *Toxicological Sciences*:
Taylor, N. S. and Viant, M. R. Discriminating toxicant modes of action via changes in the daphnid metabolome.

5.1 Introduction

A battery of standardised toxicity testing strategies exists for assessing the potential hazards of chemicals that may enter the environment; these and their limitations are discussed in Chapter 1. The potential role and importance of metabolomics in toxicity testing and ecological risk assessment is currently being evaluated (Ankley 2008), for example as a tool to discover the mode(s) of action (MOA) of toxicants at a metabolic level (Bundy *et al.* 2009). Such an application would exploit several of the strengths of metabolomics, including its ability to characterise multiple metabolic pathways simultaneously and in a relatively rapid and non-targeted manner. After having catalogued a library of sub-lethal metabolic responses to a series of defined MOAs, this approach could be used as a discovery tool for identifying the MOA of a new drug or emerging environmental contaminant, (Edwards and Preston 2008) with subsequent use in screening and/or prioritisation of chemicals in risk assessment. However, for this to be achieved it is first necessary to confirm that different chemical MOAs do indeed elicit specific and distinct metabolic response profiles that can predict toxicity (Guo *et al.* 2009). As detailed in Section 1.4.1, this has been achieved in mammalian toxicology by the COMET group (Ebbels *et al.* 2007; Lindon *et al.* 2005) and yet there remain relatively few studies published that have applied metabolomics to investigate the specificity of toxicant MOAs in ecotoxicology (Guo *et al.* 2009; McKelvie *et al.* 2009; Viant *et al.* 2006b). Furthermore, all such studies to date have utilised NMR based metabolomics only. FT-ICR MS provides ca. 10 times greater coverage of the metabolome than that achieved using standard NMR approaches. Building on the findings from our previous work (Chapters 3 and 4), which established FT-ICR MS based metabolomics as an effective

technique for assessing toxicity in both the whole-organism and haemolymph metabolome of *D. magna*; the main objective of this investigation is to develop robust multivariate models to predict toxicant MOA using FT-ICR MS metabolomics data derived from *D. magna* toxicity tests. These investigations are focussed on four model toxicants: cadmium (Cd; an inducer of oxidative stress; (Stohs and Bagchi 1995)), fenvalerate (induces hyper-excitation through prolonged opening of sodium channels; (Ray and Fry 2006)), 2,4-dinitrophenol (DNP; an uncoupler of oxidative phosphorylation; (Drysdale and Cohn 1958)) and propranolol (a non-selective β -blocker; (Huggett *et al.* 2002)). The first aim was to attempt to detect metabolic responses, following acute exposures to each toxicant, in both the whole organism metabolome (derived from homogenate of an *individual* daphnid) and the haemolymph metabolome (sampled from an *individual* animal). The second aim was to determine if the four different MOAs could be distinguished based upon the measured metabolic responses, using supervised multivariate modelling coupled to robust cross-validation and permutation testing. The final aim was to determine whether the metabolome of haemolymph or of whole organism homogenates was the more discriminatory of toxicant MOA.

5.2 Materials and Methods

5.2.1 Optimisation of FT-ICR MS analysis of individual daphnid haemolymph

Since the studies detailed in Chapter 4 utilised pooled haemolymph samples, the first stage of this investigation was to determine if FT-ICR MS of haemolymph from an individual daphnid was feasible. Haemolymph and metabolite extraction from individual daphnids was as detailed in Section 2.3.2 with varying resuspension volumes of 16, 20 and 30 μL (n=5

daphnids per resuspension volume) of 80:20 methanol:water containing 20 mM ammonium acetate. FT-ICR MS analysis in negative ion mode and data processing were conducted on all samples (Sections 2.4 and 2.5 respectively) and the results assessed to determine the optimal resuspension volume for an individual daphnid haemolymph sample.

5.2.2 Determination of sub-lethal concentrations

To determine the appropriate sub-lethal concentrations for each of the four toxicants (cadmium, 2,4-dinitrophenol, fenvalerate and propranolol; all Sigma Aldrich, UK), initial 24 h acute toxicity studies were carried out. Groups of 30 neonates (< 24-h old), in 250 mL of clean media were exposed to a range of concentrations of one of the toxicants (0-1000 μgL^{-1} Cd; 0-20 mgL^{-1} DNP; 0-20 μgL^{-1} fenvalerate and 0-24 mgL^{-1} propranolol), with n=3 exposure vessels per concentration. All toxicants were solubilised in deionised water with the exception of fenvalerate, which used dimethyl sulfoxide (DMSO) as a solvent (0.00001%) with a corresponding solvent control. No food or supplements were provided during this exposure and any mortality after 24 h was recorded. PROBIT analysis (SPSS v16, SPSSInc, Chicago) was used to establish the neonatal LC_{50} for each of the four toxicants.

5.2.3 Adult *Daphnia magna* acute toxicity studies

The nominal exposure concentration for each of the four toxicants was standardised to 10% of the calculated neonatal LC_{50} to ensure that any metabolic effects were sublethal. This approach also effectively normalised the exposure concentration to a defined biological effect. The nominal concentrations were 71 μgL^{-1} cadmium (measured as Cd^{2+} ions), 1.5 mgL^{-1}

DNP, $0.6 \mu\text{gL}^{-1}$ fenvalerate (0.00001% DMSO) and 1.4 mgL^{-1} propranolol. For all toxicity exposures, third brood neonates were obtained and cultured as normal until 14 days of age, and then individual daphnids were transferred to 250 mL of clean media and exposed to the relevant toxicant for 24 h. Four sample groups were used for each toxicant: control (n=10 individuals) and toxicant-exposed (n=10) for whole organism sampling, and control (n=10) and toxicant-exposed (n=10) for haemolymph sampling. Again, no food or supplements were provided during the exposures.

5.2.4 Animal capture and metabolite extraction

Following 24 hours of exposure, daphnids were captured and metabolites extracted using one of two methods (Sections 2.2 and 2.3). For whole organism homogenate studies, daphnids were captured by filtration through a fine mesh gauze, transferred rapidly to a Precellys™ homogenisation tube, flash frozen in liquid nitrogen, and then stored at -80°C until metabolite extraction. Metabolite extraction used the two-step methanol:chloroform:water protocol detailed in Section 2.3.1, including the preparation of an extract blank. For haemolymph studies, animals were transferred onto clean microscope slides, carefully blotted dry and approximately $1 \mu\text{L}$ of haemolymph was extracted by piercing the carapace close to the heart using a 21 gauge needle and collecting the haemolymph using a micropipette as described by Mucklow and Ebert (Mucklow and Ebert 2003). Each haemolymph sample was placed in an individual Eppendorf™ tube and again stored at -80°C . Metabolites from the haemolymph samples were extracted and an extract blank prepared, as described in Section 2.3.2. The evening prior to FT-ICR MS analysis, each ca. $1 \mu\text{L}$

haemolymph sample was diluted with 30 μ L of 80:20 methanol:water containing 20 mM ammonium acetate, vortexed, and stored at -20°C overnight to facilitate protein precipitation.

5.2.5 FT-ICR MS, data processing and metabolite identification

On the day of FT-ICR analysis, one aliquot of each of the dried polar extracts from the whole daphnid extractions was resuspended in 30 μ L 80:20 methanol:water containing 20 mM ammonium acetate. The protein-precipitated haemolymph samples were used directly. All biological samples and extract blanks were then prepared, analysed in triplicate, in negative ion mode, by DI FT-ICR MS, utilising the SIM-stitching method, as described in Section 2.4. Mass spectra were processed as detailed in Section 2.5; the sample filter set to retain only those peaks that occurred in at least 50% of all samples using a 1.8ppm spread along the m/z axis for defining unique peaks, and blank peaks were retained only if twice as intense in the biological sample.

For the individual analyses of each of the four toxicants, mass spectral processing was applied to each of the whole organism homogenate datasets and to each of the haemolymph datasets, resulting in eight data matrices in total (each comprising n=10 controls and n=10 exposed). For the analysis of all toxicants together, mass spectra were reprocessed (as stated above, except that in this case all peaks in the “extract blank” were removed from the biological samples) to obtain one whole organism homogenate dataset and one haemolymph dataset (each comprising n=30 controls, n=10 solvent controls, and n=10 exposed to each of the four toxicants). Subsequently, every matrix was further processed by the addition of

missing values, normalised and g-log transformed (transformation parameter $\lambda=7.31\times 10^{-11}$) as detailed in Section 2.5. Putative identification of peaks was as described in Section 2.6, which consequently enabled the identification of peaks directly related to the parent toxicants, which were subsequently removed from the datasets prior to statistical analysis.

5.2.6 Statistical analysis

To assess the effects of each individual toxicant on both the whole organism and haemolymph metabolomes of *D. magna*, eight principal components analyses (PCA) were conducted on the processed data matrices (Section 2.7.1). The significance of separation between the control and exposed classes – along the first several principal components (PCs) – was evaluated via t-tests of the PC scores. Univariate statistical tests (t-tests; Section 2.7.2) were used to determine if individual peaks (i.e. metabolites) changed significantly between control and exposed classes.

To distinguish between the four toxicant MOAs, in both whole organism and haemolymph metabolome datasets, two partial least squares discriminant analyses (PLS-DA) were conducted (Section 2.7.1). Here, internal cross validation and permutation testing were employed, as described below, to calculate robust classification error rates associated with the prediction of toxicant MOAs. Results are presented as “balanced” error rates, i.e. the average of false positive and false negative error rates (Fleuret 2004). First the number of latent variables (LVs) for each PLS model (i.e. whole organism and haemolymph) was chosen to minimise the classification errors. Then the following strategy was employed: an optimal PLS-DA model was built and internally cross validated (venetian blinds with 8 splits) to yield

the “optimal model” classification error rate (derived from repeating the internal cross-validation process 1000 times) for each class: control, solvent control, Cd, DNP, fenvalerate and propranolol. Next, to evaluate the statistical significance of these error rates (i.e. to ensure that the optimal model was not over-fitting the dataset) the class labels were randomly permuted and another PLS-DA model was built. Internal cross validation was used to calculate a “permuted” classification error rate (for control, solvent control, Cd, DNP, fenvalerate and propranolol classes); this permutation and model building process was repeated 1000 times. Statistical significance, for the prediction of each class, could then be assessed by comparing the optimal model classification error rate to the null distribution of permuted error rates (Westerhuis *et al.* 2008). Specifically the number of instances for which the permuted classification error rate was less than the optimal model error rate was determined and then divided by the total number of permutations (1000), generating a p -value, with $p < 0.05$ indicating that the metabolic profile associated with that toxicant MOA could be discriminated from all other metabolic profiles.

5.3 Results and Discussion

5.3.1 Optimisation of FT-ICR MS analysis of individual daphnid haemolymph

FT-ICR analysis of samples resuspended in both 16 and 20 μL of MS solvent only enabled each of the samples to be run in duplicate rather than triplicate, potentially due to disturbance of particulates in the sample when loading the samples causing poor spray stability. The samples resuspended in 30 μL of MS solvent were all successfully analysed in triplicate, allowing data processing to be performed as detailed in Section 2.5. Furthermore

this achieved high quality mass spectra detecting ca. 2500 signals, therefore 30 µL of MS solvent was determined to be sufficient for this approach and utilised for all FT-ICR MS analysis of individual daphnid haemolymph samples.

5.3.2 Determination of sublethal concentrations

Preliminary acute toxicity tests were conducted in order to determine the *D. magna* neonatal lethality concentrations for each of the four toxicants. The objective of these preliminary exposures was to facilitate the selection of an exposure concentration for the acute toxicity studies of the adult daphnids that would not induce any mortality, thus ensuring that any observed metabolic effect was sublethal. The incidence of neonate mortality during these exposures is summarised in Table 5.1, with the calculated neonatal LC₅₀ for each of the toxicants listed in Table 5.2. The nominal exposure concentrations selected for the acute toxicity studies using adult *D. magna* were 10% of the neonatal LC₅₀ for each toxicant.

Table 5.1 Results from 24 hr *D. magna* neonate acute toxicity study summarising the mean mortality rate for each nominal concentration (n=3).

Toxicant	Nominal concentrations	Mean mortality rate (%)
Cadmium chloride *	0 µg/L	0
	200 µg/L	0
	400 µg/L	0
	600 µg/L	25
	800 µg/L	33
	1000 µg/L	52
Fenvalerate **	0 µg/L	0
	2 µg/L	2
	4 µg/L	18
	6 µg/L	47
	8 µg/L	73
	10 µg/L	93
DNP	0 mg/L	0
	5 mg/L	0
	10 mg/L	5.5
	12.5 mg/L	12
	15 mg/L	33
	17.5 mg/L	87
	20 mg/L	100
Propranolol	0 mg/L	0
	5 mg/L	2
	10 mg/L	18
	15 mg/L	33
	18 mg/L	80
	21 mg/L	92
	24 mg/L	100

* Calculated at Cd²⁺ ions

** All concentrations using 0.00001% DMSO as solvent

Table 5.2 Calculated LC₅₀ values from 24 hr neonate exposures using PROBIT analysis

Toxicant	LC ₅₀
Cadmium chloride *	713.6 ± 154 µg/L
Fenvalerate	5.9 ± 0.5 µg/L
DNP	14.9 ± 2.9 mg/L
Propranolol	13.8 ± 2.4 mg/L

* Calculated at Cd²⁺ ions

5.3.3 Effects of individual toxicants on whole organism and haemolymph metabolomes

The first aim of this study was to utilise the mass spectrometry-based metabolomics approach to attempt to detect metabolic responses to acute toxicity, in both the whole organism and haemolymph metabolomes of individual adult daphnids. Exposure to 10% of the concentration of the neonatal LC₅₀ did not cause lethality for all four toxicants tested, confirming that these studies evaluated sub-lethal metabolic responses in adult daphnids. FT-ICR mass spectrometry of whole organism extracts and haemolymph resulted in high quality metabolite profiles with a mean of 3094 signals detected in haemolymph and 4134 signals in the whole organism extracts. Putative identification of peaks following spectral processing identified any peaks that directly related to the parent toxicants, these are shown in Table 5.3, and were subsequently removed from the datasets at this stage; prior to statistical analysis.

Table 5.3 Peaks identified in the FT-ICR mass spectra that directly related to parent toxicants. These were subsequently removed from the metabolic datasets prior to statistical analysis.

Haemolymph	Whole organism homogenates
[Dinitrophenol-H] ⁻	[Dinitrophenol-H] ⁻
[Dinitrophenol(¹³ C)-H] ⁻	[Dinitrophenol (¹³ C)-H] ⁻
[Propranolol+ ³⁵ Cl] ⁻	
[Propranolol(¹³ C)+ ³⁵ Cl] ⁻	
[Propranolol+ ³⁷ Cl] ⁻	
[Propranolol(¹³ C)+ ³⁷ Cl] ⁻	

PCA was used to visualise the metabolic differences between control and toxicant-exposed samples (Figure 5.1). The scores plots show clear metabolic effects due to Cd, DNP, fenvalerate and propranolol exposures, for both the whole organism and haemolymph datasets. These effects were evaluated statistically by testing the significance of the separation between each toxicant class and its corresponding control, along the PC1, PC2, PC3 and PC4 axes (these PCs accounted for ≥60% of the total variance in each dataset; Table 5.4). All four toxicants induced a significant metabolic perturbation in both the haemolymph and whole organism homogenates (all $p < 0.0125$, Bonferroni-corrected for multiple testing), with Cd inducing the largest effect, along PC1, in both sample types.

To determine the number of peaks that changed intensity significantly in response to each toxicant (and their proportion relative to the total number of peaks detected), Student's t-tests were applied between control (n=10) and exposed (n=10) samples (adjusted for FDR<5%; Table 5.5). Consistent with the PCA results, the greatest number of (and relative proportion of) significant peaks occurred in response to Cd, totalling ca. 600 for both haemolymph and whole organism homogenates. For the other three toxicants, however, the proportion of significantly changing peaks was much higher in the whole organism homogenates (from 5-13%) than in the haemolymph samples (<1% for all three toxicants). This provides the first evidence that the whole organism metabolome's response to a toxicant is typically more extensive (and potentially contains more information) compared to the response of the haemolymph.

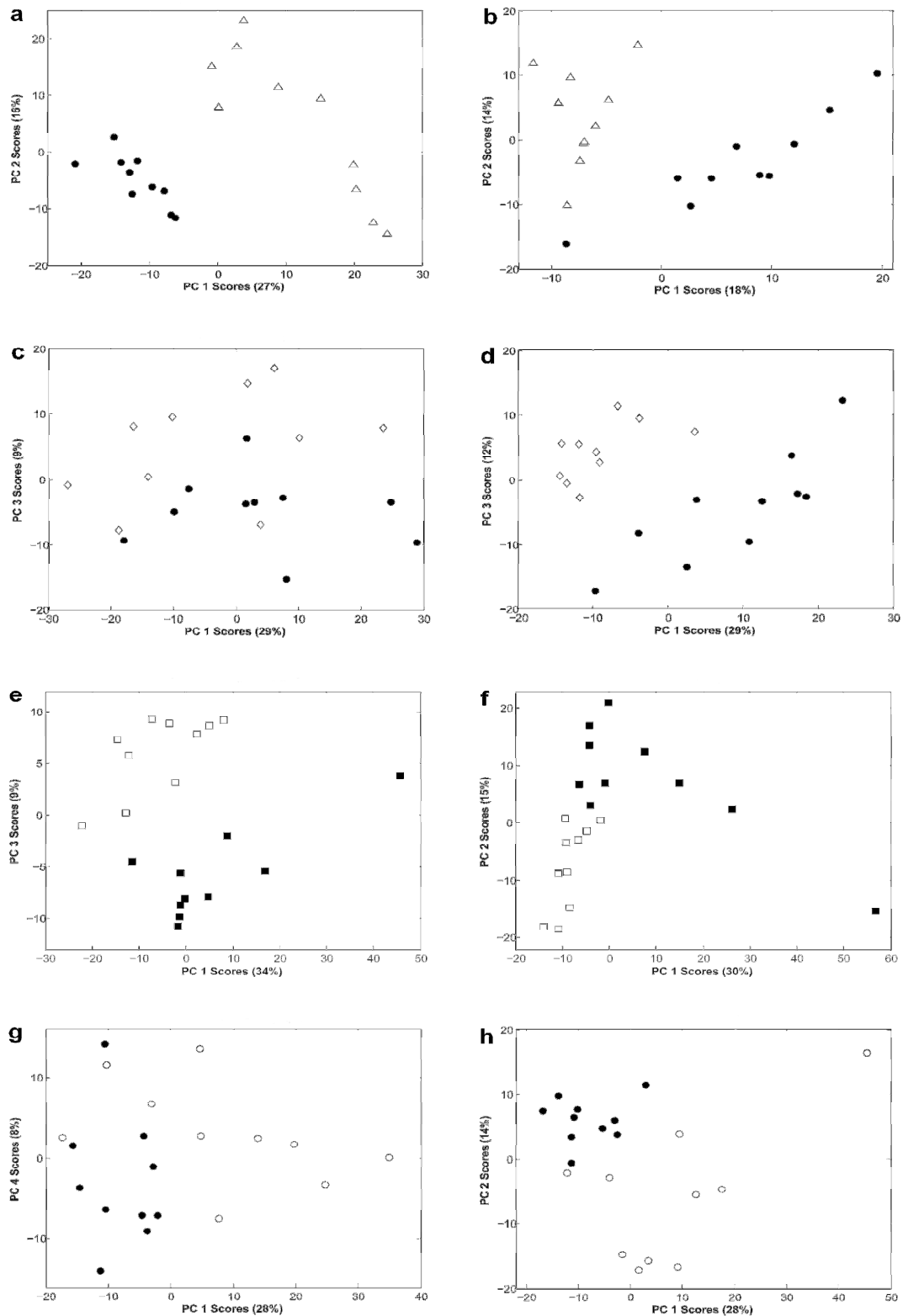


Figure 5.1 PCA scores plots from analysis of FT-ICR mass spectra of *D. magna* (a) haemolymph and (b) whole organism homogenates following Cd exposure (control ●, exposed Δ), (c) haemolymph and (d) whole organism homogenates following DNP exposure (control ●, exposed ◊), (e) haemolymph and (f) whole organism homogenates following fenvalerate exposure (control ■, exposed □), and (g) haemolymph and (h) whole organism homogenates following propranolol exposure (control ●, exposed ○). All plots show PC1 against the (next) most significant PC axis and all show a toxicant induced metabolic response.

Table 5.4 Summary of *p*-values from Student's t-tests of PC scores between control (n=10) and exposed (n=10) samples, for Cd, DNP, fenvalerate and propranolol (see Figure 1). Data are presented for both haemolymph and whole organism homogenates of *D. magna*.

Haemolymph				
Principal component	Cd	DNP	Fenvalerate	Propranolol
PC1	2.12×10^{-6} (*)	0.25	0.06	6.20×10^{-3} (*)
PC2	0.04	0.04	0.55	0.72
PC3	0.66	7.66×10^{-3} (*)	4.32×10^{-6} (*)	0.12
PC4	0.75	0.17	0.75	0.06
Whole organism homogenates				
Principal component	Cd	DNP	Fenvalerate	Propranolol
PC1	3.29×10^{-5} (*)	1.41×10^{-4} (*)	0.02	6.49×10^{-3} (*)
PC2	0.04	0.32	1.29×10^{-3} (*)	3.63×10^{-3} (*)
PC3	0.23	9.45×10^{-3} (*)	0.67	0.74
PC4	0.89	0.81	0.40	0.16

* indicates significance at the Bonferroni-corrected *p*-value<0.0125

Table 5.5 Number of peaks that significantly changed concentration (FDR<0.05, relative to controls) and their proportion relative to the total number of peaks detected, following exposure to cadmium, DNP, fenvalerate and propranolol. Data are presented for both haemolymph and whole organism homogenates of *D. magna*.

Haemolymph				
	Cd	DNP	Fenvalerate	Propranolol
Number of significant peaks	618	9	31	10
Proportion of significant peaks (%)	21	0.3	0.8	0.4
Whole organism homogenates				
	Cd	DNP	Fenvalerate	Propranolol
Number of significant peaks	660	544	398	232
Proportion of significant peaks (%)	14	13	12	5

While an extensive biochemical interpretation of the effects of each toxicant is not an objective of this study, it is however valuable to confirm that some of the putatively identified metabolites that change concentration are consistent with MOAs reported in the literature. For example, focusing on the more extensive responses within the whole organism homogenates, the uncoupler of oxidative phosphorylation (DNP) significantly induced anticipated changes to the invertebrate phosphagen system, specifically arginine ($p=0.0032$) and phosphoarginine ($p=0.0112$) (Uda *et al.* 2006). This response is comparable to a previous metabolomics investigation into the responses of Japanese Medaka embryos to Dinoseb (another herbicide that is known to uncouple oxidative phosphorylation), where the levels of phosphocreatine (part of the vertebrate phosphagen system) were significantly changed following exposure (Viant *et al.* 2006a). The study by Viant *et al.* (Viant *et al.* 2006a) also found altered levels of ATP as a further indicator of disruption to energy metabolism, however, in this current investigation ATP falls outside of the m/z range analysed so could not be detected. Another study using rat hepatocytes exposed to Dinoseb (Palmeira *et al.* 1994) found a depletion of cellular glutathione, this depletion was proposed to initiate the process of cell death. While not a significant change, a depletion of glutathione (0.6 fold change) was also putatively identified in this investigation following DNP exposure. Cd exposure, unlike the previous metabolomics study of copper toxicity in *D. magna* (Chapter 3), did not induce oxidative stress in the form of glutathione depletion. However, consistent with the reported toxicity of a low concentration of Cd (6 $\mu\text{g/L}$) to *D. magna*, in which Krebs cycle enzymes were disturbed (Connon *et al.* 2008), we detected a significant increase in isocitrate. Previously, Cd has been shown to inhibit the enzyme isocitrate dehydrogenase in

an aquatic invertebrate (Ivanina *et al.* 2008). From a comparison with the significant changes found following Cd exposure in the investigation detailed in Chapter 4, it can be determined that some of the changes putatively identified, specifically decreases in arginine, methionine, histidine and phenylalanine could also be putatively identified in this investigation. However, it needs to be noted that none of these changes are significant and the average fold change for all these metabolites is small (0.8), but could be a further indication of the initial stages of Cd toxicity causing depletion of amino acids for defence and repair mechanisms. Fenvalerate, although unrelated to its action as a neurotoxin, has also been found to reduce Krebs cycle enzyme activity, disrupting primary metabolism in catfish (Tripathi and Verma 2004). In *D. magna* it reduced feeding rate and growth (Reynaldi *et al.* 2006), and a metabolomics study into esfenvalerate toxicity to Chinook salmon (Viant *et al.* 2006b) found decreased levels of ATP and phosphocreatine, all consistent with a perturbation to energy metabolism. Our observations support this, with 1.7- and 1.8-fold increases in AMP ($p=0.1010$) and ADP ($p=0.0850$) respectively, as well as a 2.2-fold increase in phosphoarginine ($p=0.0087$). Propranolol is a non-selective β -adrenergic receptor blocker that is used to treat hypertension (Sui *et al.* 2007). The metabolic effects of this drug in non-target organisms are less well understood, potentially due to the lack of β -adrenergic receptors in cladocerans (Stanley *et al.* 2006). The metabolic rate of *D. magna* was found to decrease in response to acute metoprolol exposure (another β -adrenergic receptor blocker) thought to be a consequence of reduced heart rate (Dzialowski *et al.* 2006). Whilst not significant, small increases (1.2-2 fold changes) in the levels of many amino acids putatively identified in this investigation following acute propranolol exposure could be a build up of these metabolites

due a reduced metabolic rate meaning they are not utilised for general metabolic processes. Propranolol exposure to *D. magna* has also been reported to cause membrane destabilisation (Huggett *et al.* 2002), while mussels exhibited an increase in lipid peroxidation (Sole *et al.* 2010), however, the lipophilic metabolites were not analysed in the current study, hampering the comparison of our data with the published literature. Future analysis of the non-polar fractions would also be particularly advantageous in the case of the potential disruption to energy metabolism indicated by DNP and fenvalerate exposure, as *Daphnia* are known to store energy in the form of triglyceride droplets (Tessier and Goulden 1982).

5.3.4 Multivariate models for discriminating toxicant modes of action

The second aim was to determine if the four toxicants that induced metabolic perturbations were distinguishable according to their MOAs. The metabolic measurements from the individual acute toxicity tests were combined into two datasets (for haemolymph and whole organism homogenates) optimal PLS-DA models were derived, using internal cross-validation to assess their predictive powers. The optimal PLS models each comprised of eight LVs, based upon the minimisation of classification errors, and accounted for $\geq 50\%$ of the total variance in the metabolic data. From the scores plots for haemolymph and whole organism homogenates (LV1 vs. LV2, Figure 5.2a and 5.2b, respectively) a clear clustering of the individual samples within some of the treatment classes is evident, particularly for the whole organism homogenates. However the greatest separation within the haemolymph and whole organism homogenate scores plots, though markedly more obvious for the former, is that of the fenvalerate exposed samples and their corresponding solvent controls away from all

other samples along LV1. This suggested a strong solvent effect. Therefore scores plots showing LV2 vs. LV3 are also plotted (Figure 2c and 2d), which again show separations between some of the treatment classes. Considering both scores plots for haemolymph (Figure 2a and 2c), only the Cd-exposed class clearly separates from all other samples, consistent with the results from the individual toxicant analyses. For the whole organism homogenates (Figure 2b and 2d), there is much more distinct clustering of samples into each of their individual toxicant classes.

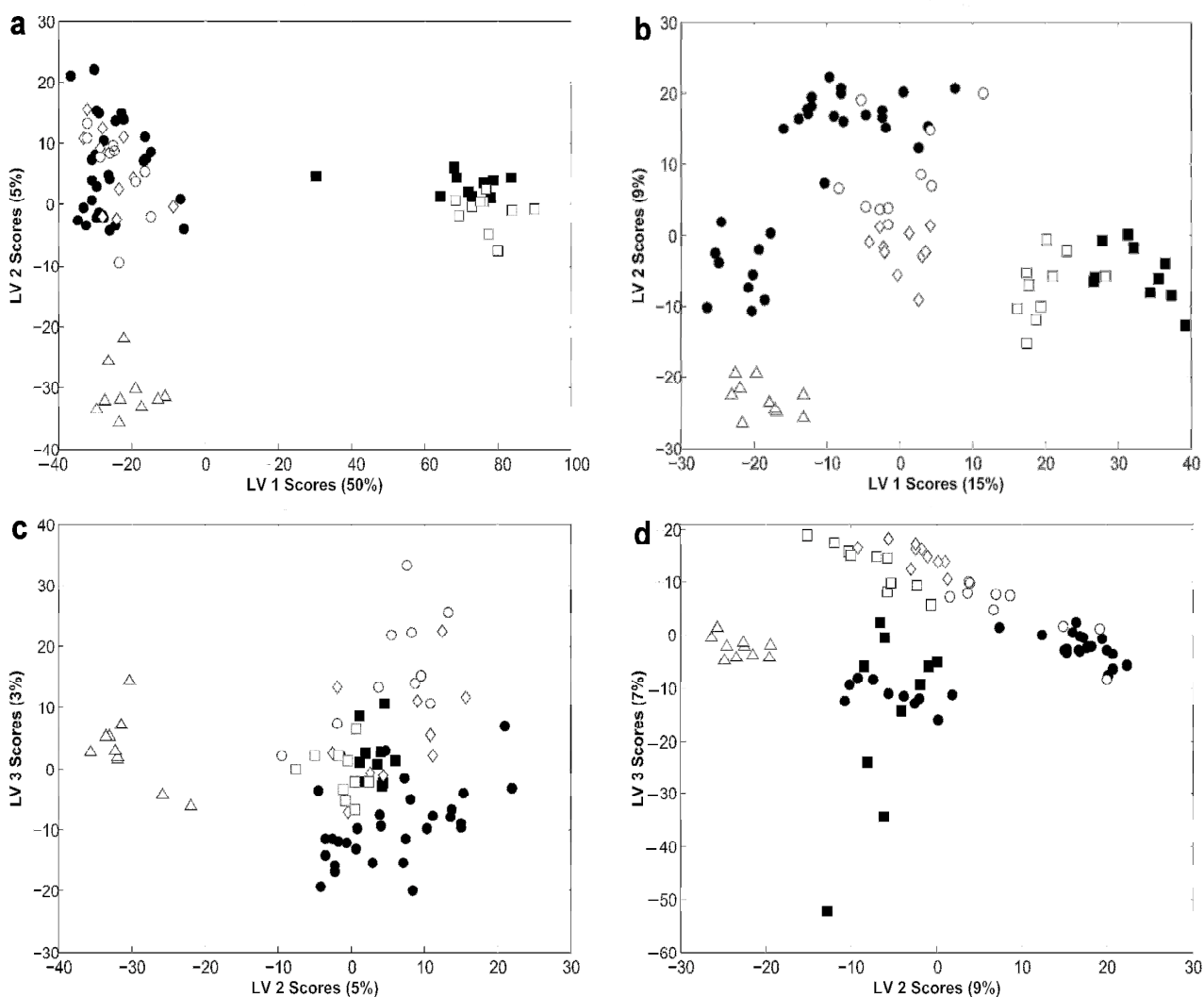


Figure 5.2 PLS-DA scores plots depicting LV1 against LV2 for (a) haemolymph and (b) whole organism homogenates, and LV2 against LV3 for (c) haemolymph and (d) whole organism homogenates of *D. magna* exposed to each of four toxicants. Classes comprise of control (●), solvent control (■), Cd exposed (Δ), DNP exposed (◇), fenvalerate exposed (□) and propranolol exposed (○). For both sample types, the separation along LV1 is dominated by a solvent effect.

Visual examination of PLS-DA scores plots, however, is not a reliable method for determining their predictive power (Westerhuis *et al.* 2008), partly because a 2-dimensional plot can only provide a limited description of the optimal 8-dimensional models calculated here. Therefore robust classification error rates for each of the treatment classes (control, solvent control, Cd, DNP, fenvalerate and propranolol) were calculated using internal cross validation, and the significance of these classification errors determined via permutation testing. The “optimal model” classification error rates for each treatment, for both the haemolymph and whole organism homogenate datasets, are low, confirming the high predictivities of the models (Table 5.6). For both sample types, prediction of Cd-exposed samples had the lowest error rates (both <1%), consistent with the visual interpretation of the PLS-DA scores plots (Figure 5.2). The mean classification error rate (across all four toxicants and two control classes) for the whole organism homogenates (3.9%) is lower than that for haemolymph (6.9%), providing evidence that the whole organism metabolome contains a greater amount of metabolic information that is specific to each of the four toxicant MOAs. These error rates clearly demonstrate that the metabolic responses to the four toxicants can each be differentiated from the others and also from the control groups. To highlight the quality of these predictive models, both Cd- and fenvalerate-induced biomarker signatures are so distinct that each enables >98% of samples to be correctly predicted; and this is true for metabolic perturbations to both the whole organism and haemolymph metabolomes.

Table 5.6 “Optimal model” and “permuted” classification error rates for each of the six exposure classes, and their mean value, for both haemolymph and whole organism homogenates of *D. magna*. The permuted classification error rates are presented as the mean values derived from 1000 random permutations of the class labels.

Haemolymph							
	Control	Solvent control	Cd	DNP	Fenvalerate	Propranolol	Mean
Optimal model classification error rate (%)	11.2	2.7	0.1	17.8	1.2	8.2	6.9
Permuted classification error rate (%)	51.1	50.2	50.8	50.1	50.1	50.8	50.5
Whole organism homogenates							
	Control	Solvent control	Cd	DNP	Fenvalerate	Propranolol	Mean
Optimal model classification error rate (%)	4.0	0.7	0.9	7.6	1.8	8.1	3.9
Permuted classification error rate (%)	50.9	50.1	50.2	50.0	50.4	50.8	50.4

For all six exposure classes, in both sample types, p -value<0.001

Although the classification error rates appear low, these values do not provide any measure of statistical significance. To assess the statistical significance of these apparently highly predictive multivariate models, permutation testing was conducted. One thousand random permutations of the class labels prior to PLS-DA analyses resulted in a distribution of “permuted” classification error rates for each class, the mean of each being ca. 50% (Table 5.6). From analyses of these distributions, the significance of the power of the optimal models to predict each of the four toxicant MOAs and two controls classes was determined to be $p < 0.001$ (i.e. none of the 1000 permuted classification error rates were less than those from the optimal models).

In principle, these predictive models can now be used to classify the metabolic perturbations induced by a toxicant of unknown MOA as similar (or not) to that caused by an inducer of oxidative stress, a sodium channel activator, an uncoupler of oxidative phosphorylation, or a non-selective β -blocker. The actual application of such an approach to chemical toxicity testing would of course require the construction of a larger library of sub-lethal metabolic responses to a series of defined MOAs.

5.3.5 Whole organism metabolome provides more discriminatory predictive models

The final aim was to determine whether the metabolome of haemolymph or of whole organism homogenates was the more discriminatory of the toxicant-induced metabolic perturbations. The univariate and multivariate analyses presented above clearly demonstrate that the whole organism metabolome provides the greatest predictivity of metabolic effect. Specifically, considering the analysis of the effects of the individual toxicants, whole organism

homogenates displayed a higher percentage of significantly changing peaks (average of 11% of all peaks detected across the four toxicants; Table 5.5) than for haemolymph (average of 5.6%). Furthermore, this value for haemolymph is skewed by the Cd exposure (21%), with the remaining three toxicants inducing an average of only 0.5% of all peaks changing significantly; i.e. Cd is the only toxicant to induce a major change in the haemolymph metabolome. Overall this provides evidence that the whole organism metabolome's response to a toxicant is typically more extensive compared to the response of the haemolymph. Further evidence for this can be derived from the PLS-DA models, in which the mean classification error rate (across all four toxicants and two control classes) for the whole organism homogenates (3.9%) is lower than that for haemolymph (6.9%). Hence this confirms that the whole organism metabolome contains a greater amount of metabolic information that is specific to each of the four toxicant-induced perturbations. It can therefore be concluded that whole organism homogenates of *D. magna* should be employed in any future applications of metabolomics in aquatic toxicity testing.

In addition to the evidence presented above, there are several further benefits of using whole organism homogenates over haemolymph. First, whole organism sampling can be applied across all daphnid life-stages while haemolymph can only feasibly be extracted from adult animals. Second, whole organism studies allow for the standardisation of the biomass per sample, this is an important criteria in FT-ICR mass spectrometry as highlighted by the studies conducted in Chapter 3, whereas the volumes of haemolymph extracted can vary

considerably across individuals. Finally, the extraction of haemolymph from daphnids is more time consuming and prone to operator error than simply flash-freezing whole animals.

5.4 Conclusion

This study represents the first reported multiple-toxicant metabolomics study in the OECD recommended test species, *Daphnia magna*. We have confirmed that a metabolic effect can be elucidated using both haemolymph samples and whole organism homogenates for four different toxicants. We have also demonstrated that individual toxicants, with differing MOAs can be distinguished using multivariate classification models with minimal classification error rates. Based upon the results of the individual acute toxicity tests and the combined analysis of all four toxicants, we conclude that whole organism homogenates are the more information-rich sample type for use in predictive toxicology. These findings strengthen the argument that omics approaches could become a valuable additional tool within toxicity testing and ecological risk assessment. Moreover, the ability to use single daphnids for such studies hints at the considerable future potential for causally relating molecular responses to internationally-recognised reproductive fitness.

The next investigation aims to exploit this potential by evaluating the possibility of using metabolic data to predict changes to the reproductive output of *D. magna*; utilising whole organism homogenates of individual *D. magna*, identified here as the more information-rich and reproducible sample type.

CHAPTER SIX:

**Discovering metabolic markers that are predictive of
reduced reproductive output in *Daphnia magna***

6.1 Introduction

Over recent decades the use of biomarker techniques in ecotoxicology has become more popular; looking for molecular indicators of exposure to toxic chemicals that ultimately leads to higher level effects and are, in principle, capable of predicting reduced performance (De Coen and Janssen 2003; Forbes *et al.* 2006; Moore *et al.* 2004). However, despite the early promise of these techniques, they have done little except increase our ability to detect stress responses at low levels of exposure (Preston 2002), and are yet to demonstrate their usefulness in predicting organism fitness and subsequent population to ecosystem level effects (Forbes *et al.* 2006). Lately, the utilisation of metabolomics techniques in toxicity testing have had some success in overcoming the problem of elucidating toxicant MOA (Ebbels *et al.* 2007; Guo *et al.* 2009; Viant *et al.* 2006b), and the previous study (Chapter 5) has also shown this to be possible in *Daphnia magna*. However, until recently the metabolic perturbations determined from metabolomic investigations have also lacked the ability to predict whole organism fitness, such as adverse effects on growth or reproductive output. One metabolomics study that attempts to address this issue was reported by Hines *et al.* (Hines *et al.* 2010) where a measure of physiological response (scope for growth; SFG) and metabolic changes in the marine mussel (*Mytilus edulis*) following exposure to copper or pentachlorophenol (PCP), found metabolic signatures that were predictive of reduced fitness. Since *D. magna* is a keystone species in the freshwater aquatic food web, any adverse effects on this species could cause ecosystem level responses (Flaherty and Dodson 2005) and as such is a vital species for any investigation that can link subcellular changes to whole organism responses. A study reported by De Coen and Janssen (De Coen and Janssen 2003)

successfully attempted to link subcellular changes in *D. magna* to population level responses by measuring chronic effects after 21 d of exposure to a series of toxicants, and building multivariate models to predict changes in pre-defined metabolite changes measured at 96 h. However, unlike metabolomics investigations, which are relatively non-targeted, this study required the selection of short-term exposure endpoints and thus some prior knowledge of toxicant MOA and expected targets of toxicity. Therefore, the main objective of this study is to attempt to find molecular biomarkers of reduced reproductive output in *D. magna*, following toxicant exposure, using FT-ICR MS-based metabolomics (of individual *D. magna* whole-organism homogenates). These investigations used three of the model toxicants investigated in Chapter 5: cadmium (Cd), 2,4-dinitrophenol (DNP) and propranolol, with the initial aim being to induce changes in the reproductive output of *D. magna* following a standard OECD chronic exposure (OECD 1998) to varying concentrations (0.05%-10% of the neonatal LC₅₀; 1% dose common to all three toxicants) of one of these toxicants. Since these studies were conducted on individual daphnids, both the reproductive output and the subsequent FT-ICR MS measurements relate to a single animal. To achieve the objective of biomarker discovery, the development of robust multivariate models using partial least squares regression (PLS-R) were employed to attempt to predict the reproductive output of an individual *D. magna* based upon its metabolic profile.

6.2 Materials and Methods

6.2.1 Determination of sub-lethal concentrations

Initial 21 d test exposures to each of the 3 toxicants were conducted to determine the appropriate concentrations at which the animals were likely to survive throughout the entire exposure period. Individual 3rd brood neonates were exposed to the relevant concentration of toxicant in 250 mL media, exposure vessels were fed daily with *Chlorella vulgaris* as per normal culturing conditions (Section 2.1) without the addition of any supplements. Media and appropriate toxicant renewal occurred every 48 hours. The starting test concentration for each of the three toxicants was 10% of the neonatal LC₅₀ concentration previously determined in Chapter 5 (n=5 exposure vessels per concentration). If mortality occurred within the 21 d exposure period then repeat exposures of a lesser concentrations were set up until a concentration was determined that allowed for survival through the entire test period.

6.2.2 *Daphnia magna* chronic exposures

Individual *D. magna* neonates (3rd brood, <24-h old), in 250 mL media, were exposed for 21 days to varying concentrations of one of the three toxicants tested (n=8 exposure vessels per concentration). Animals were fed daily with *Chlorella vulgaris* as per normal culturing conditions (Section 2.1) without the addition of any supplements, with media and toxicant renewal every 48 hours. Three separate chronic studies were conducted using cadmium, DNP or propranolol as the test chemical. Nominal concentrations were: 0, 0.35, 1.4, 3.5 and 7 µg L⁻¹ cadmium (measured as Cd²⁺ ions); 0, 0.15, 0.75 and 1.5 mg L⁻¹ DNP and 0, 0.14, 0.7 and 1.4

mgL⁻¹ propranolol. As a means of normalising to biological effect, the exposures of 7 µgL⁻¹ cadmium, 0.15 mgL⁻¹ DNP and 0.14 mgL⁻¹ propranolol all corresponded to 1% of the previously determined neonatal LC₅₀ (Chapter 5). For each of the three chronic studies a further control was set up that were not exposed to any toxicants but were fed on a half ration of algae (termed “half-feed control”), in order to see if any of the adverse metabolic effects were due to a reduction in feeding. Throughout each of the 21 d studies reproductive output was monitored and recorded, specifically the number of offspring produced per adult per brood and the day on which each brood was released. Neonates were removed from the test beakers and discarded. Any mortality during the exposure period was also recorded. At the end of the 21 d test period, the now adult daphnids were captured and flash frozen as detailed in Section 2.2, then stored at -80°C prior to metabolite extraction.

6.2.3 Metabolite extraction, FT-ICR MS, data processing and putative peak identification

At the culmination of the 21 d exposure, daphnids were captured (Section 2.2) and metabolites extracted as detailed in Section 2.3.1, including the preparation of an extract blank. FT-ICR MS analysis in negative ion mode was performed on all biological samples and extract blanks as described in Section 2.4, with all samples analysed in triplicate, utilising the SIM-stitching approach.

For each of the three toxicants studied (Cd, DNP and Propranolol), mass spectra were processed as detailed in Section 2.5; the sample filter set to retain only those peaks that occurred in at least 50% of all samples using a 1.8ppm spread along the *m/z* axis for defining unique peaks, and blank peaks were retained only if three times as intense in the biological

sample. This resulted in three separate processed data matrices, one each for Cd, DNP and Propranolol. Subsequently, each matrix was further processed by the addition of missing values, normalised and g-log transformed (transformation parameter $\lambda=7.31\times 10^{-11}$). Putative identification of peaks was as described in Section 2.6, enabling the identification of peaks directly related to the parent toxicants, which were subsequently removed from the datasets prior to statistical analysis.

6.2.4 Statistical analysis

To visualise the effects of each individual toxicant on the metabolome of *D. magna*, PCAs were conducted on the processed data matrices (Section 2.7.1) to generate scores plots. Univariate statistical tests (t-tests; Section 2.7.2) were used to determine if individual peaks (i.e. metabolites) changed significantly between the control and high dose classes. The total number of offspring produced per individual daphnid over the duration of the 21 d study was used as a measure of reproductive output of *D. magna*. For each toxicant, Grubbs statistical tests were employed for each dose group to determine any outliers in the reproductive output data (which were subsequently removed from any further analysis) and ANOVAs (across all controls and dose groups) were then conducted on this data followed by a Tukey-Kramer post-hoc test that revealed any significant differences.

Partial least squares regression (PLS-R) was then employed for each individual toxicant to analyse the metabolic data, whilst simultaneously modelling the reproductive output; this was performed for each of the three toxicants tested. The metabolic data is used as a predictor for the response variable of reproductive output (Wold *et al.* 2001) and PLS-R

attempts to find factors that both capture the variance in the metabolic data and achieves correlation with the reproductive output (Wise *et al.* 2006). Cross validation (venetian blinds with 6 splits) was employed to prevent over-fitting of the data (Wold *et al.* 2001). After cross validation, the quality of the regression model was assessed by comparing the measured and predicted values of reproductive output; this generates a cross-validated R^2 value that is indicative of how well the model might predict the reproductive output of unknown samples (Wise *et al.* 2006; Wold *et al.* 2001). Next, to evaluate the statistical significance of these cross-validated R^2 values, the class labels were randomly permuted and another PLS-R model was built. Internal cross validation was used to calculate a “permuted” R^2 value; this permutation and model building process was repeated 1000 times. Statistical significance, for the prediction of reproductive output, could then be assessed by comparing the actual PLS-R model R^2 value to the null distribution of permuted R^2 values (Westerhuis *et al.* 2008). Specifically the number of instances for which the permuted R^2 values were greater than the actual R^2 value was determined and then divided by the total number of permutations (1000), generating a p -value, with $p < 0.05$ indicating that the metabolic profile associated with exposure to that toxicant was predictive of reduced reproductive output in *D. magna*.

To determine which metabolites were predictive of changes in the reproductive output regression vectors were generated from each of the three PLS-R models; this resulted in a list of regression vectors (related to each of the peaks in the metabolic data) for Cd, DNP and propranolol. In theory, those peaks then deemed to be important predictors could be putatively identified (Wise *et al.* 2006), effectively revealing potential biomarkers of reduced reproductive output in *D. magna*. These regression vectors were subsequently ranked in

order of absolute value and plotted to visually assess what proportion of the total number of peaks dominated the PLS-R models for each toxicant. The original processed metabolic data matrices for each of the toxicant exposures were then restructured in order of their absolute regression vector values (from the highest to the lowest); this allowed further PLS-R model building. Specifically, multiple PLS-R models were built using the restructured data matrices; starting with the peak with the highest absolute regression vector value (P) then incorporating the next peak from this list (P+1, P+2, P+3, etc), until all of the peaks from the metabolic data were included in the model. This resulted in an R^2 value for each further peak included in the model, ultimately generating a list of R^2 values that corresponded to the number of peaks incorporated in the model. This multiple model building process was conducted individually for all three toxicants (Cd, DNP and propranolol), consequently producing a list of R^2 values (for each peak included in the model) for each of the three toxicants. These R^2 values could then be plotted and further assessed to determine the fewest number of peaks that needed to be included in the multi-regression analysis for each toxicant, in order to produce an “optimal” PLS-R model that is highly predictive of reproductive output.

6.3 Results and discussion

6.3.1 Chronic toxicant exposures of *Daphnia magna*

The preliminary 21 d exposures of *D. magna* to both DNP and propranolol determined that 10% of the neonatal LC_{50} (1.5 mgL^{-1} DNP and 1.4 mgL^{-1} propranolol) did not induce any mortality for the duration of the exposure. However, exposure to cadmium did induce

mortality at this concentration, with 100% survival for the duration of a chronic 21 d study only occurring at 1% of the neonatal LC₅₀ (7 µgL⁻¹). Subsequently these concentrations were used as the highest doses of each toxicant for the chronic studies. It should be noted that subjective observations of the animals exposed to Cd showed them to be very immobile and pale in colour at the end of this period.

No mortality occurred during the 21 d exposure to propranolol. Some mortality occurred during the chronic exposures in both the Cd and DNP studies. Specifically, during the Cd exposure: 1 animal died in each of the 0 and 1.4 µgL⁻¹ doses, 5 animals died at 3.5 µgL⁻¹ and 3 animals died at 7 µgL⁻¹. Due to the high levels of mortality in the Cd exposure, the 3.5 and 7 µgL⁻¹ doses were subsequently grouped together as one dose for the analysis of reproductive output. During the DNP exposure, 1 animal died in each of the 0, 0.15 and 0.75 mgL⁻¹ dose groups.

6.3.2 Metabolic effects of toxicant exposure

During FT-ICR MS analysis of the biological samples, it should be noted that one sample from the half-feed control in the propranolol exposure failed to spray. Putative identification of peaks following data processing allowed for the identification of two peaks ([Dinitrophenol-H]⁻ and [Dinitrophenol (¹³C)-H]⁻) in the DNP dataset that directly related to the parent toxicant, these were removed prior to statistical analysis. Whilst determining a toxicant induced metabolic effect was not an objective of this investigation, the metabolic data is nonetheless required for the development of the predictive models and subsequent biomarker discovery. Multivariate analysis (PCA) of the metabolic data for each toxicant is

presented in Figure 6.1. Visual interpretation of the PCA scores plots shows a clear separation between the different dose groups following exposure to both Cd and propranolol (Figure 6.1a and 6.1c respectively), indicating a toxicant induced metabolic effect. Exposure to DNP (Figure 6.1b) is less well separated suggesting less of a toxicant effect in this instance. For all three toxicant exposures the half-feed group was separated from the control and toxicant exposed groups confirming that none of the toxicants caused a starvation effect. Table 6.1 summarises the total number of peaks found in each of the three toxicant studies, along with the proportion of those peaks that were significant following univariate analysis (Student's t-tests between control and high dose samples; adjusted for FDR<5%). Consistent with the PCA results, where little class separation was visible, the proportion of significant peaks in the DNP data is only 2.6% of the total peaks detected. The high proportion of significant peaks in the Cd and propranolol datasets (59 and 44% respectively) is again consistent with the clear separation seen in the corresponding scores plots.

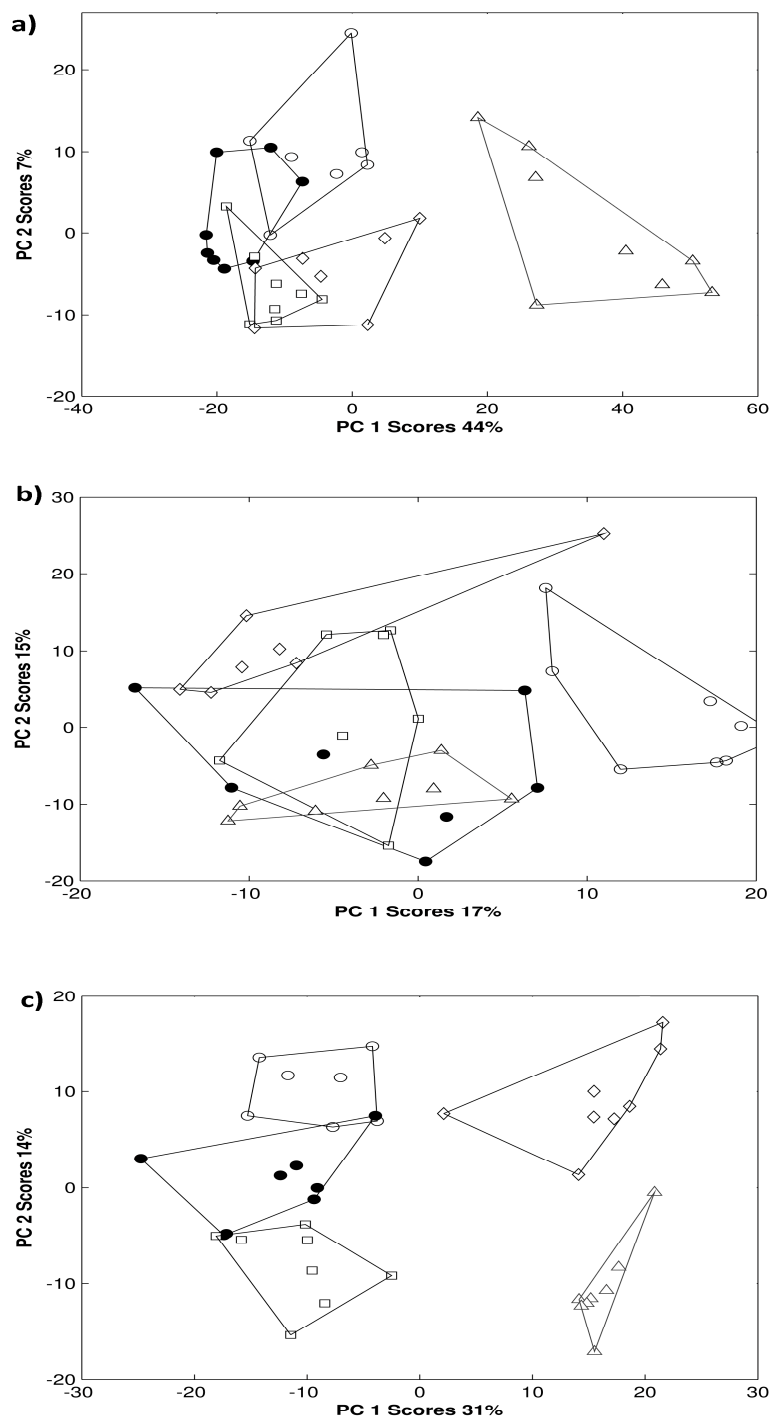


Figure 6.1 PCA scores plot from analysis of the negative ion FT-ICR mass spectra from the *D. magna* chronic studies exposed to (a) Cd, (b) DNP and (c) Propranolol. Classes comprise of control (●), half-feed control (○), Low dose (□), medium dose (◇) and high dose(s) (Δ).

Table 6.1 The total number of peaks detected and the proportion of peaks that significantly changed concentration (FDR<0.05) between the control and high dose groups, following chronic exposure of *D. magna* to cadmium, DNP and propranolol.

	Cd	DNP	Propranolol
Total Number of peaks	4056	4112	3647
Proportion of significant peaks (%)	59	2.6	44

6.3.3 Effects of chronic toxicant exposure on the reproductive output of *D. magna*

The initial aim of this study was to induce a change in the reproductive output of individual *D. magna* following chronic toxicant exposure to Cd, DNP or propranolol. The reproductive output of *D. magna* was assessed in terms of the total number of offspring produced per individual daphnid throughout the 21 d exposure period. Figure 6.2 depicts the reproductive output for every surviving animal for all three toxicants (Cd, DNP and propranolol). Grubbs outlier tests determined that the reproductive output from two animals in the DNP exposure were outliers (one in the low dose group and one in the medium dose group) and these have subsequently been removed from the data. Visual interpretation of the plots shows a distinct reduction in reproductive output with increasing toxicant dose following Cd exposure (Figure 6.2a). A clear toxicant induced effect can be seen following propranolol exposure (Figure 6.2c) but little effect can be seen on reproductive output following exposure to DNP (Figure 6.2b). Univariate statistical analysis (ANOVA across the dose groups) determined statistically significant effects on *D. magna* reproductive output for all three toxicants: Cd ($p= 1.73 \times 10^{-}$

²⁰), DNP ($p= 1.49 \times 10^{-6}$) and propranolol ($p= 1.52 \times 10^{-15}$). Subsequent Tukey-Kramer post-hoc tests revealed that significant reproductive differences in the Cd exposed daphnids occurred between all dose groups except for between the half-fed and low dose group. In the DNP exposed daphnids the control, low and medium dose groups were significantly different to the half-fed and high dose groups. The reproductive output from the control group of daphnids in the propranolol exposure were significantly different from all other dose groups, with the half-fed and low dose groups also proving to be significantly different from the medium and high dose groups. These significant findings are consistent with the plots in Figure 6.2, and establish that a reduction reproductive output of the daphnids has been induced by each of the toxicants, with the most notable reduction occurring following exposure to Cd.

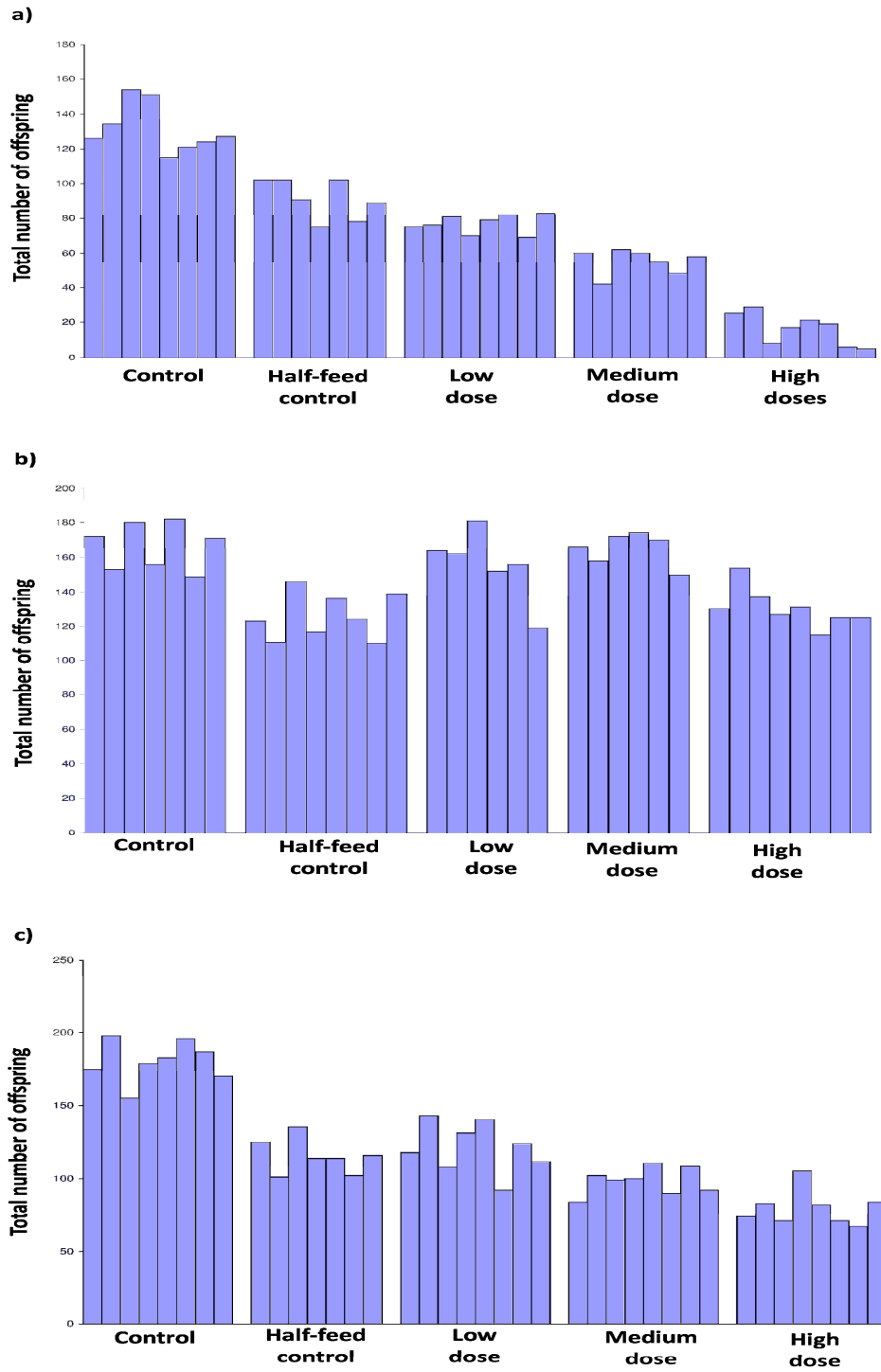


Figure 6.2 Bar charts of the reproductive output of individual *D. magna* following 21 d exposure to (a) Cd, (b) DNP and (c) Propranolol.

6.3.4 Development of predictive multivariate models

The overall objective of this study was to discover metabolic biomarkers that are predictive of reduced reproductive output in *D. magna* following toxicant exposure. In order to achieve this, cross-validated multivariate models were developed for each of the three toxicants (Cd, DNP and propranolol) using PLS-R (Figure 6.3). The models were then evaluated as to how well they might predict the reproductive output of unknown samples. The PLS-R models generated high cross-validated R^2 values for all three toxicants: Cd (4056 peaks; $R^2 = 0.822$), DNP (4112 peaks; $R^2 = 0.768$) and propranolol (3647 peaks; $R^2 = 0.735$), suggesting high predictive capabilities of each model, consistent with the highly correlated plots depicted in Figure 6.3.

To assess the statistical significance of these apparently highly predictive multivariate models, permutation testing was conducted. One thousand random permutations of the class labels prior to PLS-R analyses resulted in a distribution of “permuted” cross-validated R^2 values, the mean for each toxicant being ca. 0.05. From analyses of these distributions, the significance of the power of the actual PLS-R models to predict the reproductive output of individual *D. magna* was determined to be $p < 0.001$ (i.e. none of the 1000 permuted cross-validated R^2 values were greater than those from the actual models) for all three toxicants. The statistical significance of these highly predictive models demonstrates that signals from the mass spectra of individual *D. magna* can be utilised to predict the reproductive output of daphnids exposed to toxicants of the same or similar MOA and potentially extrapolation to subsequent population/ecosystem effects.

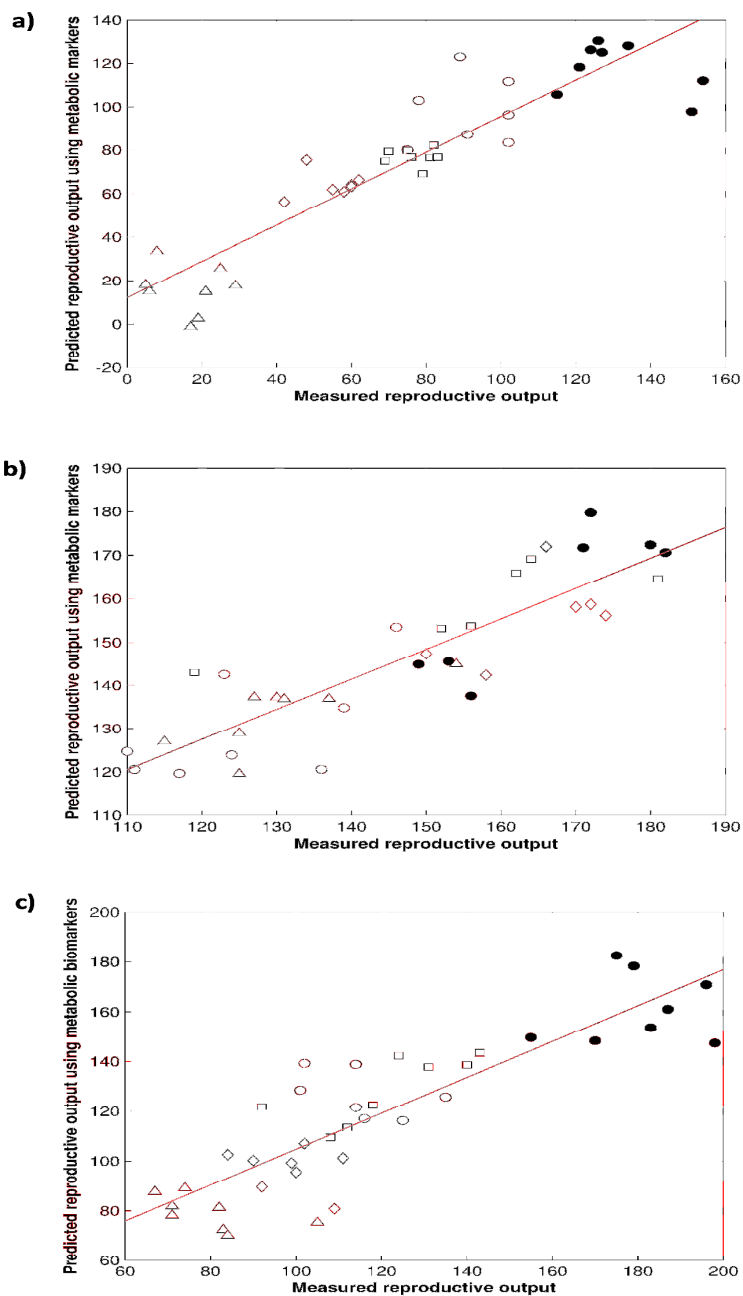


Figure 6.3 Correlation between measured and predicted reproductive output for individual daphnids, the latter derived from a PLS-R model and the metabolic signatures of individual daphnids following exposure to (a) Cd, (b) DNP and (c) propranolol, including lines of best fit. The cross-validated R^2 values are 0.822 for Cd (4056 peaks), 0.768 for DNP (4112 peaks) and 0.735 for propranolol (3647 peaks); $p < 0.001$ in all cases. Classes comprise of control (●), half-feed control (○), Low dose (□), medium dose (◇) and high dose(s) (Δ).

6.3.4.1 Development of optimal predictive models using each toxicant

When building PLS-R models, regression vectors are generated; the highest regression vectors relate to the m/z value of those peaks that are most predictive of reduced reproductive output of *D. magna* using the metabolic data. This resulted in a ranked list of absolute regression vectors for each toxicant (Cd, DNP and propranolol). These regression vectors are depicted in Figure 6.4, and clearly show that only a small proportion of the total numbers of peaks dominate the PLS-R models. As detailed in Section 6.2.4, these ranked regression vector values were then used to build multiple PLS-R models for each toxicant, incorporating increasing numbers of peaks. This strategy generated a list of R² values for each toxicant; these are depicted in Figure 6.5. Consistent with the plots of regression vectors (Figure 6.4), it can clearly be seen only a small proportion of the total peaks are required to achieve a high R² value, thus a highly predictive model, for all three toxicants. Forward selection was utilised to determine the fewest number of peaks required to build an “optimal” highly predictive model (i.e. generating a high R² value), using a cut-off point of within 1% of the greatest R² value generated by the multiple model building strategy. This determined that (in order of absolute regression vector value), the top 107 peaks from the Cd dataset, the top 502 peaks from the DNP dataset and the top 170 peaks from the propranolol dataset would build toxicant specific models that are highly predictive of reduced reproductive output in *D. magna*. The peaks determined from the forward selection strategy are detailed on the Supplementary Information CD (Tables SI3, SI4 and SI5 for Cd, DNP and propranolol respectively). The number of peaks required to build optimal predictive models is consistent with toxicant induced effects of reproductive output in Figure 6.2, the

clearest toxicant induced effect is in the Cd data (Figure 6.2a) and requires the fewest peaks in the optimal model, whereas the lack of toxicant induced effect in the DNP data (Figure 6.2b) requires the largest number of peaks in the optimal model.

Utilising the peaks from the forward selection strategy, optimal PLS-R models were then built (Figure 6.6). These models generated cross-validated R^2 values of 0.937 for Cd, 0.851 for DNP and 0.907 for propranolol. These are all noticeably higher than the values generated from the original models (0.822 for Cd, 0.768 for DNP and 0.735 for propranolol) but consistent in their predictive capabilities, with the Cd dataset being the most predictive of reduced reproductive output in *D. magna*. It is notable that, for all three toxicants, over one hundred peaks are required to build the optimal, highly predictive, PLS-R models. This indicates that a lot of metabolic data is required to predict reduced reproductive output in *D. magna*.

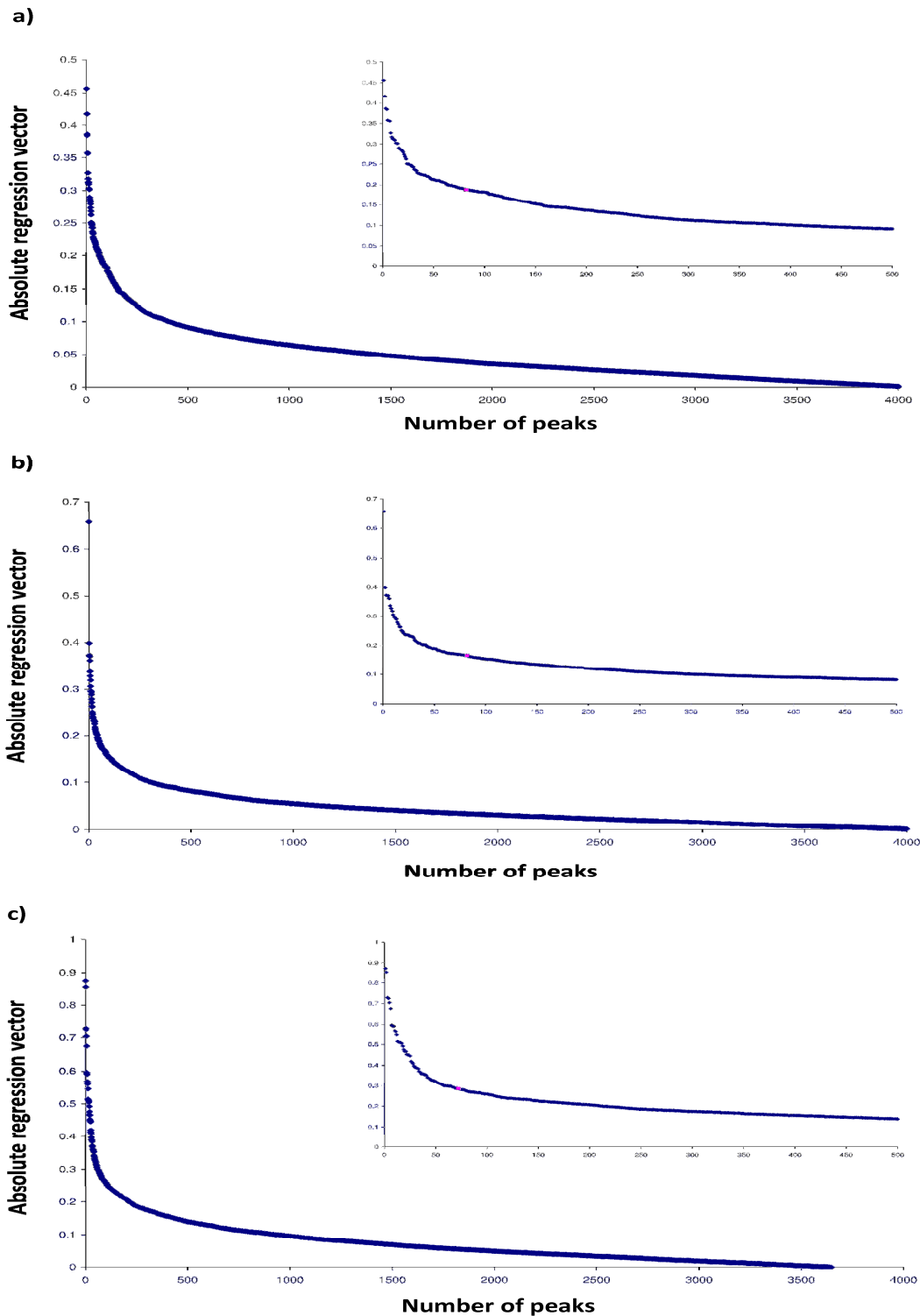


Figure 6.4 Plots of the ranked absolute regression vectors generated from the building of PLS-R models using metabolic and reproductive output data from individual *D. magna* following 21 d exposure to (a) Cd, (b) DNP and (c) Propranolol. The inset plots are the top 500 peaks in each instance.

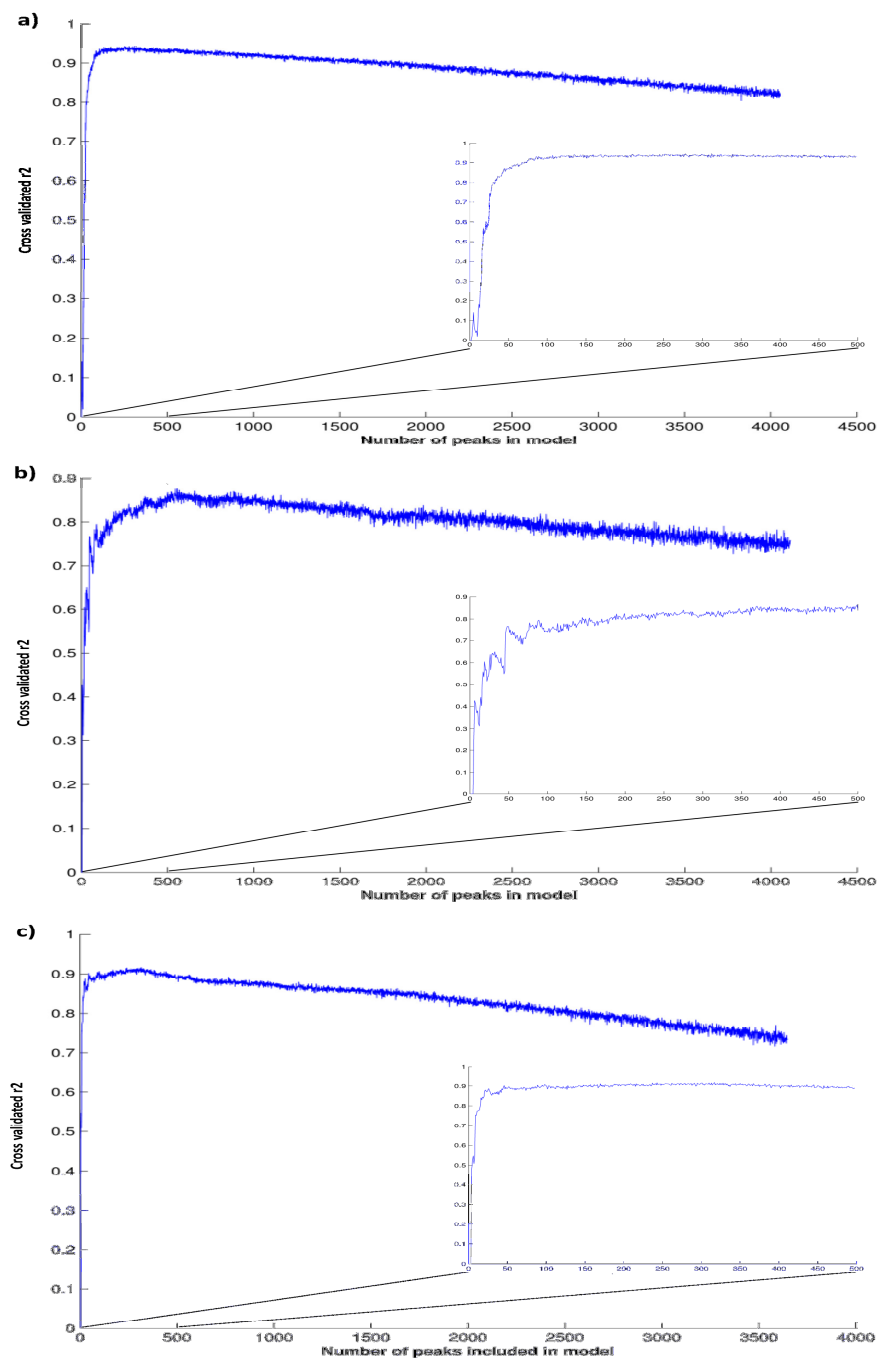


Figure 6.5 Plots of the R^2 values of increasing numbers of peaks (ranked by absolute regression vector) incorporated into the building of PLS-R models using metabolic and reproductive output data from individual *D. magna* following a 21 d exposure to (a) Cd, (b) DNP and (c) Propranolol. The inset plots are the first 500 peaks included in the model in each instance. This data was used in a forward selection strategy for building an optimal PLS-R model for each toxicant.

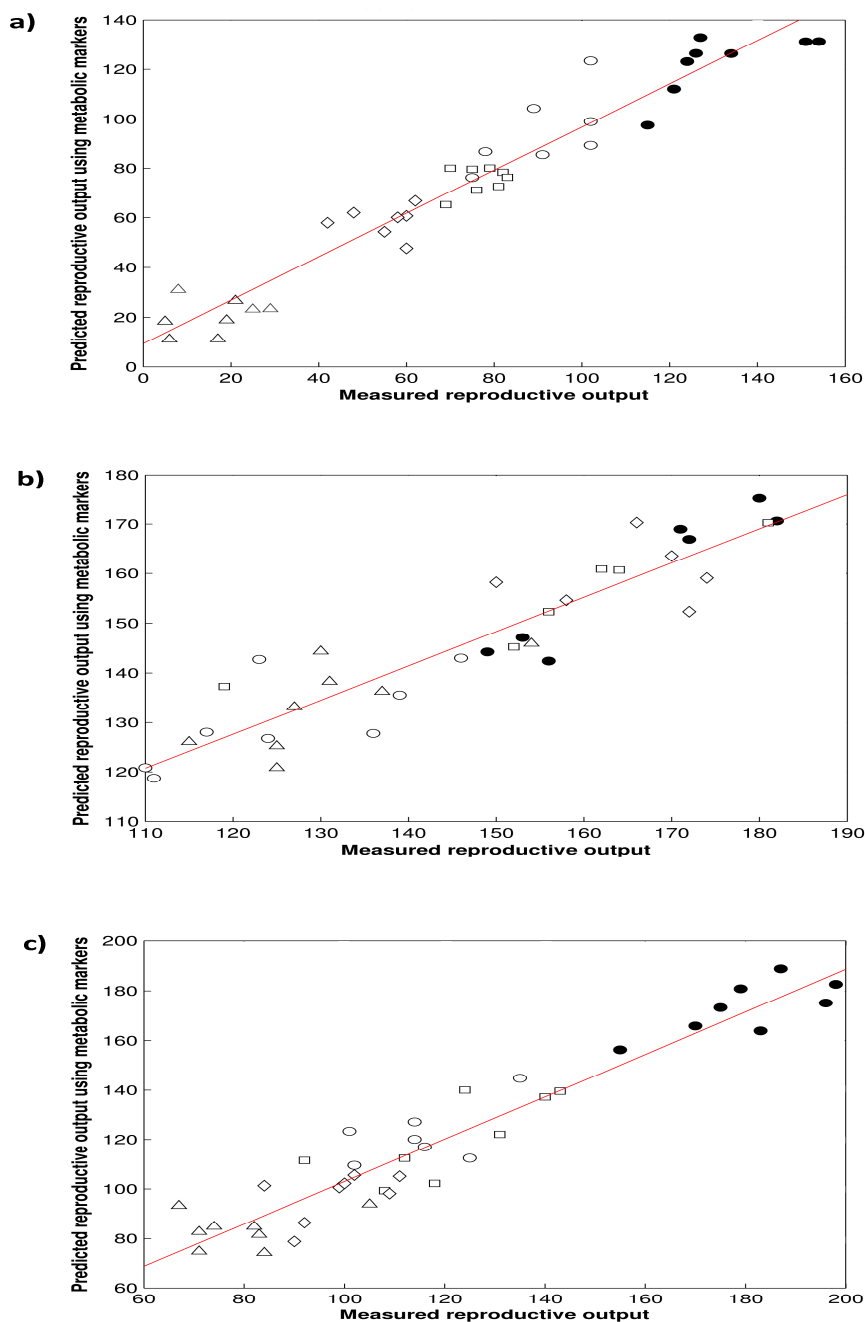


Figure 6.6 Correlation between measured and predicted reproductive output for individual daphnids, the latter derived from an optimal PLS-R model and the metabolic signatures of individual daphnids following exposure to (a) Cd, (b) DNP and (c) propranolol, including lines of best fit. The cross-validated R^2 values are 0.937 for Cd (107 peaks), 0.851 for DNP (502 peaks) and 0.907 for propranolol (170 peaks). Classes comprise of control (●), half-feed control (○), Low dose (□), medium dose (◇) and high dose(s) (Δ).

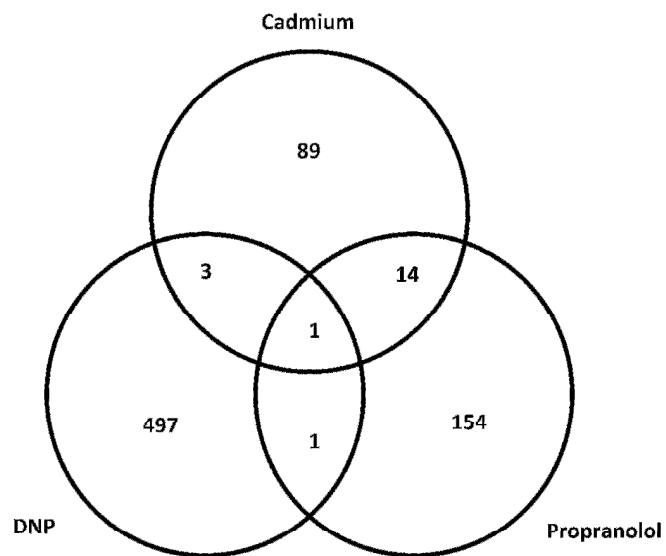
6.3.5 Discovery of biomarkers predictive of reduced reproductive output in *D. magna*

One objective of this study was to find molecular biomarkers of exposure, regardless of toxicant MOA. Therefore, the peaks that were determined from the forward selection strategy for use in the optimal (but toxicant specific) PLS-R predictive models were assessed to establish whether there were any common peaks across the three toxicant models (Cd, DNP and propranolol). Putative identification of these peaks could then identify potential biomarkers of reduced reproductive output (Wise *et al.* 2006). A peak was deemed to be common across the datasets if it occurred within a 1 ppm error range. Figure 6.7a visually depicts the common peaks from the three toxicant datasets; clearly the majority of common peaks occur between the Cd and propranolol datasets, with less overlap with the DNP data in both cases and only one peak common across all three toxicants. To confirm that the appearance of common peaks was not purely by chance due to using a large number of peaks, random permutations ($n=3$) of the datasets were utilised to assess this (Figure 6.7b). This clearly shows that no common peaks were found using the permuted data giving confidence in the occurrence of the common peaks in the real data and their potential to be biomarkers of reduced reproductive output in *D. magna*.

The common peaks across two or more of the three datasets are explicitly listed in Table 6.2, along with the putative identification of those peaks using the modified KEGG database as described in Section 2.6. Further information on the significance and fold change of these peaks (Student's t-tests between control and high dose samples; adjusted for $FDR < 5\%$) detailed in Table 6.3. There is a degree of consistency of the fold changes and significance of some of the peaks are detailed in Table 6.3 highlighting these peaks in particular as metabolic

biomarkers of reduced reproductive output, regardless of toxicant MOA. Interestingly there are also some inconsistencies (marked as bold in Table 6.3) which suggests that the predictive models are somewhat toxicant specific and the metabolic changes are related to the toxicant with the reduced reproductive output just well correlated rather than causally related.

a)



b)

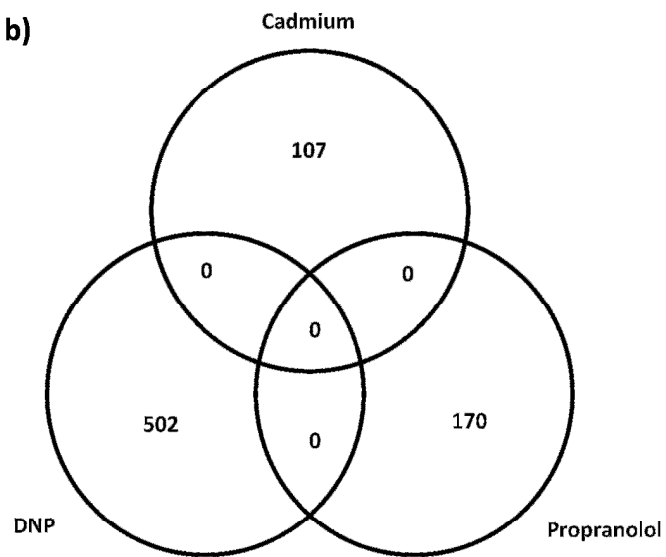


Figure 6.7 Venn diagrams depicting the common peaks from (a) the optimal PLS-R models of individual daphnids following exposure to Cd, DNP and propranolol and (b) the mean of 3 random permutations of the same data.

Table 6.2 Summary of the common peaks the optimal PLS-R models of individual *D. magna* following exposure to cadmium, DNP and propranolol. With the putative identification of metabolites using a modified KEGG database.

Cd	DNP	Propranolol	Empirical formula of putatively identified metabolite	Putative metabolite identification ^a
145.06265	145.06267			
175.02481	175.0248	175.02482	C ₆ H ₈ O ₆	Ascorbate (11)
181.07302	181.07308		C ₇ H ₁₀ N ₄ O ₂	Lathyrine
196.04518	196.04505			
237.99488		237.9949		
251.09631		251.09627		
275.00834		275.00834		
277.2178		277.2178		M1 (¹² C)
278.22116		278.22116		M1 (¹³ C)
295.99316		295.99326		
340.12549		340.12564		
	354.17616	354.17634		
359.22133		359.22124		
392.97009		392.96982		
400.14692		400.14709		
411.27628		411.27618		
441.17365		441.17369		
474.97352		474.97312		
475.17612		475.17586		

^a Following removal of assignments in which the match was a non-endogenous metabolite such as a drug, plasticiser or pesticide. However, compounds such as secondary alkaloid metabolites and bacterial metabolites have not been removed and the presence of these reflects the fact that empirical formulae are insufficient for unambiguous metabolite identification. The number in parentheses represents the total number of possible metabolites that match the stated empirical formula.

Table 6.3 Summary of the common peaks the optimal PLS-R models of individual *D. magna* following exposure to cadmium, DNP and propranolol. Showing the significance and fold change values for each of the peaks following Student's t-tests between control and high dose samples; adjusted for FDR<5%. Peaks marked in bold text show inconsistency in fold changes between toxicants.

m/z	Cd	DNP	Propranolol
145.063	0.938	0.802	-
175.025	0.498	0.636	0.571
181.073	6.722 (***)	0.574	-
196.045	2.199	0.478	-
237.995	1.354	-	7.225
251.096	0.503 (*)	-	0.188 (***)
275.008	0.704	-	0.298 (**)
277.218	0.229	-	0.736
278.221	0.260	-	0.753
295.993	0.438 (*)	-	0.383 (**)
340.125	11.993	-	5.284 (***)
354.176	-	0.571	0.375
359.221	0.337	-	0.931
392.970	0.128 (***)	-	0.204 (**)
400.147	20.737	-	7.558 (***)
411.276	0.164	-	1.433
441.174	0.534	-	1.011
474.973	0.182 (***)	-	0.209 (**)
475.176	10.705 (**)	-	0.625

*** p=0.005

** p=0.01

* p=0.05

6.3.5.1 Potential biomarker of reduced reproductive output in *D. magna*

Ultimately, the ideal route forward is extensive metabolite identification of the peaks that were utilised in the optimal PLS-R models for each of the three toxicants. A biomarker signature of >100 peaks rather than a single or several peaks is a more robust approach to relating subcellular changes to whole organism response. This would create models of metabolic signatures that are predictive of toxicant specific induced reduction in reproduction in *D. magna*. However, such extensive metabolite identification is extremely challenging and new methods are being developed to overcome this problem. Until this is achievable, here, we focus on the single peak that was determined to be an important predictor of reduced reproductive output in *D. magna* across all three toxicants, this has been putatively identified as ascorbate (Table 6.2). The fold change in this peak is also consistent across the three toxicants (a mean 2-fold decrease from control to high dose) indicating that a reduction in ascorbate could be a biomarker of exposure that is causally related to reduced reproductive output in *D. magna*, regardless of toxicant MOA. Ascorbate has long been associated with fertility (Loh and Wilson 1971), it is considered an essential biochemical for reproduction and potentially a significant factor in human fertility (Luck *et al.* 1995). In the aquatic environment, ascorbate is used as a supplement in the aquaculture of fish as it is deemed such an important nutrient for reproductive function, a deficiency causing reduced gamete production and quality and thus fertility (Ciereszko and Dabrowski 1995; Dabrowski and Ciereszko 2001). There is evidence that ascorbate performs a protective role against genetic defects during gametogenesis in fish (Dabrowski and Ciereszko 2001) and it has also been proposed as a biomarker of ovulation in the seabass (*Dicentrarchus labrax*)

(Guerriero *et al.* 1999). Similar findings have also been reported in the aquaculture of Penaeid shrimp, where high levels of dietary ascorbate were related to a high hatch rate of *Fenneropenaeus indicus* eggs (Wouters *et al.* 2001) and a diet high in ascorbate also increased the resistance of postlarvae shrimp (*Penaeus monodon* and *Penaeus vannamei*) to infection and stress (Merchie *et al.* 1997). The previously reported study by De Coen and Janssen (2003) which attempted to link early biomarkers of exposure to whole organism responses found that the highest contributions to the predictive models for growth and survival were obtained from cellular energy allocation measurements (particularly lipid content) and parameters related to oxidative stress (catalase and DNA damage) (De Coen and Janssen 2003). The lipid fractions of the samples used in this investigation were not analysed, however, the potential discovery of a reduction in ascorbate, combined with its well known anti-oxidant properties (Padayatty *et al.* 2003) are consistent with the speculation that damage caused by oxidative stress is predictive of reduced survival capabilities of *D. magna* (De Coen and Janssen 2003).

Our findings indicate that a decrease in ascorbate levels in *D. magna*, could be predictive of reduced reproductive output as it features highly in all three optimal PLS-R models (for Cd, DNP and propranolol). The reported evidence of high levels of ascorbate relating to high levels of fertility and reproductive function gives confidence in the putative identification of this predictive peak as ascorbate, however, further work is required to confirm the identity of this peak, and indeed of the other peaks that could potentially be predictive of reduced reproductive output in *D. magna*. Techniques such as tandem MS (MS/MS) can be used,

allowing structural identification of metabolites from interpretation of fragment ions and fragmentation patterns (Dunn and Ellis 2005).

6.4 Conclusion

This study has established that metabolic signatures from individual *D. magna* exposed to toxicants can be used to develop multivariate models that are highly predictive of reduced reproductive output. Furthermore, it has determined that biomarkers of reduced reproductive output can be elucidated that are either toxicant specific (Cd, DNP or propranolol) or generic. One particular example from this work is the possibility that decreased ascorbate levels could be a generic biomarker of reduced reproductive function in *D. magna*. However, this investigation has also highlighted that a lot of metabolic data is required to build highly predictive models and, despite the challenge of metabolite identification, metabolomics studies are ideal for measuring hundreds of metabolites simultaneously requiring no prior knowledge of toxicant MOA. Since chronic studies are both resource and time expensive, methods that reduce these costs are the ultimate aim for ecotoxicological studies that are predictive of whole organism responses (Santojanni *et al.* 1998). The greatest validation of this approach would therefore be to determine if short-term (acute) exposure to these toxicants could establish the same metabolic perturbations and biomarkers of toxicity. Overall, this investigation highlighted the considerable potential of using non-targeted metabolomics to find measurements of subcellular responses that can be predictive of higher level biological responses, with subsequent implications for population and ecosystem dynamics.

CHAPTER SEVEN:

Final Conclusions and Future Work

At the start of this research four aims were outlined (Section 1.8) in order to achieve the primary objective of this thesis in exploring the potential for FT-ICR mass spectrometry based metabolomics in regulatory toxicity testing using *Daphnia magna*. Initially the feasibility of using this approach with the small, freshwater invertebrate, *D. magna* had to be assessed (Chapters 3 and 4). The concept of a metabolic biomarker signature that informs upon toxicant MOA (Chapter 5) and on reproductive fitness (Chapter 6) was then explored, using different metabolite signatures for each outcome. How well these aims were addressed will be considered and what further work is necessary, either to entirely fulfil these aims or in light of the findings from each investigation.

7.1 The feasibility of FT-ICR MS-based metabolomics for toxicity testing using *Daphnia magna*

The first aim of this thesis was to optimise an FT-ICR mass spectrometry based metabolomics approach using whole organism homogenates of *D. magna*; subsequently validating this technique using copper as a model toxicant and assessing its feasibility for use in first-tier toxicity testing.

The studies detailed in Chapter 3 are the first reported metabolomics investigations utilising the keystone freshwater aquatic invertebrate *D. magna*. The findings confirm that FT-ICR MS, coupled with the SIM-stitching spectral processing approach, is an effective method of toxicity testing using *D. magna* whole organism homogenates. Specifically, during the optimisation studies it was highlighted that this approach was a highly sensitive technique, detecting many thousands of signals, and was reproducible, capable of discriminating between different life-stages of *Daphnia*. A further discovery during the optimisation studies

was that the technique also discriminated between differing masses of biological material drawing an important conclusion that the amount of biological material used in this approach needs to be standardised for any direct comparison of the results. This finding is important for FT-ICR MS metabolomics studies of any biological sample. The feasibility of this approach for future first-tier toxicity testing was confirmed by the results from the acute copper toxicity tests. Here, supervised multivariate analysis (PLS-DA) enabled the classification of samples into differing degrees of copper toxicity, with a high degree of consistency of the copper induced metabolic changes between the positive and negative ion mode mass spectrometry measurements. Putative identification of peaks identified potential biomarkers of toxicity that were consistent with the known MOA of copper, including known biomarkers of oxidative stress such as depleted GSH and a decrease in the amino acid pool. In addition to this, the discovery of increased N-acetylspermidine following copper exposure as a potential new biomarker highlighted the potential of this approach for metabolic biomarker discovery and mechanistic insight into toxicant MOA. Further analysis would be required to confirm N-acetylspermidine as a novel biomarker of copper toxicity, such as tandem MS to confirm the metabolic identity of this signal in the mass spectrum or targeted analysis such as HPLC on levels of N-acetylspermidine following copper, or indeed other heavy metals, exposures. These findings have validated the FT-ICR MS approach as an effective approach, ideal for high throughput first-tier screening of chemicals in *D. magna*. Future studies using other toxicants with well documented MOAs would add further validity to this approach.

An area where this approach has its limitations is in the identification of metabolites. Each peak could comprise of more than one metabolite as structural isomers will not be separated

by the direct infusion FT-ICR approach and none of the metabolite assignments reported in this study can be regarded as unambiguous since they depend only on accurate mass. To overcome these issues, a hyphenated technique such as LC-MS or tandem MS could be employed, however, these techniques would prevent this being a high-throughput approach. Since the overall objective of these studies was to assess this approach for use in high-throughput screening and prioritisation of toxicants for further testing then it can be concluded that the outcomes of these studies have met this aim.

7.2 The FT-ICR MS-based metabolomics approach using *Daphnia magna* haemolymph

Following the achievement of the first aim of optimising and validating the FT-ICR MS metabolomics approach for toxicity testing using whole body homogenates of *D. magna* the second aim of this thesis was to optimise the same approach using *D. magna* haemolymph. The premise for using haemolymph as a biological sample being that it could provide a “cleaner” biological sample for detecting significant metabolic changes when compared to whole organism homogenates that could mask subtle toxicant induced effects (i.e. organ or tissue specific effects). The toxicant induced metabolic effects on *D. magna* haemolymph were evaluated in conjunction with the findings from a transcriptomics study of further *D. magna* whole organism samples, both using cadmium (Cd) as a model toxicant.

The findings from the studies in Chapter 4 determined that the FT-ICR MS approach was feasible for use with small pools of daphnid haemolymph. Several thousand unique signals were detected, clearly distinguishable from an extract blank sample that contains no biological material. This is comparable to the signals detected by the previous studies that

utilised whole organism homogenates of *D. magna* (Chapter 3) which were concluded to be suitable for first-tier toxicity testing (Section 7.1). In assessing the validity of using haemolymph for high-throughput toxicity testing, an acute exposure using Cd as a model toxicant was employed. Following unsupervised multivariate analysis (PCA), the results of this exposure demonstrated a clear and significant Cd induced metabolic effect on the daphnid haemolymph samples. Univariate analysis determined which peaks were changing significantly due to Cd exposure and these were then putatively identified, specifically significant changes included decreases in amino acids, fatty acids and nucleic acids.

The primary objective of these studies was to evaluate the use of *D. magna* haemolymph as a biological sample for high-throughput toxicity testing using FT-ICR MS-based metabolomics. The high quality mass spectra produced during this study, along with the significant metabolic changes induced by exposure to Cd, permits the conclusion that using this approach with small pooled samples of haemolymph is feasible for determining toxicant induced effects in *D. magna*. Consequently this determines that daphnid haemolymph could also be utilised for first-tier screening and prioritisation of toxicants. The second objective of using both metabolomic and transcriptomic investigations to examine the toxicity of Cd to *D. magna* was also achieved. A level of consistency between the findings from the two approaches allowed for the development of a model of Cd toxicity, where a depletion of both lipid and protein reserves would likely result in decreased fitness and survival during prolonged exposure. Again, further studies using other toxicants with well documented MOAs would be necessary to completely establish that the use of *D. magna* haemolymph is a viable sample type for the FT-ICR MS approach.

The major limitation with this investigation is the use of two different biological sample types between the metabolomics and transcriptomics investigation. Whereas the metabolomics investigation utilised haemolymph samples, the transcriptomic analyses were conducted on separate whole organism samples. Ideally for a direct comparison of findings, these two omics methods would utilise the same biological material. It is unclear from this investigation as to whether the use of daphnid haemolymph provides a “cleaner” biological sample for toxicity studies. It would therefore be beneficial to conduct a metabolomics investigation that utilises both whole organism homogenates and haemolymph samples of *D. magna*, which can then be used to assess which would be the better sample type to use for future omics approaches to toxicity testing.

7.3 The discrimination of toxicant MOA via changes in the daphnid metabolome

It has now been concluded that both whole organism homogenates and haemolymph samples of *D. magna* are both feasible sample types for use with the FT-ICR MS approach for high-throughput toxicity testing (Sections 7.1 and 7.2). In order to build upon these findings, the third aim of this thesis was to develop robust multivariate (PLS-DA) models that can discriminate toxicant modes of action in *D. magna* acute toxicity tests, and to evaluate whether the haemolymph or whole organism metabolome is better at discriminating toxicant mode of action (Chapter 5). The model toxicants chosen for this investigation were cadmium (Cd; an inducer of oxidative stress), fenvalerate (induces hyper-excitation through prolonged opening of sodium channels), 2,4-dinitrophenol (DNP; an uncoupler of oxidative

phosphorylation) and propranolol (a non-selective β -blocker), and each sample related to an individual adult daphnid.

To achieve this aim, it was first necessary to establish that each of these toxicants induced a detectable metabolic effect following an acute exposure, in both the whole organism and haemolymph metabolome. Unsupervised multivariate analysis confirmed that significant metabolic perturbations were induced by each toxicant in both sample types, the most notable following Cd exposure for both the whole organism homogenates and the haemolymph samples. Subsequent univariate analysis determined that the proportion of significant peaks was also greatest following Cd exposure for both sample types, although in general, the proportion of significant peaks was greater in the whole organism metabolome.

With the conclusion that a significant toxicant induced effect could be determined in all cases, the second aim was to determine if the four different MOAs could be distinguished in daphnids based upon the measured metabolic responses. The development of supervised multivariate models, coupled to robust cross-validation and permutation testing, was employed to evaluate this. The models generated were highly predictive for both the whole organism and haemolymph metabolomes, with small classification error rates of 3.9% for the whole organism homogenates and 6.9% for haemolymph. The predictive power of these models was determined to be significant following permutation testing for both sample types. It can therefore be concluded that the metabolome of *D. magna* can be used to discriminate between toxicant MOA, using either whole organism homogenates or haemolymph samples.

The final aim of these investigations was to evaluate whether the metabolome of haemolymph or of whole organism homogenates was the more discriminatory of toxicant MOA. The first evidence that the whole organism metabolome's response to a toxicant is typically more extensive (and potentially contains more information) compared to the response of the haemolymph comes from the analysis of the individual toxicants. Here the proportion of significantly changing peaks is greater in the whole organism metabolome, particularly when comparing the results from the DNP, fenvalerate and propranolol exposures. Secondly the development of the predictive multivariate models determined that the predictive capabilities of the whole organism metabolome are higher than in the haemolymph metabolome, highlighted by the smaller classification error rate in this case. In addition to the results of the experimental data, further support for using the whole organism metabolome is that; whole organism sampling can be applied across all daphnid life-stages while haemolymph can only feasibly be extracted from adult animals. Moreover, whole organism studies allow for the standardisation of the biomass per sample, an important issue highlighted in Section 7.1, whereas the volumes of haemolymph extracted can vary considerably across individuals with the extraction of haemolymph from daphnids being more time consuming and prone to error.

The overall conclusion from these investigations is that different toxicant MOAs can be distinguished using highly predictive multivariate classification models, and that the whole organism metabolome of *D. magna* is the better sample type for use in predictive toxicology. In principle, these predictive models can now be used to classify the metabolic perturbations induced by a toxicant of unknown MOA as similar (or not) to that caused by an inducer of

oxidative stress, a sodium channel activator, an uncoupler of oxidative phosphorylation, or a non-selective β -blocker. Ideally, more confidence in these predictive models would come from having more than one toxicant in each category of MOA which should, in theory, produce the same metabolic perturbations to daphnids. Another consideration that needs to be taken into account is the degree of toxicity of similar chemicals. In this investigation the selection of 10% of the neonatal LC₅₀ as the dose was intended to “normalise” the study to a fixed degree of biological effect. However chemicals with similar MOAs may incur toxic effects over differing timescales so a more robust approach would have been to design a dose-response study with a range of sampling time-points for a thorough comparison of multiple toxicant MOAs. However, constraints on both time and resources prevented such an exhaustive investigation in this thesis. Nevertheless, the actual application of such an approach to chemical toxicity testing is certainly feasible but would require the construction of a larger library of sub-lethal metabolic responses to a series of defined MOAs.

7.4 The discovery of metabolic markers which are predictive of reduced reproductive output in *Daphnia magna*

Subsequent to discovering that FT-ICR MS-based metabolomics can be used to discriminate between toxicant MOAs (Section 7.3) the final aim of this thesis was to attempt discover metabolic markers in individual *D. magna* exposed to model toxicants that are predictive of reproductive output, regardless of toxicant MOA (Chapter 6). This is an exceptionally important step in any toxicity study as previous attempts to link metabolic markers of toxicity

to relevant higher level biological effects have been relatively unsuccessful, yet are the ultimate aim in ecotoxicology (Section 1.2.2).

The first step in achieving this final aim was to induce changes in the reproductive output of *D. magna* following a standard OECD chronic exposure to Cd, DNP or propranolol. A chronic 21 d exposure of individual daphnids to each of these toxicants induced a significant reduction in the reproductive output of *D. magna*, successfully achieving this initial aim. FT-ICR MS analysis of the same individual daphnids was then conducted and the metabolic data, coupled with the reproductive output data, was used to build multivariate (PLS-R) models and their ability to predict the reproductive output of unknown samples was evaluated. For all three toxicants significant and highly predictive PLS-R models were developed, demonstrating that signals from the mass spectra of individual *D. magna* can be utilised to accurately predict the reproductive output of daphnids exposed to these toxicants. To achieve the overall objective of biomarker discovery, regression vectors, generated from the PLS-R predictive models were utilised to identify those peaks that were most predictive of reduced reproductive output of *D. magna* for each toxicant. Following a forward selection strategy that established the fewest number of these peaks required to build an optimal (the most predictive) PLS-R model for each toxicant, a comparison of these selected peaks across all three datasets generated a list of common peaks. Putative identification of these peaks (based upon accurate mass measurements) could then be employed to identify biomarkers of toxicity that are predictive of reduced reproductive function in *D. magna*. The comparison of common peaks across all three toxicant datasets revealed only a limited number of potential biomarkers and only a single peak that was common to all three toxicants. This

peak was putatively identified as ascorbate, and was found to be decreased following toxicant exposure. Whilst this is consistent with previous reports of the role of this metabolite in reproductive function, it is dangerous to assume that this single metabolite can act as a biomarker of reduced reproductive function in *D. magna*. In fact, considering that the optimal PLS-R models in this study required a contribution from many metabolites (over 100 signals for each toxicant), it is highly unlikely that ascorbate alone is predictive of reproductive output; i.e. these findings highlight the fact that to generate highly predictive models, a signature of metabolic biomarkers is required rather than just a single or even a few measurements. This in turn highlights how a metabolomics approach is ideally suited to acquiring this kind of signature as one of its greatest advantages is the ability to measure several hundred markers simultaneously, with no prior knowledge of toxicant MOA required. Such studies into signatures of biomarkers would allow for the identification of the top rated regression vectors for each of the individual toxicants, producing a list of toxicant specific biomarkers for reduced reproductive output. However, as stated in Section 7.1, one of the limitations with metabolite identification of FT-ICR MS data is its ambiguity. With this in mind, future studies would require techniques such as tandem MS (MS/MS), which can attempt to confirm the identity of these peaks, creating a signature of biomarkers that are predictive of reduced reproductive output in *D. magna*. The ultimate validation of this approach would be to link acute biomarkers of exposure to reproductive output, thus removing the need for time and resource expensive chronic tests. Therefore, further studies that involve an acute exposure of *D. magna* to these model toxicants would be necessary to elucidate whether the same metabolic biomarkers of toxicity can be identified at 24 h as

occur after 21 d of exposure. Overall though, this investigation can conclude that multivariate models can be built, generating biomarkers which are predictive of reduced reproductive function in *D. magna*, even if identification of these markers requires further analysis.

7.5 Future work

Firstly it needs to be noted that all the toxicant concentrations stated in this thesis are nominal concentrations and the actual exposure concentrations may well be less than those stated, due factors such as the toxicant adhering to the glass exposure vessels. Therefore, any future work should incorporate the analysis of media samples to determine the exact toxicant concentrations. Whilst the metabolomics approach used in this thesis was relatively non-targeted, in effect only a proportion of the metabolome was actually investigated. In particular, analysis of the non-polar metabolites (i.e. lipophilic compounds) would be extremely beneficial for all of the investigations conducted in this thesis. Alongside this, for the investigations detailed in Chapters 4, 5 and 6, FT-ICR MS analysis was only conducted in negative ion mode so effectively only those metabolites that ionise well in this mode would be detected. Therefore, further analysis of the polar fractions of these samples in positive ion mode would also allow for a more definitive idea of how the metabolome responded in each investigation. Another limiting factor applied in all the investigations in this thesis is that the metabolome was only analysed from 70-500 m/z , this could be expanded to incorporate a larger m/z scale, in order to detect higher mass metabolites, such as ATP which occurs outside of this region and could be an important indicator of changes to energy metabolism. Although, this would require a longer analysis time and specifically taking into account the

small sample size available when using *D. magna*, there is a finite length of time for which the sample can be delivered into the mass spectrometer. These results would provide more insight into the biochemistry of toxicant effects in *D. magna*, corroborating the current findings and enabling further comparisons with other reported studies.

Biochemical insight into the MOA of toxicants is highly valuable for the future of regulatory toxicity testing; being able to identify the target(s) of toxicity will enable confidence in the extrapolation of effects across species. It can be determined if the species under consideration is at risk by knowing these target sites, if the organism has the relevant receptors/pathways then it is likely to be susceptible to the toxicant, thus driving the need for higher level toxicity testing. As yet it is unknown whether the metabolic changes determined by the approach used in this thesis are the direct results of, for example, a toxicant induced increase or inhibition of metabolite production. To determine this, further experiments such as flux analysis could be utilised by radio-labelling the food source and investigating which metabolites have incorporated these stable isotopes, allowing for determining which biochemical pathways have been perturbed. Having said this, in order for gaining true insight into the metabolic changes, the greatest challenge that needs to be overcome in this approach is that of metabolite identification. Until this is achieved only putative identifications can be given to the signals in the mass spectra. In this approach, incorporation of more adducts into the empirical formula algorithm could potentially allow more putative identifications; specifically this could be advantageous for metal exposures where the metal itself could be incorporated as an additional adduct. As yet, the only way to

be certain of the identity of any metabolite is to employ fragmentation approaches such as MS/MS, which in turn reduce the capabilities of this being a high throughput technique.

One final consideration is that all the studies in this thesis used a single strain of *D. magna* as the test organism and could be considered specific to just this particular species, or indeed strain. Future studies may therefore benefit from using multiple strains or species of *Daphnia* to determine if toxicant effects are generic or dependent upon the sensitivity of the target organism. However, even if these effects are determined to be specific to only this particular strain of *D. magna*, adverse effects caused by toxicant exposure could lead to a subsequent loss of genetic diversity within this species, with wider implications for future population dynamics in response to further stress. It should also be noted that all the metabolic investigations detailed in this thesis apply to strictly controlled laboratory experiments and do not reflect the natural environment of *D. magna*. Whilst this was a suitable approach for the objectives of this thesis in evaluating the metabolomics approach for use in toxicity testing and chemical screening/prioritisation, any future studies that aim to reflect potential effects of toxicant exposure in the natural environment need to consider fluctuating environmental parameters such as day length, temperature, pH and water chemistry.

7.6 Final conclusions

The driving force behind the investigations detailed in this thesis was to evaluate the potential of FT-ICR mass spectrometry based metabolomics for use in regulatory toxicity testing using *Daphnia magna*. Each study has appropriately addressed and met its individual aims (Sections 7.1 to 7.4) with a high degree of success and ultimately highlighting areas that

need further exploration (Section 7.5), yet outside of the scope of this thesis due to time and resource limitations. These investigations have determined that this novel approach to toxicity testing in *D. magna* can be used with both whole organism homogenates and haemolymph samples, bringing to light the advantages of using the whole organism metabolome. Toxicants with differing MOAs can be discriminated using this approach and models can be built that predict reduced reproductive function, a highly valuable advantage for regulatory decision making as this could prove beneficial when attempting to extrapolate results to predict population/ecosystem dynamics. In view of these findings it can be concluded that the FT-ICR mass spectrometry based metabolomics approach for use in regulatory toxicity testing using *Daphnia magna* is extremely viable.

CHAPTER EIGHT:

References

Ahlers, J., Stock, F., and Werschkun, B. (2008). Integrated testing and intelligent assessment- new challenges under REACH. *Environmental Science and Pollution Research International* **15**, 565-72.

Ankley, G. T. (2008). *Genomics in regulatory ecotoxicology : applications and challenges. In collaboration with the Society of Environmental Toxicology and Chemistry*. CRC Press, Boca Raton ; London.

Arambasic, M. B., Bjelic, S., and Subakov, G. (1995). Acute toxicity of heavy metals (copper, lead and zinc), phenol and sodium on *Allium cepa* L, *Lepidium sativum* L and *Daphnia magna* ST - comparative investigations and the practical applications. *Water Research* **29**, 497-503.

Baldovin, A., Wu, W., Centner, V., JouanRimbaud, D., Massart, D. L., Favretto, L., and Turello, A. (1996). Feature selection for the discrimination between pollution types with partial least squares modelling. *Analyst* **121**, 1603-1608.

Barata, C., Navarro, J. C., Varo, I., Riva, M. C., Arun, S., and Porte, C. (2005). Changes in antioxidant enzyme activities, fatty acid composition and lipid peroxidation in *Daphnia magna* during the aging process. *Comparative Biochemistry and Physiology B-Biochemistry & Molecular Biology* **140**, 81-90.

Benjamini, Y., and Hochberg, Y. (1995). Controlling the False Discovery Rate - a Practical and Powerful Approach to Multiple Testing. *Journal of the Royal Statistical Society Series B-Methodological* **57**, 289-300.

Benson, W. H., Gallagher, K., and McClintock, J. T. (2007). U.S. Environmental Protection Agency's activities to prepare for regulatory and risk assessment applications of genomics information. *Environmental and Molecular Mutagenesis* **48**, 359-62.

Berlett, B. S., and Stadtman, E. R. (1997). Protein oxidation in aging, disease, and oxidative stress. *Journal of Biological Chemistry* **272**, 20313-20316.

Bligh, E. G., and Dyer, W. J. (1959). A rapid method of total lipid extraction and purification. *Canadian Journal of Biochemistry and Physiology* **37**, 911-917.

Bopp, S. K., Abicht, H. K., and Knauer, K. (2008). Copper-induced oxidative stress in rainbow trout gill cells. *Aquatic Toxicology* **86**, 197-204.

Breitholtz, M., Ruden, C., Hansson, S. O., and Bengtsson, B. E. (2006). Ten challenges for improved ecotoxicological testing in environmental risk assessment. *Ecotoxicology and environmental safety* **63**, 324-35.

Breitling, R., Pitt, A. R., and Barrett, M. P. (2006). Precision mapping of the metabolome. *Trends in Biotechnology* **24**, 543-548.

Breitling, R., Vitkup, D., and Barrett, M. P. (2008). New surveyor tools for charting microbial metabolic maps. *Nature Reviews Microbiology* **6**, 156-161.

Brendonck, L., and De Meester, L. (2003). Egg banks in freshwater zooplankton: evolutionary and ecological archives in the sediment. *Hydrobiologia* **491**, 65-84.

Brown, S. C., Kruppa, G., and Dasseux, J. L. (2005). Metabolomics applications of FT-ICR mass spectrometry. *Mass Spectrometry Reviews* **24**, 223-231.

Bundy, J. G., Davey, M. P., and Viant, M. R. (2009). Environmental metabolomics: a critical review and future perspectives. *Metabolomics* **5**, 3-21.

Bundy, J. G., Keun, H. C., Sidhu, J. K., Spurgeon, D. J., Svendsen, C., Kille, P., and Morgan, A. J. (2007). Metabolic profile biomarkers of metal contamination in a sentinel terrestrial species are applicable across multiple sites. *Environmental Science & Technology* **41**, 4458-4464.

Bundy, J. G., Lenz, E. M., Bailey, N. J., Gavaghan, C. L., Svendsen, C., Spurgeon, D., Hankard, P. K., Osborn, D., Weeks, J. M., and Trauger, S. A. (2002). Metabonomic assessment of toxicity of 4-fluoroaniline, 3,5-difluoroaniline and 2-fluoro-4-methylaniline to the earthworm *Eisenia veneta* (Rosa): Identification of new endogenous biomarkers. *Environmental Toxicology and Chemistry* **21**, 1966-1972.

Bundy, J. G., Osborn, D., Weeks, J. M., Lindon, J. C., and Nicholson, J. K. (2001). An NMR-based metabonomic approach to the investigation of coelomic fluid biochemistry in earthworms under toxic stress. *Febs Letters* **500**, 31-5.

Bundy, J. G., Sidhu, J. K., Rana, F., Spurgeon, D. J., Svendsen, C., Wren, J. F., Sturzenbaum, S. R., Morgan, A. J., and Kille, P. (2008). 'Systems toxicology' approach identifies coordinated metabolic responses to copper in a terrestrial non-model invertebrate, the earthworm *Lumbricus rubellus*. *Bmc Biology* **6**, -.

Casero, R. A., and Pegg, A. E. (1993). Spermidine Spermine N1-Acetyltransferase - the Turning-Point in Polyamine Metabolism. *Faseb Journal* **7**, 653-661.

Chapman, P. M. (2002). Integrating toxicology and ecology: putting the "eco" into ecotoxicology. *Marine pollution bulletin* **44**, 7-15.

Ciereszko, A., and Dabrowski, K. (1995). Sperm Quality and Ascorbic-Acid Concentration in Rainbow-Trout Semen Are Affected by Dietary Vitamin-C - an across-Season Study. *Biology of Reproduction* **52**, 982-988.

Coen, M., Holmes, E., Lindon, J. C., and Nicholson, J. K. (2008). NMR-based metabolic profiling and metabonomic approaches to problems in molecular toxicology. *Chemical Research in Toxicology* **21**, 9-27.

Coffino, P., and Poznanski, A. (1991). Killer Polyamines. *Journal of Cellular Biochemistry* **45**, 54-58.

Colbourne, J. K., Singan, V. R., and Gilbert, D. G. (2005). wFleaBase: the Daphnia genomics information system: <http://wfleabase.org/>

Connon, R., Hooper, H. L., Sibly, R. M., Lim, F. L., Heckmann, L. H., Moore, D. J., Watanabe, H., Soetaert, A., Cook, K., Maund, S. J., Hutchinson, T. H., Moggs, J., De Coen, W., Iguchi, T., and Callaghan, A. (2008). Linking molecular and population stress responses in *Daphnia magna* exposed to cadmium. *Environmental Science & Technology* **42**, 2181-2188.

Dabrowski, K., and Ciereszko, A. (2001). Ascorbic acid and reproduction in fish: endocrine regulation and gamete quality. *Aquaculture Research* **32**, 623-638.

De Coen, W. M., and Janssen, C. R. (1997a). The use of biomarkers in *Daphnia magna* toxicity testing .2. Digestive enzyme activity in *Daphnia magna* exposed to sublethal concentrations of cadmium, chromium and mercury. *Chemosphere* **35**, 1053-1067.

De Coen, W. M., and Janssen, C. R. (1997b). The use of biomarkers in *Daphnia magna* toxicity testing. IV. Cellular Energy Allocation: a new methodology to assess the energy budget of toxicant-stressed *Daphnia* populations. *Journal of Aquatic Ecosystem Stress and Recovery (Formerly Journal of Aquatic Ecosystem Health)* **6**, 43-55.

De Coen, W. M., and Janssen, C. R. (1998). The use of biomarkers in *Daphnia magna* toxicity testing - I. The digestive physiology of daphnids exposed to toxic stress. *Hydrobiologia* **367**, 199-209.

De Coen, W. M., and Janssen, C. R. (2003). A multivariate biomarker-based model predicting population-level responses of *Daphnia magna*. *Environmental Toxicology and Chemistry* **22**, 2195-2201.

Dettmer, K., Aronov, P. A., and Hammock, B. D. (2007). Mass spectrometry-based metabolomics. *Mass Spectrometry Reviews* **26**, 51-78.

Dieterle, F., Ross, A., Schlotterbeck, G., and Senn, H. (2006). Probabilistic quotient normalization as robust method to account for dilution of complex biological mixtures. Application in ¹H NMR metabonomics. *Analytical Chemistry* **78**, 4281-90.

Dodson, S. I., and Hanazato, T. (1995). Commentary on effects of anthropogenic and natural organic chemicals on development, swimming behavior, and reproduction of *Daphnia*, a key member of aquatic ecosystems. *Environmental health perspectives* **103 Suppl 4**, 7-11.

Drysdale, G. R., and Cohn, M. (1958). Mode of Action of 2,4-Dinitrophenol in Uncoupling Oxidative Phosphorylation. *Journal of Biological Chemistry* **233**, 1574-1577.

Dunn, W. B. (2008). Current trends and future requirements for the mass spectrometric investigation of microbial, mammalian and plant metabolomes. *Physical biology* **5**, 11001.

Dunn, W. B., Bailey, N. J. C., and Johnson, H. E. (2005). Measuring the metabolome: current analytical technologies. *Analyst* **130**, 606-625.

- Dunn, W. B., and Ellis, D. I. (2005). Metabolomics: Current analytical platforms and methodologies. *Trends in Analytical Chemistry* **24**, 285-294.
- Dzialowski, E. M., Turner, P. K., and Brooks, B. W. (2006). Physiological and reproductive effects of beta adrenergic receptor antagonists in *Daphnia magna*. *Archives of Environmental Contamination and Toxicology* **50**, 503-10.
- Ebbels, T. M. D., Keun, H. C., Beckonert, O. P., Bollard, M. E., Lindon, J. C., Holmes, E., and Nicholson, J. K. (2007). Prediction and classification of drug toxicity using probabilistic modeling of temporal metabolic data: The Consortium on Metabonomic Toxicology screening approach. *Journal of Proteome Research* **6**, 4407-4422.
- Edwards, S. W., and Preston, R. J. (2008). Systems biology and mode of action based risk assessment. *Toxicological Sciences* **106**, 312-8.
- Ekman, D. R., Teng, Q., Villeneuve, D. L., Kahl, M. D., Jensen, K. M., Durhan, E. J., Ankley, G. T., and Collette, T. W. (2008). Investigating compensation and recovery of fathead minnow (*Pimephales promelas*) exposed to 17 alpha-ethynylestradiol with metabolite profiling. *Environmental Science & Technology* **42**, 4188-4194.
- Escher, B. I., and Hermens, J. L. (2002). Modes of action in ecotoxicology: their role in body burdens, species sensitivity, QSARs, and mixture effects. *Environmental Science & Technology* **36**, 4201-17.
- Evans, S. M., and Nicholson, G. J. (2000). The use of imposex to assess tributyltin contamination in coastal waters and open seas. *The Science of the Total Environment* **258**, 73-80.

Flaherty, C. M., and Dodson, S. I. (2005). Effects of pharmaceuticals on *Daphnia* survival, growth, and reproduction. *Chemosphere* **61**, 200-7.

Fleuret, F. (2004). Fast binary feature selection with conditional mutual information. *Journal of Machine Learning Research* **5**, 1531-1555.

Forbes, V. E., Palmqvist, A., and Bach, L. (2006). The use and misuse of biomarkers in ecotoxicology. *Environmental Toxicology and Chemistry* **25**, 272-80.

Gaetke, L. M., and Chow, C. K. (2003). Copper toxicity, oxidative stress, and antioxidant nutrients. *Toxicology* **189**, 147-63.

Griffin, J. L. (2003). Metabonomics: NMR spectroscopy and pattern recognition analysis of body fluids and tissues for characterisation of xenobiotic toxicity and disease diagnosis. *Current Opinion in Chemical Biology* **7**, 648-654.

Griffin, J. L., Walker, L. A., Shore, R. F., and Nicholson, J. K. (2001). High-resolution magic angle spinning H-1-NMR spectroscopy studies on the renal biochemistry in the bank vole (*Clethrionomys glareolus*) and the effects of arsenic (As³⁺) toxicity. *Xenobiotica* **31**, 377-385.

Guerriero, G., Paolucci, M., and Ciarcia, G. (1999). Vitamin C: A biomarker of the ovulation in sea bass, *Dicentrarchus labrax*. *Free Radical Biology and Medicine* **27**, S154-S154.

Guo, Q., Sidhu, J. K., Ebbels, T. M. D., Rana, F., Spurgeon, D. J., Svendsen, C., Sturzenbaum, S. R., Kille, P., Morgan, A. J., and Bundy, J. G. (2009). Validation of metabolomics for toxic mechanism of action screening with the earthworm *Lumbricus rubellus*. *Metabolomics* **5**, 72-83.

Han, J., Danell, R. M., Patel, J. R., Gumerov, D. R., Scarlett, C. O., Speir, J. P., Parker, C. E., Rusyn, I., Zeisel, S., and Borchers, C. H. (2008). Towards high-throughput metabolomics using ultrahigh-field Fourier transform ion cyclotron resonance mass spectrometry. *Metabolomics* **4**, 128-140.

Heckmann, L.-R., Sibly, R. M., Connon, R., Hooper, H. L., Hutchinson, T. H., Maund, S. J., Hill, C. J., Bouetard, A., and Callaghan, A. (2008). Systems biology meets stress ecology: Linking molecular and organismal stress responses in *Daphnia magna*. *Genome Biology* **9**, Article no. R40.

Hines, A., Staff, F. J., Widdows, J., Compton, R. M., Falciani, F., and Viant, M. R. (2010). Discovery of metabolic signatures for predicting whole organism toxicology. *Toxicological Sciences* doi: **10.1093/toxsci/kfq004**.

Huggett, D. B., Brooks, B. W., Peterson, B., Foran, C. M., and Schlenk, D. (2002). Toxicity of select beta adrenergic receptor-blocking pharmaceuticals (B-blockers) on aquatic organisms. *Archives of Environmental Contamination and Toxicology* **43**, 229-235.

Hutchinson, T. H., Ankley, G. T., Segner, H., and Tyler, C. R. (2006). Screening and testing for endocrine disruption in fish-biomarkers as "signposts," not "traffic lights," in risk assessment. *Environmental Health Perspectives* **114 Suppl 1**, 106-14.

Ivanina, A. V., Habinck, E., and Sokolova, I. M. (2008). Differential sensitivity to cadmium of key mitochondrial enzymes in the eastern oyster, *Crassostrea virginica* Gmelin (Bivalvia : Ostreidae). *Comparative Biochemistry and Physiology C-Toxicology & Pharmacology* **148**, 72-79.

Jobling, S., Nolan, M., Tyler, C. R., Brighty, G., and Sumpter, J. P. (1998). Widespread sexual disruption in wild fish. *Environmental Science & Technology* **32**, 2498-2506.

Jones, O. A. H., Spurgeon, D. J., Svendsen, C., and Griffin, J. L. (2008). A metabolomics based approach to assessing the toxicity of the polyaromatic hydrocarbon pyrene to the earthworm *Lumbricus rubellus*. *Chemosphere* **71**, 601-609.

Kanehisa, M., Goto, S., Hattori, M., Aoki-Kinoshita, K. F., Itoh, M., Kawashima, S., Katayama, T., Araki, M., and Hirakawa, M. (2006). From genomics to chemical genomics: new developments in KEGG. *Nucleic Acids Research* **34**, D354-D357.

Kaplan, F., Kopka, J., Haskell, D. W., Zhao, W., Schiller, K. C., Gatzke, N., Sung, D. Y., and Guy, C. L. (2004). Exploring the temperature-stress metabolome of *Arabidopsis*. *Plant Physiology* **136**, 4159-68.

Katsiadaki, I., Williams, T. D., Ball, J. S., Bean, T. P., Sanders, M. B., Wu, H. F., Santos, E. M., Brown, M. M., Baker, P., Ortega, F., Falciani, F., Craft, J. A., Tyler, C. R., Viant, M. R., and Chipman, J. K. (2009). Hepatic transcriptomic and metabolomic responses in the Stickleback (*Gasterosteus aculeatus*) exposed to ethinyl-estradiol. *Aquatic Toxicology*
doi:10.1016/j.aquatox.2009.07.005.

Keun, H. C. (2006). Metabonomic modeling of drug toxicity. *Pharmacology & Therapeutics* **109**, 92-106.

Keun, H. C., Ebbels, T. M. D., Antti, H., Bollard, M. E., Beckonert, O., Schlotterbeck, G., Senn, H., Niederhauser, U., Holmes, E., Lindon, J. C., and Nicholson, J. K. (2002). Analytical reproducibility in H-1 NMR-based metabonomic urinalysis. *Chemical Research in Toxicology* **15**, 1380-1386.

Kind, T., and Fiehn, O. (2007). Seven Golden Rules for heuristic filtering of molecular formulas obtained by accurate mass spectrometry. *BMC Bioinformatics* **8**, 105.

Kluender, C., Sans-Piche, F., Riedl, J., Altenburger, R., Hartig, C., Laue, G., and Schmitt-Jansen, M. (2009). A metabolomics approach to assessing phytotoxic effects on the green alga *Scenedesmus vacuolatus*. *Metabolomics* **5**, 59-71.

Knops, M., Altenburger, R., and Segner, H. (2001). Alterations of physiological energetics, growth and reproduction of *Daphnia magna* under toxicant stress. *Aquatic Toxicology* **53**, 79-90.

Lansing, M. B., Gardner, W. S., and Eadie, B. J. (1993). Catecholamines as Potential Sublethal Stress Indicators in Great-Lakes Macroinvertebrates. *Journal of Great Lakes Research* **19**, 569-581.

LeBlanc, G. A. (2007). Crustacean endocrine toxicology: a review. *Ecotoxicology* **16**, 61-81.

Lenz, E. M., and Wilson, I. D. (2007). Analytical strategies in metabolomics. *Journal of Proteome Research* **6**, 443-458.

Lin, C. Y., Viant, M. R., and Tjeerdema, R. S. (2006). Metabolomics: Methodologies and applications in the environmental sciences. *Journal of Pesticide Science* **31**, 245-251.

Linder, M. C., and Hazegh-Azam, M. (1996). Copper biochemistry and molecular biology. *American Journal of Clinical Nutrition* **63**, 797S-811S.

Lindon, J. C., Keun, H. C., Ebbels, T. M. D., Pearce, J. M. T., Holmes, E., and Nicholson, J. K. (2005). The Consortium for Metabonomic Toxicology (COMET): aims, activities and achievements. *Pharmacogenomics* **6**, 691-699.

Lindon, J. C., Nicholson, J. K., Holmes, E., and Everett, J. R. (2000). Metabonomics: Metabolic processes studied by NMR spectroscopy of biofluids. *Concepts in Magnetic Resonance* **12**, 289-320.

Loh, H. S., and Wilson, C. W. M. (1971). Relationship of Human Ascorbic-Acid Metabolism to Ovulation. *Lancet* **1**, 110-&.

Luck, M. R., Jeyaseelan, I., and Scholes, R. A. (1995). Ascorbic-Acid and Fertility. *Biology of Reproduction* **52**, 262-266.

Makarov, A., Denisov, E., Lange, O., and Horning, S. (2006). Dynamic range of mass accuracy in LTQ orbitrap hybrid mass spectrometer. . *Journal of the American Society for Mass Spectrometry* **17**, 977-982.

Malmendal, A., Overgaard, J., Bundy, J. G., Sorensen, J. G., Nielsen, N. C., Loeschcke, V., and Holmstrup, M. (2006). Metabolomic profiling of heat stress: hardening and recovery of homeostasis in *Drosophila*. *American Journal of Physiology-Regulatory Integrative and Comparative Physiology* **291**, R205-R212.

Martin-Creuzburg, D., Westerlund, S. A., and Hoffmann, K. H. (2007). Ecdysteroid levels in *Daphnia magna* during a molt cycle: determination by radioimmunoassay (RIA) and liquid chromatography-mass spectrometry (LC-MS). *General and Comparative Endocrinology* **151**, 66-71.

Martins, J., Oliva Teles, L., and Vasconcelos, V. (2007). Assays with *Daphnia magna* and *Danio rerio* as alert systems in aquatic toxicology. *Environment International* **33**, 414-25.

McKelvie, J. R., Yuk, J., Xu, Y. P., Simpson, A. J., and Simpson, M. J. (2009). H-1 NMR and GC/MS metabolomics of earthworm responses to sub-lethal DDT and endosulfan exposure. *Metabolomics* **5**, 84-94.

Merchie, G., Lavens, P., and Sorgeloos, P. (1997). Optimization of dietary vitamin C in fish and crustacean larvae: a review. *Aquaculture* **155**, 165-181.

Miller, M. G. (2007). Environmental metabolomics: A SWOT analysis (strengths, weaknesses, opportunities, and threats). *Journal of Proteome Research* **6**, 540-545.

Moore, M. N., Depledge, M. H., Readman, J. W., and Leonard, D. R. P. (2004). An integrated biomarker-based strategy for ecotoxicological evaluation of risk in environmental management. *Mutation Research-Fundamental and Molecular Mechanisms of Mutagenesis* **552**, 247-268.

Mucklow, P. T., and Ebert, D. (2003). Physiology of immunity in the water flea *Daphnia magna*: environmental and genetic aspects of phenoloxidase activity. *Physiological and Biochemical Zoology* **76**, 836-42.

Nicholson, J. K., Connelly, J., Lindon, J. C., and Holmes, E. (2002). Metabonomics: a platform for studying drug toxicity and gene function. *Nat. Rev. Drug Discov.* **1**, 153-161.

OECD (1998). OECD Guidelines for Testing of Chemicals 211 - *Daphnia magna* Reproduction Test, Vol. 64, p. 21.

OECD (2004). OECD guidelines for testing of chemicals, No 202, *Daphnia sp.* acute immobilisation test, p. 12. Organisation for Economic Cooperation and Development.

OECD (2009). OECD Guidelines for the Testing of Chemicals, Section 2: Effects on Biotic Systems.

Olmstead, A. W., and Leblanc, G. A. (2002). Juvenoid hormone methyl farnesoate is a sex determinant in the crustacean *Daphnia magna*. *Journal of Experimental Zoology* **293**, 736-9.

Olmstead, A. W., and LeBlanc, G. A. (2003). Insecticidal juvenile hormone analogs stimulate the production of male offspring in the crustacean *Daphnia magna*. *Environmental Health Perspectives* **111**, 919-24.

Olsen, J. V., de Godoy, L. M. F., Li, G. Q., Macek, B., Mortensen, P., Pesch, R., Makarov, A., Lange, O., Horning, S., and Mann, M. (2005). Parts per million mass accuracy on an orbitrap mass spectrometer via lock mass injection into a C-trap. *Molecular & Cellular Proteomics* **4**, 2010-2021.

Padayatty, S. J., Katz, A., Wang, Y. H., Eck, P., Kwon, O., Lee, J. H., Chen, S. L., Corpe, C., Dutta, A., Dutta, S. K., and Levine, M. (2003). Vitamin C as an antioxidant: Evaluation of its role in disease prevention. *Journal of the American College of Nutrition* **22**, 18-35.

Palmeira, C. M., Moreno, A. J., and Madeira, V. M. (1994). Metabolic alterations in hepatocytes promoted by the herbicides paraquat, dinoseb and 2,4-D. *Archives of Toxicology* **68**, 24-31.

Parsons, H. M., Ekman, D. R., Collette, T. W., and Viant, M. R. (2009). Spectral Relative Standard Deviation: A Practical Benchmark in Metabolomics. *The Analyst* **134**, 478-485.

Parsons, H. M., Ludwig, C., Günther, U. L., and Viant, M. R. (2007). Improved classification accuracy in 1- and 2-dimensional NMR metabolomics data using the variance stabilising generalised logarithm transformation. *BMC Bioinformatics* **8**, 234.

Payne, T. G., Southam, A. D., Arvanitis, T. N., and Viant, M. R. (2009). A Signal Filtering Method for Improved Quantification and Noise Discrimination in Fourier Transform Ion Cyclotron Resonance Mass Spectrometry-Based Metabolomics Data. *Journal of the American Society for Mass Spectrometry* **20**, 1087-1095.

Phalaraksh, C., Lenz, E. M., Lindon, J. C., Nicholson, J. K., Farrant, R. D., Reynolds, S. E., Wilson, I. D., Osborn, D., and Weeks, J. M. (1999). NMR spectroscopic studies on the haemolymph of the tobacco hornworm, *Manduca sexta*: assignment of H-1 and C-13 NMR spectra. *Insect Biochemistry and Molecular Biology* **29**, 795-805.

Phalaraksh, C., Reynolds, S. E., Wilson, I. D., Lenz, E. M., Nicholson, J. K., and Lindon, J. C. (2008). A metabonomic analysis of insect development: H-1-NMR spectroscopic characterization of changes in the composition of the haemolymph of larvae and pupae of the tobacco hornworm, *Manduca sexta*. *Scienceasia* **34**, 279-286.

Poynton, H. C., Loguinov, A. V., Varshavsky, J. R., Chan, S., Perkins, E. I., and Vulpe, C. D. (2008). Gene expression profiling in *Daphnia magna* part I: Concentration-dependent profiles provide support for the No Observed Transcriptional Effect Level. *Environmental Science & Technology* **42**, 6250-6256.

Poynton, H. C., Varshavsky, J. R., Chang, B., Cavigliolo, G., Chan, S., Holman, P. S., Loguinov, A. V., Bauer, D. J., Komachi, K., Theil, E. C., Perkins, E. J., Hughes, O., and Vulpe, C. D. (2007). *Daphnia magna* ecotoxicogenomics provides mechanistic insights into metal toxicity. *Environmental Science & Technology* **41**, 1044-1050.

Preston, B. L. (2002). Indirect effects in aquatic ecotoxicology: implications for ecological risk assessment. *Environmental Management* **29**, 311-23.

Ray, D. E., and Fry, J. R. (2006). A reassessment of the neurotoxicity of pyrethroid insecticides. *Pharmacology & Therapeutics* **111**, 174-93.

REACH (2006). Regulation (EC) No 1907/2006 of The European Parliament and of The Council In Registration, Evaluation, Authorisation and Restriction of Chemicals (REACH), establishing a European Chemicals Agency, amending Directive 1999/45/EC and repealing Council Regulation (EEC) No 793/93 and Commission Regulation (EC) No 1488/94 as well as Council Directive 76/769/EEC and Commission Directives 91/155/EEC, 93/67/EEC, 93/105/EC and 2000/21/EC. The European Parliament and The Council of The European Union.

.

Reynaldi, S., Duquesne, S., Jung, K., and Liess, M. (2006). Linking feeding activity and maturation of *Daphnia magna* following short-term exposure to fenvalerate. *Environmental Toxicology and Chemistry* **25**, 1826-30.

Robertson, D. G. (2005). Metabonomics in toxicology: A review. *Toxicological Sciences* **85**, 809-822.

Robertson, D. G., Reily, M. D., and Baker, J. D. (2007). Metabonomics in pharmaceutical discovery and development. *Journal of Proteome Research* **6**, 526-39.

Robosky, L. C., Robertson, D. G., Baker, J. D., Rane, S., and Reily, M. D. (2002). In vivo toxicity screening programs using metabonomics. *Combinatorial Chemistry and High Throughput Screening* **5**, 651-662.

Rubingh, C. M., Bijlsma, S., Derks, E. P. P. A., Bobeldijk, I., Verheij, E. R., Kochhar, S., and Smilde, A. K. (2006). Assessing the performance of statistical validation tools for megavariate metabolomics data. *Metabolomics* **2**, 53-61.

Samuelsson, L. M., Forlin, L., Karlsson, G., Adolfsson-Eric, M., and Larsson, D. G. J. (2006). Using NMR metabolomics to identify responses of an environmental estrogen in blood plasma of fish. *Aquatic Toxicology* **78**, 341-349.

Sandbacka, M., Christianson, I., and Isomaa, B. (2000). The acute toxicity of surfactants on fish cells, *Daphnia magna* and fish—a comparative study. *Toxicology in Vitro* **14**, 61-8.

Sangster, T. P., Wingate, J. E., Burton, L., Teichert, F., and Wilson, I. D. (2007). Investigation of analytical variation in metabolomic analysis using liquid chromatography/mass spectrometry. *Rapid Communications in Mass Spectrometry* **21**, 2965-70.

Santojanni, A., Gorbi, G., and Sartore, F. (1998). Prediction of fecundity in chronic toxicity tests on *Daphnia magna*. *Water Research* **32**, 3146-3156.

Schmidt, C. W. (2004). Metabolomics: What's happening downstream of DNA. *Environmental Health Perspectives* **112**, A410-A415.

Skoog, D. A., Holler, F. J., and Nieman, T. A. (1998). *Principles of Instrumental Analysis*. Harcourt Brace & Company, Orlando; Florida.

Smolders, R., Baillieul, M., and Blust, R. (2005). Relationship between the energy status of *Daphnia magna* and its sensitivity to environmental stress. *Aquatic Toxicology* **73**, 155-70.

Snape, J. R., Maund, S. J., Pickford, D. B., and Hutchinson, T. H. (2004). Ecotoxicogenomics: the challenge of integrating genomics into aquatic and terrestrial ecotoxicology. *Aquatic Toxicology* **67**, 143-154.

Soetaert, A., Moens, L. N., Van der Ven, K., Van Leemput, K., Naudts, B., Blust, R., and De Coen, W. M. (2006). Molecular impact of propiconazole on *Daphnia magna* using a

reproduction-related cDNA array. *Comparative Biochemistry and Physiology C-Toxicology & Pharmacology* **142**, 66-76.

Soetaert, A., van der Ven, K., Moens, L. N., Vandenbrouck, T., van Remortel, P., and De Coen, W. M. (2007a). *Daphnia magna* and ecotoxicogenomics: Gene expression profiles of the anti-ecdysteroidal fungicide fenarimol using energy-, molting- and life stage-related cDNA libraries. *Chemosphere* **67**, 60-71.

Soetaert, A., Vandenbrouck, T., van der Ven, K., Maras, M., van Remortel, P., Blust, R., and de Coen, W. M. (2007b). Molecular responses during cadmium-induced stress in *Daphnia magna*: Integration of differential gene expression with higher-level effects. *Aquatic Toxicology* **83**, 212-222.

Soga, T., Baran, R., Suematsu, M., Ueno, Y., Ikeda, S., Sakurakawa, T., Kakazu, Y., Ishikawa, T., Robert, M., Nishioka, T., and Tomita, M. (2006). Differential metabolomics reveals ophthalmic acid as an oxidative stress biomarker indicating hepatic glutathione consumption. *Journal of Biological Chemistry* **281**, 16768-16776.

Sole, M., Shaw, J. P., Frickers, P. E., Readman, J. W., and Hutchinson, T. H. (2010). Effects on feeding rate and biomarker responses of marine mussels experimentally exposed to propranolol and acetaminophen. *Analytical and Bioanalytical Chemistry* **396**, 649-656.

Southam, A. D., Easton, J. M., Stentiford, G. D., Ludwig, C., Arvanitis, T. N., and Viant, M. R. (2008). Metabolic changes in flatfish hepatic tumours revealed by NMR-based metabolomics and metabolic correlation networks. *Journal of Proteome Research* **7**, 5277-85.

Southam, A. D., Payne, T. G., Cooper, H. J., Arvanitis, T. N., and Viant, M. R. (2007). Dynamic Range and Mass Accuracy of Wide-Scan Direct Infusion Nanoelectrospray Fourier Transform

Ion Cyclotron Resonance Mass Spectrometry-Based Metabolomics Increased by the Spectral Stitching Method. *Analytical Chemistry* **79**, 4595-4602.

Stanley, J. K., Ramirez, A. J., Mottaleb, M., Chambliss, C. K., and Brooks, B. W. (2006). Enantiospecific toxicity of the beta-blocker propranolol to *Daphnia magna* and *Pimephales promelas*. *Environmental Toxicology and Chemistry* **25**, 1780-1786.

Stentiford, G. D., Viant, M. R., Ward, D. G., Johnson, P. J., Martin, A., Wei, W., Cooper, H. J., Lyons, B. P., and Feist, S. W. (2005). Liver tumours in wild flatfish: a histopathological, proteomic and metabolomic study. *OMICS - Journal of Integrative Biology* **9**, 281-299.

Stohs, S. J., and Bagchi, D. (1995). Oxidative mechanisms in the toxicity of metal ions. *Free Radical Biology and Medicine* **18**, 321-36.

Sugimoto, H., Matsuzaki, S., Hamana, K., Yamada, S., and Kobayashi, S. (1991). Alpha-Tocopherol and Superoxide-Dismutase Suppress and Diethyldithiocarbamate and Phorone Enhance the Lipopolysaccharide-Induced Increase in N1-Acetylspermidine Concentrations in Mouse-Liver. *Circulatory Shock* **33**, 171-177.

Sui, J. J., Tan, T. L., Zhang, J. H., Ching, C. B., and Chen, W. N. (2007). ITRAQ-coupled 2D LC-MS/MS analysis on protein profile in vascular smooth muscle cells incubated with S- and R-enantiomers of propranolol: Possible role of metabolic enzymes involved in cellular anabolism and antioxidant activity. *Journal of Proteome Research* **6**, 1643-1651.

Sumner, L. W., Amberg, A., Barrett, D., Beale, M. H., Beger, R., Daykin, C. A., Fan, T. W. M., Fiehn, O., Goodacre, R., Griffin, J. L., Hankemeier, T., Hardy, N., Harnly, J., Higashi, R., Kopka, J., Lane, A. N., Lindon, J. C., Marriott, P., Nicholls, A. W., Reilly, M. D., Thaden, J. J., and Viant, M. R. (2007). Proposed minimum reporting standards for chemical analysis. *Metabolomics* **3**, 211-221.

Takahashi, H., Kai, K., Shinbo, Y., Tanaka, K., Ohta, D., Oshima, T., Altaf-Ul-Amin, M., Kurokawa, K., Ogasawara, N., and Kanaya, S. (2008). Metabolomics approach for determining growth-specific metabolites based on Fourier transform ion cyclotron resonance mass spectrometry. *Analytical and Bioanalytical Chemistry* **391**, 2769-82.

Tatarazako, N., and Oda, S. (2007). The water flea *Daphnia magna* (Crustacea, Cladocera) as a test species for screening and evaluation of chemicals with endocrine disrupting effects on crustaceans. *Ecotoxicology* **16**, 197-203.

Tessier, A. J., and Goulden, C. E. (1982). Estimating food limitation in cladoceran populations. *Limnological Oceanography* **27**, 707-717.

Tripathi, G., and Verma, P. (2004). Fenvalerate-induced changes in a catfish, *Clarias batrachus*: metabolic enzymes, RNA and protein. *Comparative Biochemistry and Physiology C-Toxicology & Pharmacology* **138**, 75-79.

Truhaut, R. (1977). Ecotoxicology: objectives, principles and perspectives. *Ecotoxicology and Environmental Safety* **1**, 151-73.

Turner, M. A., Viant, M. R., Teh, S. J., and Johnson, M. L. (2007). Developmental rates, structural asymmetry, and metabolic fingerprints of steelhead trout (*Oncorhynchus mykiss*) eggs incubated at two temperatures. *Fish Physiology and Biochemistry* **33**, 59-72.

Uda, K., Fujimoto, N., Akiyama, Y., Mizuta, K., Tanaka, K., Ellington, W. R., and Suzuki, T. (2006). Evolution of the arginine kinase gene family. *Comparative Biochemistry and Physiology D-Genomics & Proteomics* **1**, 209-218.

US-EPA (2004). Potential Implications of Genomics for Regulatory and Risk Assessment Applications at EPA, p. 70. United States Environmental Protection Agency.

Van Straalen, N. (2003). Ecotoxicology becomes stress ecology. *Environmental Science & Technology* **37**, 324A-330A.

Verslycke, T., Ghekiere, A., Raimondo, S., and Janssen, C. (2007). Mysid crustaceans as standard models for the screening and testing of endocrine-disrupting chemicals. *Ecotoxicology* **16**, 205-219.

Viant, M. R. (2007). Metabolomics of aquatic organisms: the new 'omics' on the block. *Marine Ecology-Progress Series* **332**, 301-306.

Viant, M. R. (2008). Recent developments in environmental metabolomics. *Molecular Biosystems* **4**, 980-986.

Viant, M. R., Bundy, J. G., Pincetich, C. A., de Ropp, J. S., and Tjeerdema, R. S. (2005). NMR-derived developmental metabolic trajectories: An approach for visualizing the toxic actions of trichloroethylene during embryogenesis. *Metabolomics* **1**, 149-158.

Viant, M. R., Pincetich, C. A., Hinton, D. E., and Tjeerdema, R. S. (2006a). Toxic actions of dinoseb in medaka (*Oryzias latipes*) embryos as determined by *in vivo* ³¹P NMR, HPLC-UV and ¹H NMR metabolomics. *Aquatic Toxicology* **76**, 329–342.

Viant, M. R., Pincetich, C. A., and Tjeerdema, R. S. (2006b). Metabolic effects of dinoseb, diazinon and esfenvalerate in eyed eggs and alevins of Chinook salmon (*Oncorhynchus tshawytscha*) determined by ¹H NMR metabolomics. *Aquatic Toxicology* **77**, 359–371.

Viant, M. R., Rosenblum, E. S., and Tjeerdema, R. S. (2003a). NMR-based metabolomics: A powerful approach for characterizing the effects of environmental stressors on organism health. *Environmental Science & Technology* **37**, 4982-4989.

Viant, M. R., Werner, I., Rosenblum, E. S., Gantner, A. S., Tjeerdema, R. S., and Johnson, M. L. (2003b). Correlation between heat-shock protein induction and reduced metabolic condition in juvenile steelhead trout (*Oncorhynchus mykiss*) chronically exposed to elevated temperature. *Fish Physiology and Biochemistry* **29**, 159-171.

Watanabe, H., Takahashi, E., Nakamura, Y., Oda, S., Tatarazako, N., and Iguchi, T. (2007). Development of a *Daphnia magna* DNA microarray for evaluating the toxicity of environmental chemicals. *Environmental Toxicology and Chemistry* **26**, 669-676.

Weber, R. J. M., and Viant, M. R. (submitted). MI-Pack: Increased confidence of metabolite identification in mass spectra by integrating accurate masses and metabolic pathways. *Chemometrics and Intelligent Laboratory Systems*

Westerhuis, J. A., Hoefsloot, H. C. J., Smit, S., Vis, D. J., Smilde, A. K., van Velzen, E. J. J., van Duijnhoven, J. P. M., and van Dorsten, F. A. (2008). Assessment of PLS-DA cross validation. *Metabolomics* **4**, 81-89.

Wise, B. M., Gallagher, N. B., Bro, R., Shaver, J. M., Windig, W., and Koch, R. S. (2006). *PLS_Toolbox 4.0 for use with MATLAB (user manual)*. Eigenvector Research, Inc, Wenatchee, USA.

Wold, S., Sjostrom, M., and Eriksson, L. (2001). PLS-regression: a basic tool of chemometrics. *Chemometrics and Intelligent Laboratory Systems* **58**, 109-130.

Wouters, R., Lavens, P., Nieto, J., and Sorgeloos, P. (2001). Penaeid shrimp broodstock nutrition: an updated review on research and development. *Aquaculture* **202**, 1-21.

Wu, H., Southam, A. D., Hines, A., and Viant, M. R. (2008). High throughput tissue extraction protocol for NMR- and MS-based metabolomics. *Analytical Biochemistry* **372**, 204-212.

Zhang, L. K., Rempel, D., Pramanik, B. N., and Gross, M. L. (2005). Accurate mass measurements by Fourier transform mass spectrometry. *Mass Spectrometry Reviews* **24**, 286-309.

CHAPTER NINE:

Appendix

Publication List and Author Contributions

Taylor, N. S.; Weber, R. J. M.; Southam, A. D.; Payne, T. G.; Hrydziuszko, O.; Arvanitis, T. N.; Viant, M. R. A new approach to toxicity testing in *Daphnia magna*: Application of high throughput FT-ICR mass spectrometry metabolomics. *Metabolomics*. **2009**, 5 (1), 45-58.

Taylor, N.S.: Experimental design, exposure studies, FT-ICR MS analysis, data analysis and writing of manuscript

Weber, R.J.M.: development of algorithm for calculating empirical formulae and KEGG identification

Southam, A.D.: Optimisation of FT-ICR MS and SIM-stitch approach

Payne, T.G.: Optimisation of SIM-stitch approach, including data pre-processing and three-stage filtering algorithm.

Hrydziuszko, O.: Development of algorithm for replacing missing values and software visualisation tool for determining common peaks

Arvanitis, T.N.: Optimisation of SIM-stitch approach, including data pre-processing and three-stage filtering algorithm.

Viant, M.R.: Experimental design, FT-ICRMS and data analysis optimisation, editing of manuscript.

Poynton, H. C.; **Taylor, N. S.;** Hicks, J.; Colson, K.; Chan, S.; Clark, C.; Scanlan, L.; Louginov, A. V.; Vulpe, C.; Viant, M. R. Integration of metabolomics and transcriptomic signatures offers a coordinated model of cadmium toxicity in *Daphnia magna*. *Environmental Science and Technology* (submitted).

Taylor, N.S.: FT-ICR MS analysis and subsequent data processing and analysis, writing of manuscript

Poynton, H.C.: Exposures for transcriptomic analysis, microarray analysis and q-RT-PCR analysis, writing of manuscript.

Hicks, J. and Chan S.: NMR analysis, manuscript editing

Vulpe, C., Colson, K., Clark, C. Scanlan, L and Louginov, A.: Daphnia exposures and haemolymph extraction for metabolomic analysis, manuscript editing

Viant, M.R.: FT-ICR MS metabolomic data analysis, manuscript editing.

Taylor, N. S. and Viant, M. R. Discriminating toxicant modes of action via changes in the daphnid metabolome. *Toxicological Sciences* (submitted)

Taylor, N.S.: Experimental design, exposure studies, FT-ICR MS analysis, data analysis and writing of manuscript

Viant, M.R.: Data analysis, manuscript editing.